DIFFUSION OF PURE LIQUID HYDROCARBONS IN HIGH SILICA PENTASIL ZEOLITES

A THESIS

SUBMITTED TO THE

UNIVERSITY OF POONA

FOR THE DEGREE OF

MASTER OF SCIENCE

IN

PHYSICAL CHEMISTRY

BY

A. S. MAMMAN

NATIONAL CHEMICAL LABORATORY

PUNE - 411 008 (INDIA)

1988

DEDICATED TO

MY LATE BROTHER

SIMRAN

ACKNOWLEDGEMENT

I wish to place on record my heartfelt sense of gratitude to Dr. V.R. Choudhary, Asst. Director, Chemical Engineering Division, National Chemical Laboratory, Pune, for his invaluable guidance and encouragement throughout the course of this work.

I am grateful to Dr. O.G.B. Nambiar (Head of Analytical Group) for useful discussions and suggestions for the appropriate methods for chemical analysis. My thanks are due in no small measure to Dr.(Mrs.) A. Mitra (SIL) for SEM. I owe my sincere thanks to Mr. S.S. Tamhankar (Inorganic Divn.) for his invaluable help rendered for the analysis of some of the samples.

I am thankful to Mr. D.B. Akolekar, Dr. A.P. Singh, Dr. S.D. Sansare and Mr. A.M. Rajput for their timely help and cooperation in some of the experimental work. I am also thankful to Dr. V.S. Nayak for providing ZSM-5 zeolite samples.

I also take this opportunity to thank Mr. V.B. Bonde, S.T. Choudhary, V.H. Rane, Miss R.V. Gadre, Dr. S.G. Pataskar and Mrs. Mayadevi for their constant cheerful cooperation.

My special thanks go to Dr. R.A. Mashelkar, Head, Chemical Engineerig Division, for his constant encouragement to persue the present work.

Lastly, I am indebted to the Director, N.C.L., for permitting me to undertake the present research work.

Pune *[A. S. MAMMAN]*

April 1988

CONTENTS

.....

SUMMARY AND CONCLUSIONS

SUMMARY AND CONCLUSIONS

Intracrystalline diffusion plays a very vital role in pentasil zeolites in deciding the product distribution in catalytic processes and also in adsorption separation processes in which the adsorption is kinetically controlled. The diffusional and/or shape selective properties of these medium pore size zeolites could be altered by the modification of the zeolites.

A number of studies have been reported on the diffusion of gaseous compounds in ZSM-5 zeolites. However, studies on diffusion of liquid species in ZSM-5 are very scarce. Also, no detailed investigation has been reported so far on the diffusion and/or catalytic reactions in modified ZSM-8 zeolites. The present investigation was undertaken with following objectives:

1. *To study diffusion of liquid cumene in ZSM-5 and factors (viz. type of cation, calcination temperature and poisoning of zeolite) affecting the diffusion.*
2. *To study influence of modification of H-ZSM-8 by MgO, P_2O_5 and B_2O_3 on its acid strength distribution, diffusional properties (i.e. diffusion of liquid cumene) and catalytic activity/selectivity in the cumene cracking, o- and m- xylene isomerisations and methanol and ethanol conversion reactions.*

Diffusion of Cumene in ZSM-5

Diffusion of cumene in ZSM-5 zeolites from liquid phase at 283-328 K has been studied using a novel volumetric apparatus. Influence of temperature and zeolite parameters such as cation type (viz. H^+, Na^+ and NH_4^+), dehydroxylation and poisoning of the strong acid sites (by pyridine) of the zeolite on the diffusion has been investigated. The diffusion of cumene in ZSM-5 and the activation energy of diffusion are found to be strongly affected by the above zeolite parameters. The influence of the parameters on the diffusion is explained by considering the changes in the effective channel diameter, particularly at channel intersections, and the interaction

of diffusing species with cations in the zeolite.

Acidity of Modified H-ZSM-8 Zeolite

The acidity distribution on the H-ZSM-8 and MgO-, P_2O_5- and B_2O_3- modified H-ZSM-8 has been measured using the gc pulse method based on TPD under chromatographic conditions and the stepwise thermal desorption of pyridine from 473 to 673 K. The modification of the zeolite in all the cases has resulted in a very significant decrease in the strong acid sites and also in the number of total acid sites, because of the blockage of existing acid sites on the zeolite by the modifying agents.

Diffusion of Cumene in Modified H-ZSM-8

The modification of H-ZSM-8 by MgO, P_2O_5 and B_2O_3 caused a decrease in the cumene diffusivity and also an increase in the activation energy for the diffusion in the zeolite. This is mostly due to a reduction in the effective channel diameter and also partly due to the partial blocking of some of the channel openings on the external surface of the zeolite crystals.

Catalytic Activity of Modified H-ZSM-8 Zeolite

The catalytic activity of H-ZSM-8 and MgO-, P_2O_5- and B_2O_3- modified zeolites in cumene cracking and o- and m- xylene isomerisation, and also alcohol (viz. methanol and ethanol) conversion reaction has been investigated using a pulse microreactor attached to a gas chromatograph.

The modification of H-ZSM-8 with MgO has resulted in the decrease of catalytic activity in the cumene cracking, o- and m- xylene isomerisation and aromatization in methanol and ethanol conversion reactions. The shape selectivity of the zeolite, on the other hand, is found to be increased significantly eventhough the concentration of MgO in the zeolite is as low as 0.1%.

The modification of H-ZSM-8 with P_2O_5 has resulted in the decrease in the aromatization activity (in both the alcohol conversion reactions) of the zeolite.

However, the cumene cracking and o- and m-xylene isomerisation activity of the zeolite is increased and also the para selectivity in the xylene isomerisation and ethanol conversion is increased after the modification. The modification of H-ZSM-8 with B_2O_3 has resulted in the decrease in the aromatization activity (in both the alcohol conversion reactions) of the zeolite but in the large increase in the conversion of cumene, o- and m- xylene. In general, the shape selectivity (or para selectivity) of H-ZSM-8 in the above reactions is reduced after the modification.

The reasons for the observed changes in the catalytic properties of H-ZSM-8 after its modifications are discussed.

Chapter–1 : INTRODUCTION

1. INTRODUCTION

1.1 PENTASIL ZEOLITES

Since the introduction of ZSM-5 zeolite [1] by Mobil Oil Corporation in 1972, this zeolite has gained increasing importance as a high potential catalyst in a number of commercially important chemical processes[2-6].ZSM-8 zeolite[7] was also introduced by Mobil Oil Corporation around the same period. All these zeolites belong to a group of pentasil zeolites as their secondary building units (SBU) contains 5-1 T (i.e. Si + Al) atoms. The SBU in ZSM-5 zeolite [8,9] is shown in Fig. 1.1(a). The configuration and linkage of these SBU within chains in ZSM-5 [8] are shown in Fig. 1.1(b). The low energy complex 5-1 SBU (which are thermodynamically very stable) in the framework of pentasil zeolite are responsible for their very high thermal and acid/base stability.

The above pentasil zeolites are superior to the conventional ones like X, Y and mordenite because of their following unique properties:

(i) High thermal and hydrothermal stability and also stability to most mineral acids (except HF).

(ii) Molecular shape-selectivity arising from steric restrictions during sorption and catalytic reactions at active sites.

(iii) The constraint that, normally, hydrocarbons containing more than eleven carbon atoms are not formed in the alcohol and hydrocarbon conversion processes.

(iv) High resistance to deactivation due to coke deposition and hence, very long life in the catalytic conversion processes as compared to other zeolites.

1.1.1 ZSM-5 Type Zeolites

The discovery of the new shape-selective high silica zeolite, designated as ZSM-5, by Mobil Oil Corporation [1] has resulted in a number of high potential

catalysts for obtaining synthetic fuel and hydrocarbons from methanol [2,3] as well as catalysts for other industrial hydrocarbon conversion processes [2,6]. The importance of the zeolite has been steadily increasing as can be seen from the large number of patents [2-6] for the following processes employing ZSM-5 class catalysts:

(i) Production of gasoline from methanol and oxygenated compounds.

(ii) Production of gasoline by reforming of hydrocarbons.

(iii) Production of gasoline/hydrocarbons from synthesis gas.

(iv) Production of aromatics from lower hydrocarbons.

(v) Processing and upgrading of alkenes and alkanes.

(vi) Conversion of methanol to olefins.

(vii) Conversion of methanol to aromatics.

(viii) Isomerization of alkylbenzenes (mostly xylenes and ethylbenzene) and o-cresol.

(ix) Disproportionation of toluene.

(x) Alkylation of aromatic hydrocarbons - ethylation of benzene, selective methylation of toluene to p-xylene and ethylation and propylation of toluene.

(xi) Upgrading of Fischer-Tropsch synthesis products.

(xii) Dewaxing and hydrodewaxing of hydrocarbons.

(xiii) Cracking and hydrocracking of hydrocarbon oils.

(xiv) Synthesis of aliphatic amines from ether and ammonia and of pyridine derivatives from carbonyl compounds and ammonia.

(xv) Removal of p-dialkylbenzenes from their isomers by cracking and other miscellaneous processes.

Mobil MTG (methanol-to-gasoline) process, based on the use of ZSM-5 zeolite catalyst, is in operation in the synfuel plant at Motunui, New Zealand). This plant is expected to supply a third of the country's needs for petrol [5].

The unique catalytic properties of the zeolite including its high resistance towards deactivation due to coking are attributed [10,11] to the presence of strong

acid sites as well as the unique molecular shape-selective properties imparted to the zeolites by the three dimensional system of intersecting channels present in them.

The structure and properties of ZSM-5 type zeolites are discussed below.

(a) Structure of ZSM-5 Zeolite [8,9]

The unit cell composition of Na-form of ZSM-5 can be expressed as follows:

$$Na_nAl_nSi_{96-n}O_{192} \sim 16H_2O \quad (\text{where, } n < 27)$$

A model of the pore structure of ZSM-5 is shown in Fig. 1.2. The framework of the zeolite (Fig. 1.2(b)) consists of a three dimensional system of intersecting near circular zig-zag channels (0.54 x 0.56 nm) defined by 10 rings of oxygen ions in all three directions running parallel to [001] and crosslinked by elliptical straight channels [0.51 x 0.55 nm] parallel to [010] plane. A large fraction of the crystal structure is made up of five membered rings of silicon-oxygen tetrahedra (Fig. 1.2(a)). In ZSM-5 linkage of chains (Fig. 1.1(b)) occurs through 4-, 5- and 6- membered rings [12]. The crystallographic data of ZSM-5 [8,9] are presented in Table-1.1.

ZSM-5 crystals are orthorhombic. However, monoclinic symmetry has also been observed. Wu et al. [13] have studied the factors affecting the crystal symmetry of ZSM-5. They have observed that the crystal symmetry of TPA-ZSM-5 is orthorhombic; however, it changes to apparent monoclinic when certain treatments such as calcination and ion exchange are given to the zeolite. They have further observed that this change in crystal symmetry is reversible and displacive transformation between the two symmetric forms of the zeolite and does not cause any basic change in the structure of the framework.

(b) Structural Stability of ZSM-5

ZSM-5 zeolites possesses high thermal (upto 1283 K) and steam stability,

(a)

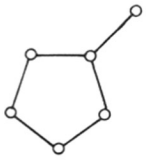

(b)

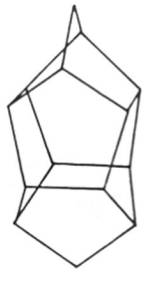

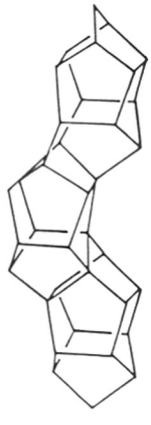

FIG. 1·1 (a) SECONDARY BUILDING UNITS (SBU) IN ZSM-5 AND ZSM-11 ZEOLITES (REF. 8)

(b) CONFIGURATION AND ITS LINKAGE WITHIN CHAINS IN ZSM-5 (REF. 8)

(a)

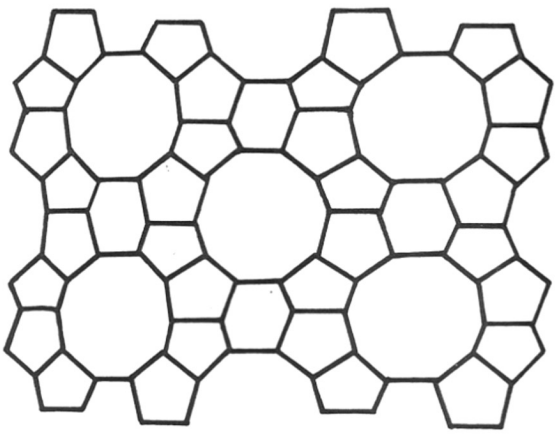

(b)

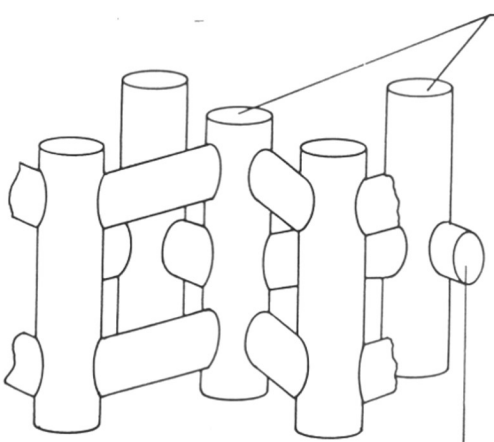

FIG. 1·2: PROJECTION AND CHANNEL NETWORK OF ZSM-5 ZEOLITE

TABLE-1.1

Crystallographic data of ZSM-5

Crystallographic parameters	ZSM-5 (Ref. 8, 9)
Secondary building units	Complex 5-1
Framework density	17.9 (Si + Al) per nm^3
Channels	10-membered ring, intersecting Zig-zag 0.54 x 0.56 nm, parallel to [001] Straight 0.51x 0.55 nm, parallel to [010]
Fault planes	(100)
Unit cell composition	$Na_nAl_nSi_{96-n}O_{192} \sim 16H_2O$ (with $n < 27$ and typically about 3)
Crystal symmetry/space group symmetry	Orthorhombic/Pnma
Unit cell dimensions	a = 2.01 nm, b = 1.99 nm, c = 1.34 nm

and are also stable to most mineral acids (except HF) compared to the other catalytically important zeolites [1,14-16]. Its structure is stable even to heavy thermal shocks [15]. These properties permit reactions to be carried out in the presence of water vapor (which can be one of the products) and the regeneration of the deactivated catalyst at relatively high temperatures.

(c) Shape-Selectivity of ZSM-5

Apart from the high thermal and hydrothermal stability of ZSM-5 zeolite, this zeolite is superior to the conventional ones like mordenite, X and Y type because of its typical molecular shape-selectivity resulting in a desirable product or product distribution and also, a long catalyst life in catalytic processes.

Selective formation of hydrocarbon products restricted to a maximum of 10-carbon atoms in aromatics and 11-carbon atoms in paraffins in the conversion of methanol-to-gasoline on ZSM-5 has been observed [17]. According to Derouane and coworkers [11,18,19], this product selectivity is probably controlled mostly by molecular shape-selective constraints on the formation of intermediate complex structures. Steric inhibition is attributed to the particular dimension of the channel intersections, which restrains the oligomerization of iso-olefins and precludes the accommodation of bimolecular complexes of more than 10-carbon atoms.

Modifications of the zeolite with compounds of phosphorous, boron, magnesium etc. [20-26] results in forms that are more and more shape-selective. These compounds alter the diffusional characteristics of the zeolite such that the diffusivity of para isomers of alkylbenzenes is relatively much higher than that of the other isomers, thus favouring the formation of p-isomers in the catalytic processes.

Selective formation of particular products or a range of products has also been interpreted [27] in terms of a diffusion/reaction interaction. Recently, Derouane and Gabelica [28] have put forward the concept of molecular traffic control in

ZSM-5 type zeolite which has been further generalised by Derouane et al. [29] to include transformations in which '..... (some of the) reactant molecules and (some of the) product molecules have different pathways ..... less readily accessible to the desorbing products ..... and vice-versa ..... ' .

Chen and Garwood [30] have investigated the shape-selective behaviour of ZSM-5 by studying a series of diagnostic catalytic reactions and observed that the zeolite possesses a wide dynamic range of shape-selective properties which are strongly temperature dependent, and that it does not exhibit a cage effect with respect to the chain length of the molecule. The critical dimension of the molecule is more important than the length of the molecule in determining its rate of diffusion through the zeolite. Thus, the diffusion rate is probably controlled by the matching of the size and shape of the molecule with those of the pore opening, rather than by the tortuosity of the channel as in the case of erionite.

The shape-selective nature of ZSM-5 can also be used for the separation of hydrocarbons. Namba et al. [31] studied the relative sorption of 2-methylpentane and 2,2-dimethylbutane on H-ZSM-5 and have observed that only 2-methylpentane was sorbed on the zeolite. This offers a process for a complete separation of the two hydrocarbons.

The deposition of carbonaceous residues on ZSM-5 occurs essentially on its external surface as bulky polyalkyl aromatics which act as coke precursors are not easily formed inside the zeolite channels because of restricted transition state molecular shape-selectivity [32]. The deposition of coke (which is more graphitic in nature) on the outer surface of the crystallites of the zeolite results only in a slight modification of its molecular shape-selective properties and produces a high resistance to ageing.

A detailed discussion on the shape-selective behaviour of ZSM-5 has been given in a number of recent reviews [33-36].

(d) Active Sites/Acidity of ZSM-5 Zeolite

Among the zeolites, the acidic properties of ZSM-5 zeolites have been thoroughly investigated by temperature programmed desorption (TPD) of ammonia [40, 37-39] and pyridine [15,16,41,42], chemisorption and stepwise thermal desorption (STD) of ammonia [43] and pyridine [15,16,41,42], microcalorimetric measurement of heats of ammonia adsorption [44-47] and by the IR spectroscopic study of adsorbed pyridine [38,45,46] on the zeolite. Influence of the conditions of thermal decomposition of TPA-ZSM-5 to H.Na-ZSM-5 [48], the conditions of deammoniation of NH_4-ZSM-5 to H-ZSM-5 [15], the degree of H^+-exchange of H.Na-ZSM-5 [15,42,49], the Si/Al ratio of H-ZSM-5 [41,49] and of the various hydrothermal treatments of H-ZSM-5 [16] on its acidity distribution and catalytic activity in the cumene cracking, o-xylene isomerization and methanol and ethanol to hydrocarbons conversion reactions has been thoroughly investigated. Excellent correlations between the number of strong acid sites measured in terms of pyridine adsorbed irreversibly at 673 K, and the catalytic activity in the above reactions have been obtained [15,16,49]. It was observed [15] that pyridine selectivity measures protonic acid sites on H-ZSM-5 zeolite as Lewis acid sites, formed due to the dehydroxylation, are not easily accessible to it.

The number of active sites and the minimum acid strength required to be possessed by acid site for it to be active in the conversion of C_2-C_6 olefins, cyclohexane, methanol and ethanol to aromatics [50] and hydrocarbon conversion reactions (viz. isomerization of o-xylenes, disproportionation of toluene, trans alkylation between benzene and mesitylene) [51-53] on H-ZSM-5 have been determined by selectively poisoning the stronger acid sites in the order of their strength by pyridine. In the conversion of alcohols on H-ZSM-5, the dehydration occurs on weak acid sites but the aromatization requires strong acid sites [50]. In the hydrocarbon conversion reactions, the requirement of the strength of acid sites is in the following

order [51,52].

Isomerization < Dealkylation < Disproportionation

The high catalytic activity of ZSM-5 is attributed [54,55] to the protonated tetrahedral aluminium atoms (which are the highly reactive ingredients even at levels of parts per million or less). The protonic acid site in H-ZSM-5 and its interaction with a base is shown in Fig. 1.3. In absence of a base, the aluminium atom in tetrahedral environment is asymmetric. Whereas, on interaction with an added base, the aluminium is in a highly symmetrical tetrahedral coordination. According to Weisz, "the quality of Bronsted Al sites is the same - atleast for the 'dilute' siliceous zeolites - regardless of 'acidity' in terms of Al site density" [55].

Lago et al. [56] have observed that carefully prepared H-ZSM-5 zeolites contain sites of equal activity regardless of Al-content and mild steaming generates acid sites of increased activity. For the cracking of hexane at 811 K they are 45 to 75 times more active than conventional sites. The number of enhanced sites created is a strong function of Al content of the zeolite and in particular, is dependent upon the number of paired Al sites in the unsteamed parent. Haag and coworkers [57,58] have observed that the catalytic activity of H-ZSM-5 in the cracking of hexane and hexene and also, in the disproportionation of toluene varies linearly with tetrahedral Al-content of the zeolite over a wide composition range and extrapolates to zero activity at zero Al-content. Such a linear correlation has also been observed by Chen and Reagan [59] in the conversion of methanol to hydrocarbons and by Chang and coworkers [60] in ethylbenzene dealkylation and cyclopentane isomerization on H-ZSM-5.

1.1.2 ZSM-8 Type Zeolites

Mobil Oil Corporation introduced ZSM-8 zeolite [61] in 1971. Though this zeolite is known about one year earlier than ZSM-5 somehow it did not attract

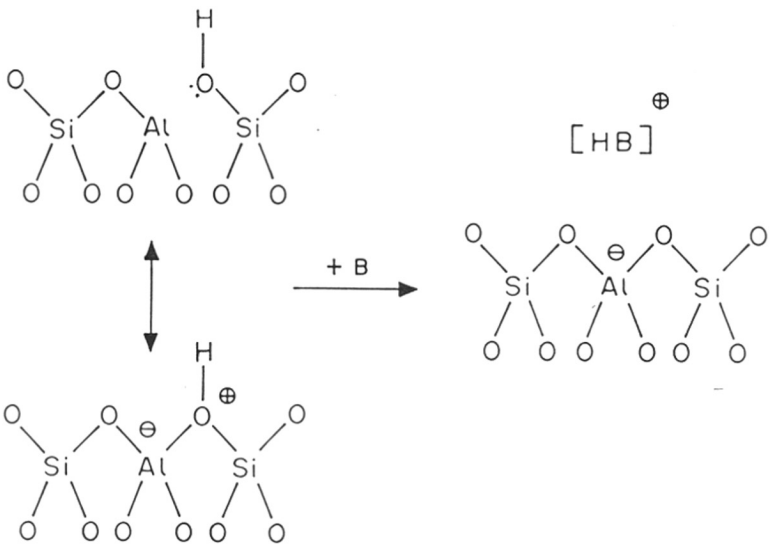

FIG. 1·3: BRÖNSTED ACID SITES IN H-ZSM-5 AND ITS INTERACTION WITH A BASE (REF. 54)

attention of the investigators and has been neglected probably because of a very small difference in XRD data of these two zeolites [62]. Detailed analysis of the crystal structure and channel system of ZSM-8 has not yet been done.

It is interesting that X-ray powder diffraction spectra for ZSM-5 and ZSM-8 zeolites are somewhat similar; the difference lies mostly in the group reflections in the region 2θ = 22-25°, as shown in Fig. 1.4 [63]. ZSM-8 shows a splitting in the highest peak which is not observed for ZSM-5 [11,61]. It is not yet clear whether the structure of ZSM-8 is significantly different from that of ZSM-5 or both these zeolites have a somewhat similar structures [63].

Only a few patents [61,64,65] on the synthesis and application of ZSM-8 as a catalyst and the adsorption capacity of ZSM-8 for water, ammonia, and aliphatic hydrocarbons have been reported. Recently, Park and Chou [66] reported the selective formation of alkylaromatics in the alkylation of toluene with ethanol on ZSM-8. Chou et al. [67] observed that the molecular shape-selective characteristics of ZSM-8 and ZSM-5 zeolites are quite similar.

Recently, Choudhary and Akolekar [68] have thoroughly investigated the acidity and catalytic activity and shape-selectivity [in hydrocarbon conversions (viz. cumene cracking, isomerization of xylenes, and disproportion of toluene) and methanol-to-aromatics reactions] of H.Na-ZSM-8 with different degree of H^+-exchange and of H-ZSM-8 pretreated under different conditions, influence of poisoning of stronger acid sites on its catalytic activity and product selectivity has also been investigated. The physical, acidic and catalytic properties, shape-selectivity behaviour and catalyst deactivation characteristics of ZSM-8 and ZSM-5 zeolites are compared.

1.1.3 Modified ZSM-5 and ZSM-8 Zeolites

The studies on modified pentasil zeolites are summarised in Table-1.2.

When the medium pore size (0.5-0.6 nm) pentasil zeolites are modified by the introduction of phosphorous, boron and magnesium compounds (mostly as their

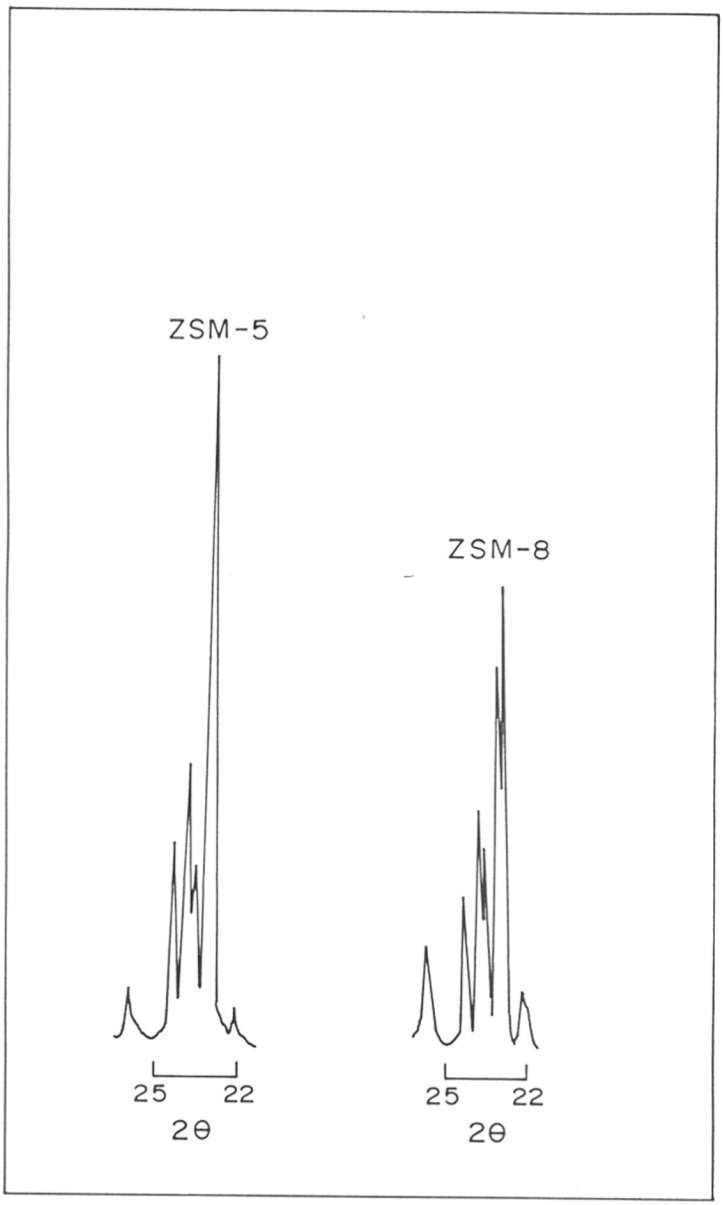

FIG. 1·4 : XRD SPECTRA OF ZSM-5 AND ZSM-8 ZEOLITES AROUND 2θ=22-25° (REF. 63)

TABLE-1.2

Summary of Studies on Modified Pentasil Zeolites

S.No.	Zeolite/ modified zeolite	Catalytic reaction or other studies	Remarks	References
1	2	3	4	5
1.*	H-ZSM-5 and phosporous and boron modified H-ZSM-5	Toluene alkylation with methanol	The zeolite modification caused dramatic increase in p-selectivity in the reaction	Kaeding, et al. (69)
2.	Various modified ZSM-5 zeolites	Toluene alkylation with methanol	On the modified zeolites high purity p-xylene for conversion to fibre grade terephthalic acid obtained	Kaeding et al. (70)
3.	Modified zeolites	Hydrocracking of gasoline fractions	-	Nadirov et al. (71)
4.	Phosphorous modified zeolites	Conversion of xylenes containing ethyl benzene	High p-selectivity in the xylene conversion observed	Iwayama et al. (72)
5.	Phosphorous modified ZSM-5 zeolites (1.1 & 2.0 wt.% phosphorous)	Methanol conversion	Physical properties of modified zeolite determined and mechanism for changes in selectivity discussed	Vedrine et al. (73)
6.	Magnesium/phosphorous modified ZSM-5 zeolite	Alkylation of toluene with ethylene	High selectivity for p-isomers (97.6%)	Kaeding et al. (74)

.....

1	2	3	4	5
7.	Phosphorous treated ZSM-5 zeolite (3.2 - 4.3% P_2O_5)	o-xylene & ethyl benzene isomerisation and aromatization of 1-heptene	Treatment with phosphorous compounds results in longer life of ZSM-5 catalysts	Young et al. (75)
8.*	Phosphorous or B modified H-ZSM-5 zeolites	Sorption studies	The modification with phosphorous or boron affected the catalyst surface only by partly blocking the pores but did not affect the internal pore volume or structure	Gabelica et al. (76)
9.	Phosphorous oxides modified H-ZSM-5	Alkylation of toluene with methanol	High selectivity for p-xylene (94.6%) obtained	Chu (77)
10.*	Phosphorous or magnesium modified ZSM-5 zeolites	Methanol conversion	Surface properties of phosphorous and magnesium modified zeolites and results correlated with methanol conversion reaction	Cai et al. (78)
11.	P Modified H-ZSM-5/ Al_2O_3 catalyst	Methanol conversion	Process variables optimized	Zatroski et al. (79)
12.	Phosphorous modified H-ZSM-5	Methanol conversion	Effect of process variables on product yields studied	Zatroski et al. (80)
13.	P, Mg and/or its oxide modified H-ZSM-5 zeolite	Methylation of toluene	High selectivity for p-xylene	Teijin Petrochem. Industries Ltd. (81)
14.*	Boron modified H-ZSM-5	Microcalorometric studies of ammonia sorption	The modification results in decrease in acidity of the zeolites	Auroux et al. (82)

1	2	3	4	5
15.*	Phosphorous modified H-ZSM-5 zeolites	n-Hexane cracking TPD of NH_3, IR of adsorbed pyridine	Increase in P-content causes increase in activation energy for n-hexane cracking and decrease in acid strength	Lercher et al. (83)
16.*	Mg and phosphorous modified H-ZSM-5 zeolite	Toluene-methanol alkylation and methanol conversion	Modification causes plugging of channels and changes in catalyst hydrophilicity. Introduction of P blocked all strong acid centres but Ni and Mg had small effect on the acidity distribution	Derewenski et al. (84)
17.	Phosphorous modified ZSM-5	Acidity measurement	Controlled decrease of acid strength by o-phosphoric acid on ZSM-5. Higher P-loading caused deposition of plates on crystal surface	Lercher and Rumplmayr (85)
18.	Magnesium and phosphorous modified H-ZSM-5	Alkylation and disproportionation of ethyl-benzene to p-diethyl benzene	ZSM-5 modified with P and Mg gives 98-99% p-diethyl benzene	Kaeding et al. (86)
19.	H-ZSM-5 zeolites treated with BF_3	Hexane cracking and methanol conversion	100% conversion of methanol at 573 K achieved at very high space velocity for the modified zeolite	Rodewald (87)
20.	Modified H-ZSM-5 zeolites	Alkylation of toluene with methanol	Diffusion plays more significant role in enhancing p-selectivity than Bronsted acid sites	Huang et al. (88)

.....

1	2	3	4	5
21.	Boron-modified ZSM-5	Calorimetric studies of NH_3 adsorption	Increase in concentration of B causes decrease in acidity of the zeolite. Modification also results pore plugging	Sayed et al. (89)
22.	Boron-modified high silica zeolites	Xylene isomerisation	Boron modified zeolites are less active but have more stability at higher temperature	Nefedov et al. (90)
23.	Mg-modified zeolites	Cracking reaction	-	Gulf Research & Development Co. (91)
24.	Phosphorous modified ZSM-5	Aromatization reactions	99.8% conversion of propylene with high selectivity for aromatics	Chu (92)
25.	H-ZSM-5 zeolite modified with oxides of group IIIA, IVA, and VA elements	Conversion of paraffin to aromatics	Complete conversion of octane with yields of 29% aromatics	Chu (93)
26.	Mg-modified H-ZSM-5 and H-ZSM-8 zeolites	Isomerisation and alkylation of toluene with C_2H_5OH	High p-ethyl toluene selectivity	Chon et al. (94)
27.	Phosphorous, magnesium modified H-ZSM zeolites	Diffusion properties by adsorption kinetics	--	Wu et al. (95)

.....

1	2	3	4	5
28.	Phosphorous and Boron modified high silica pentasil zeolites	Dehydration of aldehydes, isomerisation of 2-alkyl acroliens	-	Hoeldrich et al. (96)
29.	Phosphorous and rare earth elements modified ZSM-5	Disproportionation of toluene	H_3PO_4 treatment caused the disappearance of strong acid centre. The zeolite modification results in high p-selectivity	Chen et al. (97)
30.*	Boron modified H-ZSM-5	Disproportionation and alkylation of toluene	At low concentrations, B exists only in zeolite channels as boric anhydride. But at higher concentrations it exists also on the external crystal surface. Selectivity for p-xylene varies with time in a non-regular way, indicating B mobility with in the zeolite grains	Sayed et al. (98)
31.	Boron modified high silica zeolites	Thermogravimetric and IR spectroscopic studies	Thermal stability of H form zeolites is not affected by addition of B but that of Na-form is affected.	Chukin et al. (99)
32.	Boric acid impregnated H-ZSM-5	Micro calorimetric study of ammonia adsorption	The modification results in reduction in overall acidity	Auroux et al. (100a)
33.	MgO-modified ZSM-5 zeolites	Acidity by IR spectroscopy of adsorbed pyridine & quinoline	The modification causes decrease in concentration of protonic acid sites. MgO penetrates the zeolite pores and coats their walls, blocking active acid sites in channels	Musa et al. (100b)

oxides) in the zeolite the shape selectivity of the zeolites is dramatically increased [20-26,69,70]. This is mainly because of the fact that the diffusional characteristics of the zeolites are altered such that the diffusivity of p-isomers of alkyl benzenes is relatively much higher than that of the other isomers. Hence, the formation of p-isomer in the catalytic processes on the modified zeolites is favoured.

A number of studies on ZSM-5 zeolites modified with phosphorous [69,70, 72-81,83-86,92,95-97], boron [69,70,76,82,87,89,90,96,98,100] and magnesium [74,78, 81,84-86,91,94,95] compounds have been reported in the literature. But no detailed investigation on the acidity, catalytic and shape selectivity properties of modified ZSM-8 zeolites have been reported so far.

1.2 DIFFUSION IN ZEOLITES (General)

Diffusion in zeolites, in general, does not belong to any of the conventional types, like bulk diffusion or Knudsen diffusion, but to the configurational type [101]. Since the diffusing species are in very close contact with zeolite channel walls, their diffusivity is strongly influenced by the chemical and physical interactions with the structural elements and the cations in the zeolite. The diffusion in zeolites is, therefore, expected to be dependent on the effective channel diameter, the chemical nature of the structural elements and the cations present, and also on the size and configuration, chemical nature and concentration of the diffusing species.

A number of critical reviews on diffusion in zeolites has been published by Barrer [102,103], Ruthven [104,105], Riekert [106], Eberly, Jr. [107], Breck [108], Walker et al. [109] and Palekar and Rajadhyaksha [110].

True zeolite diffusion occurs in the fine micropore structure that is found within the zeolite crystals. A generalised equation that relates the diffusion constant to the properties of the molecule, size and shape of the intracrystalline pore, pressure and temperature is difficult to arrive at. The intimate contact between the diffusing molecules and the pore walls makes the flow strongly dependent on these

variables as well as on the chemical nature of the pore walls. These are the factors that contribute to the non-ideality of the diffusion in zeolites. Consequently, the diffusivity is, in general, a function of the pressure, (or concentration) or more explicitly, a function of the concentration of the sorbed species. This dependence is expressed by the equation,

$$D = D_o \left[\frac{\ln p}{\ln c} \right] \qquad (1)$$

The limiting diffusivity, D_o is a more fundamental constant. Only when the sorption isotherm is linear, D_o becomes equal to D, in which case $\ln p / \ln c = 1$. The expected dependence of diffusivity upon sorbate concentration for a number of other sorption isotherms is given by Barrer [102].

The strong temperature dependence of diffusion is one of its most important characteristics. The diffusion increases exponentially with temperature as expressed by the Arrhenius type relationship,

$$D \text{ or } D_o = D^* e^{-E/RT} \qquad (2)$$

The reported activation energies are in the range 0.5 - 20 kcal.mol.$^{-1}$ [102].

Single-component diffusion in zeolites is investigated by studying the kinetics of sorption or desorption controlled by intracrystalline diffusion, using static volumetric or gravimetric methods, and self-diffusion by NMR and tracer methods.

1.2.1 Analysis of Sorption/Desorption at Constant Pressure (or Concentration) [2]

: For the case of sorption/desorption being carried out at constant pressure, the boundary conditions for any crystallite are as follows:

$C = C$ at the crystallite surface for all $t > 0$

$C = C_o$ throughout the crystalline at $t = 0$

$C = C_\infty$ throughout the crystallite at $t = \infty$

where, C is the concentration of sorbed or desorbed species. Assuming a concentration independent diffusion coefficient, Crank [111] has formulated the following equations for spherical particles of radius r :

$$\frac{Q_t - Q_o}{Q - Q_o} = 1 - \frac{6}{\pi^2} \sum_{n=1}^{\infty} \frac{1}{n^2} \exp\left[- \frac{Dn^2 \pi^2}{r^2} t \right] \qquad (3)$$

where, Q represents the total amount sorbed or desorbed at the various indicated times.

However, for small values of t detailed knowledge of the shape and size distribution of the zeolite crystals is not required and the solution of the diffusion equation [Eqn. (3)] for crystallites of different geometry reduces to a simple form (called $\sqrt{t}$ law) :

$$\frac{Q_t - Q_o}{Q - Q_o} = 6 \left[\frac{D}{r^2} \right]^{1/2} . \; t^{1/2} \qquad (4)$$

The diffusivity can be calculated from the slope of the plot of the LHS vs. $t^{1/2}$. This manner of expressing experimental results is often employed [102].

Barrer [102] has noted that for larger values of t, Eqn. (3) reduces to

$$\ln \frac{Q - Q_t}{Q - Q_o} = \ln \left(\frac{6}{\pi^2} \right) - \left(\frac{D \pi^2}{r^2} \right) t \qquad (5)$$

The values of D can be estimated from the plot of the LHS vs. t. This treatment is used less frequently than Eqn. (4).

1.2.2 Analysis of Sorption/Desorption at Constant Volume and Variable Pressure(or Concentration)

When the sorption/desorption is carried out at constant volume and the variation of pressure is followed as a function of time, the solution to the diffusion equation for spherical particles for the initial brief duration (i.e. for small t) is given by,

$$\frac{Q_t - Q_o}{Q - Q_o} = \frac{6}{r_o}\left[\frac{K+1}{K}\right]\left[\frac{dt}{\pi}\right]^{1/2} \qquad (6)$$

$$= \frac{6}{r}\left[\frac{(Q_o)_g + Q_o}{(Q_o)_g - (Q - Q_o)}\right]\left[\frac{D\,t}{\pi}\right]^{1/2}$$

provided the sorption follows Henry's law [102]. Here, K denotes the equilibrium ratio of sorbate in the gas phase to that in the crystal and $(Q_o)_g$, the amount of sorbate present initially in the gas phase.

1.2.3 Special Features of the $\sqrt{t}$ - Law

Apart from its simplicity, a very special feature of the $\sqrt{t}$ law [Eqns.(5) and (6)] is that it holds whatever the size and shape distribution, provided the time is small enough for each crystal to act as a semi-infinite medium. In this case, r in Eqns. (5) and (6) is replaced by 3V/A. Thus the $\sqrt{t}$ law for crystals of different sizes and shapes can be expressed [102] as,

$$\frac{Q_t - Q_o}{Q - Q_o} = \frac{2A}{V}\left[\frac{Dt}{\pi}\right]^{1/2} \qquad (7)$$

for sorption/desorption at constant pressure, and

$$\frac{Q_t - Q_o}{Q - Q_o} = \frac{2A}{V}\,\frac{1+K}{K}\left[\frac{Dt}{\pi}\right]^{1/2} \qquad (8)$$

for sorption/desorption at constant volume (Henry's law). Here A and V denote the external surface area and the volume of the zeolite crystal, respectively.

In case the sorption/desorption data cannot be collected in the initial short period, it is very essential to consider the shape and size distribution of the zeolite crystals for obtaining reliable values of diffusion coefficients [112,113].

Doelle and Riekert [114] have studied the kinetics of sorption and desorption, respectively, of n-butane in zeolite X and of CO_2 in zeolite A and observed that only the initial rates of uptake or release of the sorbate are controlled by mass transfer alone, whereas, ultimately they also depend on the rate of heat transfer from the sorbent to its surroundings or vice versa. Thus the effect of heat transfer can be neglected if the experimental data pertains to the very short initial period of sorption or desorption.

The effects of heat transfer and temperature changes during sorption/desorption has been considered by Kondis and Dranoff [115-117], Eagan et al. [118] and Ruthven [105]. The possibility of the sorption/desorption rates being controlled by various mass transfer processes occurring in series (intercrystalline diffusion, transfer through skin on crystal surface and intracrystalline diffusion) has been discussed by Barrer [103].

Intracrystalline diffusion coefficients for sorption and desorption of n-butane in NaX found to be independent of the direction of flux [119]. However, in case of shape-selective zeolite like ZSM-5 (a medium pore zeolite), the diffusion coefficients for bulkier sorbate molecule, obtained from its sorption and desorption measurements may differ from each other [120]. This is expected because of the fact that the rate of sorption of bulkier sorbate in the medium pore zeolite is expected to be controlled by the entrance of the sorbate molecule into the zeolite channel or by the configurational diffusion of the molecule inside the channels or by the

combination of both the intracrystalline mass transfer resistances. Whereas, since in the desorption, the sorbed molecules (which are already in their favourable conformation in the channels are coming out through the channel openings, the rate of desorption is expected to be controlled only by the configurational diffusion of the molecule in the zeolite channels.

1.3 DIFFUSION IN ZSM-5 AND ZSM-8 ZEOLITES

The ZSM-5 framework (Fig. 1.2) contains two types of intersecting channels made up of 10-membered rings, the channel diameter being intermediate between those of classical shape-selective zeolites (erionite, offretite, etc.) and of large pore zeolites (faujasite, X, Y, etc.). Hence, rather than the molecular screening, which is observed in classical shape-selective zeolites, the slightly higher channel diameter of ZSM-5 imposes some configurational restrictions [121], that is, there is a continuous matching of size and shape of the diffusing species and the host channels.

A summary of sorption and diffusion of various sorbates in ZSM-5 type and other pentasil (viz. ZSM-8, ZSM-11) zeolites is presented in Table-1.3.

Diffusion in ZSM-5 type zeolites depends very strongly on the critical size/or the configuration of sorbate molecules [122,125-130]. In case of sorbates diffusing freely in the zeolite channels, the diffusion depends on the length and polarity of the sorbate molecules [129,130]. The diffusion in ZSM-5 is also strongly influenced by zeolite factors [viz. Si/Al ratio, nature of cation and its degree of exchange, calcination temperature and pretreatment given to the zeolite before its use, poisoning and addition or introduction of foreign substance(s) in the zeolite channels], which affect the effective channel diameter and/or chemical environment of diffusing species in the zeolite channels [123,124,127].

In general, diffusion in ZSM-5 is highly activated one (i.e. highly temperature dependent) [120,121,127-131]. The diffusion of benzene in H.Na.ZSM-5 zeolites has

TABLE-1.3

Summary of the studies on diffusion of various sorbates in pentasil zeolites

S.No.	Sorbate/ diffusing species	Zeolite	Zeolite properties			Temp. (K)	Method used	Ref.
			Si/Al	Degree of cation exchange	Crystal size (um)			
1	2	3	4	5	6	7	8	9
1.	n-Hexane, cyclo-hexane, B,EB,o-, m- and p-X	Silicalite-I	-	-	2	293-473	Gravimetric-sorption (constant volume - constant pressure)	Wu et al. (122)
2.	n-Hexane, DME & B	H-ZSM-5	17.5	-	14 ± 2	293-333	Gravimetric-sorption (constant volume, variable pressure)	Heering et al. (132)
3.	DME, B & m-X	H-ZSM-5	17-65	-	0.5-14	293-313	-do-	Doelle et al. (133)
4.	B, T & p-X	H-ZSM-5	22-50	-	0.5-1	298	-do-	Nayak and Riekert (123)
5.	Ethane & propane	Silicalite-I	-	-	19.7±1.35	298-338	NMR (frequency response)	Bulow et al. (134)
	Propane	H.Na-ZSM-5	135	-	24.6±2.6	298-338	Gravimetric-sorption (constant volume-variable pressure)	-do-
6.	Methane,ethane & propane	Silicalite-I	12.30	-	19.7±1.35	296-338	NMR (pulse gradient technique)	Caro et al. (135)

1	2	3	4	5	6	7	8	9
	Methane, propane	H.Na-ZSM-5	-	-	30	403	NMR (pulse gradient technique)	Caro et al. (135)
7.	Methane & propane	Silicalite-I	-	-	-	293-403	Gas chromatographic	Chiang et al. (136)
8.	Benzene	H-ZSM-5	22.0	99	1.46	523-673	Dynamic-sorption/ desorption	Choudhary & Srinivasan (19)(120a, 120b)
9.	Benzene	H-ZSM-5	13.6-39.7	H^+ (51-99)	0.8-6	523	-do-	Choudhary & Srinivasan (28) (124)
10.	1,3,5-TMB,, o- & m-X	H-ZSM-5 (extrudes)	38	-	-	303	Gravimetric-liquid sorption (specific gravity bottle method)	Choudhary & Singh (125)
11.	Olefins, iso-olefins, paraffins & iso-paraffins	ZSM-5	36	-	0.05-3.0	811	Reaction on zeolite of different crystal sizes	Hang et al. (30) (126)
12.	p- & m- xylenes	H-ZSM-5	43-46	-	10	313	Gravimetric-sorption (at constant pressure)	Mao et al. (31) (137)
13.	o- and m-X & 1,3,5-TMB	ZSM-5	-	-	-	623	Sorption	Gorring (32a)(127); Olson et al. (128)

1	2	3	4	5	6	7	8	9
14.	n-Hexane, MeOH 1,2,4-TMB, p- , m- or o-X	Silicalite - I or II	-	-	7	303	Gravimetric-sorption (constant volume - constant pressure)	Ma et al. (138)
15.	2,2-Dimethyl butane	H-ZSM-5	17-100	-	0.1-5	373-563	Gravimetric-sorption (constant volume - variable pressure) and GC techniques	Post et al. (127)
16.	n- and Iso-butane	Silicalite-I	-	-	200	297-334	Single crystal zeolite membrane system (pressure difference measurement across the membrane)	Parvar and Hayhurst (139)
17.	Water, MeOH, butane and butene	Silicalite-I	-	-	10	360-420	NMR (pulse gradient technique)	Lechert et al. (128)
	-do-	H or Na-ZSM-5	29-84	-	25	166-500	-do-	-do-
18.	MeOH, DME, n-hexane, B, p-X	Silicalite-I	-	-	2	303	Gravimetric-sorption (constant volume - constant pressure)	Wu and Ma (140)
	-do-	H,Li,Na,K,Rb or C_s-ZSM-5	16	-	2	303	-do-	-do-
19.	Xylenes	H-ZSM-5	43.0	-	8-10	313 K	Gravimetric-sorption (at constant pressure)	Ragaini, et al. (129)
20.	Aromatics	ZSM-5	-	-	1-7.5	613-713 K	GC pulse method	Forni and Viscardi (130)

.....

1	2	3	4	5	6	7	8	9
21.	n-Hexane, iso-octane, n-C_{2-8} alcohols and butanol isomers, n-butylamine	H-ZSM-5	39.7	99	0.8,6	273-353	Volumetric (liquid sorption)	Choudhary & Nayak (131)
22.	Cyclic compounds [cyclohexane, B,T, p-, o-X, EB, n-PB, iso-PB, aniline and pyridine]	H-ZSM-5	17.2-39.7	99	0.8, 6	273-353	Volumetric (liquid sorption)	Choudhary & Nayak (141)
23.	n-Hexane and benzene	H-ZSM-5, H-offetite	-	-	-	273 K	Gravimetric sorption (constant volume - constant pressure)	Cointot et al. (142)
24.	Cyclohexane	H-ZSM-5 H-ZSM-8	-	-	-	386 K	-	Chon et al. (143)
25.	Methane and propane	Pentasil zeolites	-	-	-	-	NMR technique	Kaerger, et al. (144)
26.	Aromatics (single and multi component diffusion)	H-ZSM-5	45.4	0.97	3.0	288-320	Sorption from iso-octane solution	Choudhary et al. (145)
27.	Cumene	H-ZSM-5 H-ZSM-5(poisoned) H.Na-ZSM-5	31.1 31.1 31.1	99 99 45	2.1 2.1 2.1	283-323	Volumetric (liquid sorption)	Present work
28.	Cumene	H-ZSM-8 and MgO, B_2O_3 and P_2O_5 modified H-ZSM-8	29.7	8-96	4.0	283-323	-do-	-do-

also been found to be highly concentration dependent [120,124].

1.4 OBJECTIVES AND SCOPE OF PRESENT INVESTIGATION

Intracrystalline diffusion plays a vital role in ZSM-5 zeolites in deciding the product distribution in catalytic processes via diffusion-reaction interactions [146] and also in adsorption separation processes involving kinetically controlled adsorption [147]. The understanding of diffusion in these zeolites and also the factors affecting the diffusion is of great interest.

Diffusion in ZSM-5 Zeolites

Most of the previous studies on diffusion in ZSM-5 zeolites (Table-1.3) have been carried out using gaseous sorbate species. Only a few studies [125,131,141,145] on diffusion/sorption in ZSM-5 zeolites from pure liquids or solutions have been carried out. For using these zeolites in adsorption-separation processes in which adsorption occurs from liquid phase it is desirable to investigate sorption/diffusion in the zeolites from liquid phase.

In the present investigation sorption/diffusion of pure liquid in ZSM-5 (at 288-328 K) using cumene (which has an intermediate diffusivity in the zeolite) as a model sorbate has been investigated. Influence of type and/or degree of cation exchange, calcination temperature and presence of foreign compound (or poison viz. pyridine) in the zeolite channels on the diffusion has been studied. The sorption kinetic data at 288-328 K were obtained using a novel volumetric apparatus which is similar in principle to that used earlier by Satterfield and Cheng [148] but less cumbersome and very easy to operate.

Diffusion and Reaction in H-ZSM-8 and MgO, P_2O_5 and B_2O_3 Modified H-ZSM-8 Zeilites

The literature search on the diffusion and the reaction in the modified pentasil zeolites (which is summarised in Table-1.1) shows that extensive studies have

been reported on modified ZSM-5 zeolites. However, such studies on H-ZSM-8 and modified ZSM-8 zeolites are very scarce.

The present investigation on H-ZSM-8 and modified H-ZSM-8 zeolites was undertaken with following objectives:

1. To study the acidity distribution on the MgO, P_2O_5 and B_2O_3 modified H-ZSM-8 zeolites at close to catalytic reaction conditions using the gas chromatographic chemisorption [149] and stepwise thermal desorption (STD) of pyridine [150].

2. To study product distribution in the cumene cracking, o- and m- xylene isomerisation, and alcohol (methanol and ethanol) - to - aromatic conversion reactions on the modified H-ZSM-8 zeolites.

3. To study sorption/diffusion of pure cumene from liquid phase in the modified zeolites using a novel volumetric apparatus.

REFERENCES

1. Arganer, R.J., and Landolt, G.R., US Patent, 3, 702, 886 (1972).

2. Scott, J. (Ed.), 'Zeolite Technology and Applications - Recent Advances', Noyes Data Corp., NJ, 1980.

3. Chang, C.D., Catal. Rev. Sci. Eng., 25, 1 (1983).

4. Chang, C.D., Catal. Rev. Sci. Eng., 26, 323 (1984).

5. Chemistry in New Zealand, Vol. 50, No. 1, Feb. 1986.

6. Kaeding, W.W., Barile, G.C., and Wu, M.M., Catal. Rev. Sci. Eng., 26, 597 (1984).

7. Mobil Oil Corp., Netherlands Patent, 7, 014, 807 (1971).

8. Kokotailo, G.T., Lawton, S.L., Olson, D.H., and Meier, W.M., Nature, 272, 437 (1978).

9. Meier, W.M., and Olson, D.H., 'Atlas of Zeolite Structure Types', Structure Commission of the International Zeolite Association, Zurich (1978).

10. Dejaifve, P., Auroux, A., Gravelle, P.C., and Derouane, E.G., Stud. Surf. Sci. Catal., 5, 29 (1980).

11. Dejaifve, P., Vedrine, J.C., Bolis, V., and Derouane, E.G., J. Catal., 63, 331 (1980).

12. Kokotailo, G.T., Lawton, S.L., Chu, P., and Meier, W.M., Nature, 275, 119 (1978).

13. Wu, E.L., Lawton, S.L., Olson, D.H., Rohrmann, A.C., Jr., and Kokotailo, G.T., J. Phys. Chem., 83, 2777 (1979).

14. Wang, I., Chen, T.J., Chao, K.J., and Tasai, T.C., J. Catal., 60, 140 (1979).

15. Nayak, V.S., and Choudhary, V.R., J. Catal., 81, 26 (1983).

16. Nayak, V.S., and Choudhary, V.R., Appl. Catal., 10, 137 (1984).

17. Meisel, S., McCullough, J.P., Lechthaler, C.H., and Weisz, P.B., Chem. Tech., 6, 86 (1976).

.....

18. Derouane, E.G., and Vedrine, J.C., J. Mol. Catal., 8, 479 (1980).

19. Derouane, E.G., Dejaifve, P., Gabelica, Z., and Vedrine, J.C., Disc. Faraday Soc., 72, 331 (1981).

20. Kaeding, W.W., and Butter, S.A., J. Catal., 61, 155 (1980).

21. Kaeding, W.W., Chu, C., Young, L.B., Weinstein, B., and Butter, S.A., J. Catal., 67, 159 (1981).

22. Chen, N.Y., Kaeding, W.W., and Dwyer, F.G., J. Am. Chem. Soc., 101, 6783 (1979).

23. Kaeding, W.W., and Butter, S.A., US Patent, 3, 911, 041 (1975).

24. Kaeding, W.W., US Patent, 4, 067, 920 (1978).

25. Kaeding, W.W., and Young, L.B., US Patent, 4, 034, 053 (1977).

26. Kaeding, W.W., Chu, C., Young, L.B., and Butter, S.A., J. Catal., 69, 392 (1981).

27. Weisz, P.B., Pure and Appl. Chem., 52, 2091 (1980).

28. Derouane, E.G., and Gabelica, Z., J. Catal., 65, 486 (1980).

29. Derouane, E.G., Gabelica, Z., and Jacobs, P.A., J. Catal., 70, (1981).

30. Chen, N.Y., and Garwood, W.E., J. Catal., 52, 453 (1978).

31. Namba, S., Yoshimura, A., and Yashima, T., Chem. Lett., 759 (1979).

32. Dejaifve, P., Auroux, A., Gravelle, P.C., Vedrine, J.C., Gabelica, Z., and Derouane, E.G., J. Catal., 70, 123 (1981).

33(a) Csicsery, S.M., Zeolites, 4, 202 (1984).

33(b) Weisz, P.B., Stud. Surf. Sci. Catal., 7A, 3 (1981).

34. Chen, N.Y., and Garwood, W.E., Catal. Rev. Sci. Eng., 28, 185 (1986).

35. Maxwell, I.E., J. Inc. Phenomen., 4, 1 (1986).

36. Derouane, E.G., Catalysis on the Energy Scene, Eds. Kaliaguine, S., and Mahay, A., Elsevier Sci. Publ. B.V., Amsterdam, p. 1 (1984).

.....

37. Jacobs, P.A., Uytterhoeven, J.B., Steyns, M., Froment, G., and Weitkamp, J., 'Proc. 5th Int. Conf. Zeolites', Naples, Ed. Rees, L.V.C., Heydon, London, p. 607 (1980).

38. Topsoe, N.Y., Pederson, K., and Derouane, E.G., J. Catal., 70, 41 (1981).

39. Babu, G.P., Hegde, S.G., Kulkarni, S.B., and Ratnasamy, P., J. Catal., 81, 471 (1983).

40. Anderson, J.R., Foger, K., Mole, T., Rajadhyaksha, R.A., and Sanders, J.V., J. Catal., 58, 114 (1979).

41. Choudhary, V.R. and Nayak, V.S., Materials Chem. Phys., 11, 515 (1984).

42. Choudhary, V.R., and Nayak, V.S., Zeolites, 5, 15 (1985).

43. Choudhary, V.R., and Pataskar, S.G., Zeolites, 6, 307 (1986).

44. Auroux, A., Wierzchowski, P., and Gravelle, P.C., Thermochimica Acta, 32, 165 (1979).

45. Auroux, A., Bolis, V., Wierzchowski, P., Gravelle, P.C., and Vedrine, J.C., J. Chem. Soc., Faraday Trans. II, 75, 2544 (1979).

46. Vedrine, J.C., Auroux, A., Bolis, V., Dejaifve, P., Naccache, C., Wierzchowski, P., Derouane, E.G., Nagy, J.B., Gilson, J.P., van Hooff, J.H.C., van den Berg, J.P., and Wolthuizen, J., J. Catal., 59, 248 (1979).

47. Auroux, A., Gravelle, P.C., and Vedrine, J.C., 'Proc. 5th Int. Conf. Zeolites', Naples, Ed. Rees, L.V.C., Heydon, London, p. 433 (1980).

48. Choudhary, V.R., and Singh, A.P., J. Catal., 94, 573 (1985).

49. Choudhary, V.R., and Nayak, V.S., Zeolites, 5, 325 (1985).

50. Nayak, V.S., and Choudhary, V.R., Appl. Catal., 9, 251 (1984).

51. Nayak, V.S., and Choudhary, V.R., Appl. Catal., 4, 333 (1982).

52. Nayak, V.S., and Choudhary, V.R., Indian J. Technol., 21, 376 (1983).

53. Choudhary, V.R., and Nayak, V.S., Acta Phys. Chem., 31, 167 (1985).

54. Haag, W.O., Lago, R.M., and Weisz, P.B., Nature, 309, 589 (1984).

.....

55. *Weisz, P.B., I&EC Fundament., 25, 53 (1986).*

56. *Lago, R.M., Haag, W.O., Mikovsky, R.J., Olson, D.H., Hellring, S.D., Schmitt, K.D., and Kerr, G.T., Proc. 7th Int. Zeolite Conf., Tokyo, Eds. Murakami, Y., Iijima, A., and Ward, J.W., p. 677 (1986).*

57. *Olson, D.H., Haag, W.O., and Lago, R.M., J. Catal., 61, 390 (1980).*

58. *Haag, W.O., 'Proc. 6th Int. Zeolite Conf.', Reno, USA, Ed. Olson, D.H., and Bisio, A., p. 466 (1984).*

59. *Chen, N.Y., and Reagan, W.J., J. Catal., 59, 123 (1979).*

60. *Chu, C.T-W., Kuehl, G.H., Lago, R.M., and Chang, C.D., J. Catal., 93, 451 (1985).*

61. *Mobil Oil Corp., Netherlands Patent, 7, 014, 807 (1971).*

62. *Breck, D.W., 'Zeolite Molecular Sieve', Willey and Sons, New York (1974).*

63. *Lechert, H., NATO ASI Ser., Ser. E80, 151 (1984).*

64. *Vybihal, J., Czechoslovakian CS 211, 981 (Cl. C018 33/28), 29 Jul. 1983, Appl. 80/7, 602, 4 (1980).*

65. *Chen, N.Y., Lucki, S.J., and Garwood, W.E., US Patent, 3, 700, 585 (1972).*

66. *Park, S., and Chou, H., Chem. Eng. Commun. 34, 137 (1985).*

67. *Chou, H., Ahn, B.J., and Park, S.E., 'Proc. 8th Int. Congr. Catal., 1984', Vol. 4, IV, 555, Verlag Chemie, Weinheim, 1985.*

68. *Akolekar, D.B., and Choudhary, V.R., J. Catal., 105, 416 (1987).*

69. *Kaeding, W.W., Chu, C., Young, L.B., Weinslein, B., Butter, S.A., J. Catal. 67, 159 (1981).*

70. *Kaeding, W.W., Chu, C., Young, L.B., Weinstein, B., Butter, S.A., J. Appl. Polym. Sci., Appl. Polym. Symp., 36, 209 (1981).*

71. *Nadirov, N.K., Serikov, T.P., Postnov., V.V., Lykova, L.F., (USSR), Primenenic Tscolitov V. Katalize, Z-Ya Uses Konf., 89 (1981).*

72. *Iwayama, K., and Inoue, T., Eur. Pat. Appl. EP 42, 754, 30 Dec. (1981).*

.....

73. Vedrine, J.C., Auroux, A., Dejaifve, P., Ducarme, V., Hoser, H., Zhou, S., J. Catal., 73, 147 (1982).

74. Kaeding, W.W., US Patent 4, 365, 104 (21 Dec. 1982).

75. Young, Z.B., US Patent 4, 356, 338 (26 Dec. 1982).

76. Gabelica, Z., Debras, G., Gilson, J.P., Derouane, E.G., Calorim. Anal. Therm. 14, 371 (1983).

77. Chu, C.C., US Patent 4, 384, 155 (17 May 1983).

78. Cai, G., Xin, Q., Wang, X., Wang, Q., Wang, Z., Li, S., Chen, G., Cuihua Xuebao, 6(1), 50 (1985).

79. Zatroski, L.W., Wierzchowski, P.T., Przem. Chem., 63(5), 242 (1984).

80. Zatroski, L.W., Wierzchowski, P.T., Cichowlas, A.A., Bull. Pol. Acād. Sci. Chem., 32(3-6), 217 (1984).

81. Teijin Petrochemical Industries Ltd., Jpn. Kokai Tokkyo Koho JP 6067, 437 [8567, 437] (17 Apr. 1985).

82. Auroux, A., Sayed, M.B., Vedrine, J.C., Thermochim. Acta, 93, 557 (1985).

83. Lercher, J.A., Rumplmayr, G., Noiler, H., Acta Phys. Chem., 31, 71 (1985).

84. Derewinski, M., Haber, J., Pataszynski, J., Shiralkar, V.P., Dzwigaj, S., Stud. Surf. Sci. Catal., 18, 209 (1984).

85. Lercher, J.A., and Rumplmayr, G., Appl. Catal., 25, 215 (1986).

86. Kaeding, W.W., J. Catal., 95, 512 (1985).

87. Rodewald, P.G., US Patent 4, 567, 310 (28 Jan. 1986).

88. Huang, T., Dai, S., Huang, J., Wang, G., Xiamen Daxue Xuebao Ziran Kexueban, 24(2), 218 (1985).

89. Sayed, M.B., Auroux, A., Vedrine, J.C., Appl. Catal. 23(1), 49, (1 9 8 6) .

90. Nefedov, B.K., Chukin, G.D., Lupina, M.I., Polinnia, E.V., Khushid, B.L., Morgachena, N. Yu., Kukushkin, V.B., Agievskii, D.A., Nefdekhimiya, 26 (1), 16 (1986).

.....

91. Gulf Research and Development Co. Neth. Appl. NL 8402085 (16 Jan. 1986).

92. Chu, C.C., (Mobil Oil Corp.), US Patent 4, 590, 321 (20 May 1986).

93. Chu, C.C., (Mobil Oil Corp.), US Patent 4, 590, 323 (20 May 1986).

94. Chon, H., Ahu, B.J., Park, S.E., Intl. Congr. Catal. (Proc.), 8th, 4, IV-555, (1984).

95. Wu, C., Qin, G., Xie, Y., Stud. Surf. Sci. Catal. 28, 481 (1986).

96. Hoelderich, W., Stud. Surf. Sci. Catal., 28, 827 (1986).

97. Chen, L., Sun, D., Wang, J., Wang, X., Dalian Gongxueyuan Xuebao, 25(3), 33 (1986).

98. Sayed, M.B., Vedrine, J.C., J. Catal., 101(1), 43 (1986).

99. Chukin, G.D., Nefedov, B.K., Surin, S.A., Polinina, E.V., Khusid, B.L., Sidelkovskaya, V.G., Kinet. Katal., 26(5), 1262 (1985).

100(a) Auroux, A., Sayed, M.B., Vedrine, J.C., Thermochim. Acta, 93, 557 (1985).

100(b) Musa, M., Goidea, D., Blum, J., Mihaikscu, M., Goidea, N., Georghe, G., Russu, R., Manoiu, D., Stud. Surf. Sci. Catal. 23, 205 (1985).

101. Weisz, P.B., Chemtech., P 498 (1973).

102. Barrer, R.M., Adv. Chem. Ser., 102, 21 (1971).

103. Barrer, R.M., 'Properties and Application of Zeolites', Chemical Society, London, p. 3 (1980).

104. Ruthven, D.M., Proc. 4th Int. Conf. Zeolites, Chicago, Ed., Katzu, J.R., ACS Sym. Ser., 40, 320 (1977).

105. Ruthven, D.M., 'Properties and Application of Zeolites', Chemical Society, London, p. 43 (1980).

106. Riekert, L., Adv. Catal., 21, 281 (1970).

107. Eberly Jr., P.E., 'Zeolite Chemistry and Catalysis', Ed. Raba, J.A., ACS Monograph, 171, 392 (1976).

108. Breck, D.W., Zeolite Molecular Sieves, John Wiley and Sons, New York, p. 671 (1974).

.....

109. Walker, Jr., P.L., Austin, G.L., and Nandi, S.P., Chem. Phys. Carbon, 2, 257 (1966).

110. Palekar, M.G., and Rajadhyaksha, R.A., Catal. Rev.-Sci. Eng., 28, 371 (1986).

111. Crank, J., 'The Mathematics of Diffusion, Clarendon Press, Oxford, 1956.

112. Loughlin, K.F., Derrah, R.I., and Ruthven, D.M., Can. J. Chem. Eng., 49, 66 (1971).

113. Ruthven, D.M., and Loughlin, K.F., 'Adsorption Technology', AIChE Symp. Ser., (No. 117), 67, 35 (1971).

114. Doelle, H.J., and Riekert, L., Angew. Chem. Int., Ed. Engi., 18, 266 (1979).

115. Kondis, E.F., and Dranoff, J.S., Ind. Eng. Chem. Proc. Des. Dev., 10, 108 (1971).

116. Kondis, E.F., and Dranoff, J.S., 'Adsorption Technology', AIChE Symp. Ser., 67, 25 (1971).

117. Kondis, E.F., and Dranoff, J.S., Adv. Chem. Ser., 102, 171 (1971).

118. Eagan, J.D., Kindi, B., and Anderson, R.B., Adv. Chem. Ser., 102, 164, (1971).

119. Doelle, H.J., and Riekert, L., ACS Symp. Ser., 40, 401 (1977).

120. Choudhary, V.R., and Srinivasan, K.R., J. Catal., 102, 316 (1986).

121. Chen, N.Y., and Garwood, J. Catal., 52, 453 (1978).

122. Wu, P., Debebe, A., and Ma, Y.H., Zeolites, 3, 118 (1983).

123. Nayak, V.S., and Riekert, L., Int. Sym. Zeolite. Catal., May 13-16, 1985, Siofok (Hungary).

124. Choudhary, V.R., and Srinivasan, K.R., J. Catal., 102, 328 (1986).

125. Choudhary, V.R., and Singh, A.P., Zeolites, 6, 206 (1986).

126. Haag, W.O., Lago, R.M., and Weisz, P.B., Disc. Faraday Soc., 72, 317, (1982).

127. Gorring, R.L., Laboratory data [cited by Haag, W.O., Proc. 6th Intl. Zeolite Conf., Reno, Eds. Olson, D., and Bisio, A, Butterworths, Surrey, p. 466 (1983).

.....

128. Olson, D.H., Kokotailo, G.T., Lawton, S.L., and Meir, J., Phys. Chem., 85, 2283 (1981).

129. Raigini, V., Fois, R., Le van Mao, R., and Catharina, G.M., Can. J. Chem. Eng., 62, 706 (1984).

130. Forni, L., and Viscardi, C.F., J. Catal, 97, 480 (1986).

131. Choudhary, V.R., and Nayak, V.S., Chem. Eng. Sci. (communicated).

132. Heering, J., Koller, M., and Riekert, L., Chem. Eng. Sci., 37, 581 (1982).

133. Doelle, H.J., Heering, J., Riekert, L., and Marosi, L., J. Catal., 71, 27 (1981).

134. Bulow, M., Schlodder, H., Rees, L.V.C., and Richards, R.E., Proc. 7th Intl. Zeolites Conf., Tokyo Eds. Murakami, Y., Iijima, A., and Ward, J.W., p. 579 (1986).

135. Caro, J., Bulow, M., Karger, J., Heink, W., Sehirmer, W., Pfeifer, H., and Zolamov, S.P., J.C.S. Faraday I, 81, 2541 (1985).

136. Chiang, A.S., Dixon, A.G., and Ma, Y.H., Chem. Eng. Sci. 39, 1461 (1984).

137. Lo van Mao, R., Ragani, V., Leofauts, G., and Fois, R., J. Catal., 81, 418 (1983).

138. Ma, Y.H., Tang, T.D., Sand, L.B., and Hou, L.Y., Proc. 7th Intl. Zeolites Conf. Tokyo Eds. Murakami, Y., Iijima, A., and Ward, I.W., p. 531 (1986).

139. Paravar, A., and Hayhurst, D.T., Proc. 6th Intl. Zeolite Conf. Reno, July, 10-15, 1983, Eds. Ololon, H., and Bisio, A., Butterworths.

140. Wu, P., and Ma, Y.H., Proc. 6th Intl. Zeolite Conf., Reno, Eds. Olson, D., and Bisio, A., Butterworths, p. 251 (1983).

141. Choudhary, V.R., and Nayak, V.S., Chem. Eng. Sci. (communicated).

142. Cointot, A., Joly, G., J. Chem. Phys. Phys-Chim. Bio., 81 (5), 317 (1984).

143. Chou, H., Ahri, B.J., Park, S.E., Int. Congr. Catal. [Proc], 8th 4, IV-555, (1984).

144. Kaerger, J., Pfeifer, H., Frende, D., Caro, J., Buclow, M., Oehlmann, G., Stud. Surf. Sci. Catal. 28, 633 (1986).

145. Choudhary, V.R., Akolekar, D.B., and Singh, A.P., Chem. Eng. Sci. (accepted).

.....

146. *Weisz, P.B., Pure Appl. Chem. 52, 2091 (1980).*

147. *Dessau, R.M., ACS Symp. Ser., Adsorption of ion exch. and synth. zeolites, 135, 123 (1980).*

148. *Satterfield, C.N., and Cheng, S., 'Adsorption Technology', AIChE Symp. Ser. (117), 67, 43 (1971).*

149. *Choudhary, V.R., Srinivasan, K.R., J. Catal., 102, 316 (1986).*

150. *Choudhary, V.R., J. Chromatogr. 268, 207 (1983).*

Chapter-2 : EXPERIMENTAL

2. EXPERIMENTAL

2.1 CHEMICALS AND GASES

The following gases and chemicals have been used.

Nitrogen (High purity, IOLAR-I, obtained from Indian Oxygen Limited, Bombay) passed over activated molecular sieves (3A) to remove traces of moisture.

Pyridine : GR (guaranteed reagent) grade, obtained from Sarabhai Chemicals, Baroda.

o-xylene (Puriss, Fluka)

m-xylene (Puriss, Fluka)

Cumene (AR, BDH)

Methanol (AR, BDH)

Ethanol (Puriss, Fluka)

Hydrochloric acid (GR, Sarabhai)

Sodium nitrate (AR, BDH)

Ammonium nitrate (GR, Sarabhai)

Phosphoric acid (AR, BDH)

Boric acid (AR grade)

Magnesium acetate (AR grade)

Fumed silica (high purity, low bulk density)

Sodium silicate (chemically pure)

Aluminium sulfate (AR, BDH)

Aluminium chloride (Sarabhai, GR)

Sodium hydroxide (Sarabhai, GR)

Sulfuric acid (Sarabhai, GR)

Tetraethylammonium bromide (TEABr) (Aldrich, Gold Label, 99 + %)

Tetrapropylammonium hydroxide (TPAOH) 20 wt % in water (Fluka, AG)

Water (distilled deionised)

2.2 ZSM-5 AND ZSM-8 ZEOLITES

ZSM-5 [1] and ZSM-8 zeolites have been synthesized by the hydrothermal procedure described in the original patents [1,2] with little modification.

2.2.1 Synthesis of TPA Na.ZSM-5

TPA-Na.ZSM-5 (Si/Al = 31.1) was synthesized by crystallizing it from a gel of composition, 1.0 Al_2O_3 - 75.0 SiO_2 - 1.6 Na_2O - 4.6 $(TPA)_2O$ - 460 H_2O. The gel was prepared as follows.

An aqueous solution of tetrapropylammonium hydroxide (TPA-OH) was added to fumed silica and heated to 373 K to form tetrapropylammonium silicate solution. To this was added a mixture of aqueous solutions of sodium hydroxide and aluminium chloride slowly with constant stirring The crystallization was carried out in a closed stainless steel pressure bomb (i.d.: 7.5 cm, capacity: 2 dm^3), installed in an uniform temperature air oven, at autogenous pressure. During the period of crystallization, the reaction mixture was shaken time-to-time by rocking the bomb in the air oven. After the crystallization, the reaction mixture was cooled to room temperature and the resultant zeolite crystals were filtered, washed thoroughly with distilled-deionised water and finally dried in an air oven at 393 K for 24 h.

2.2.2 Synthesis of TEA.Na-ZSM-8

TEA.Na-ZSM-8 (Si/Al = 29.6) zeolite was synthesized by hydrothermally treating a gel of composition 5.5 TEABr .15.8 Na_2O. 48.4 SiO_2 .1.0 Al_2O_3 . 2054 H_2O in a stirred stainless-steel autoclave (capacity 20 dm^3, stirring speed 70 rpm) at 453 K for 40 h at autogenous pressure (about 1250 kPa). The gel was prepared in the stirred autoclave by mixing thoroughly an alkaline solution of 4 kg of sodium silicate (containing Na_2O, 9.57%; SiO_2, 28.43%; and H_2O, 62.0%) and 0.45 kg of TEABr in 6 dm^3 of deionized water with an acidic solution of aluminium sulfate

(prepared by dissolving 0.13 kg of anhydrous aluminium sulfate and 0.7 kg of concentrated sulfuric acid in 6 dm^3 of deionized water). After the hydrothermal synthesis, the contents of the autoclave were cooled to room temperature. The crystals of zeolite were filtered, washed thoroughly with deionized water, and dried in an air oven at 393 K for 24 h.

2.2.3 Removal of Templating Agent from Zeolite Channels

The organic template occluded in the channels of the precursor crystals of the pentasil zeolites was removed by calcining the zeolites in air at 813 K for 12 h (the temperature was increased at a heating rate of about 10 $K.min^{-1}$).

2.2.4 Preparation of H-ZSM-5 and H.Na-ZSM-5

H-ZSM-5 : In order to obtain the ZSM-5 in its NH_4-exchanged form, the calcined ZSM-5 zeolite was contacted with 1 M NH_4NO_3 solution (25 cm^3 per gram of the zeolite) at 353 K eight times. The slurry was continuously stirred during the contacting. The first exchange of the ZSM-5 was for 2 h each and next three exchanges were of four h each. After the exchange, the zeolite was thoroughly washed with deionised distilled water, and dried at 393 K in air for 4 h. The NH_4-ZSM-5 zeolite was converted to its protonated form [i.e. H-ZSM-5] by deammoniating it at 773 K for 12 h in air.

H.Na-ZSM-5 : H.Na-ZSM-5 (degree of H^+ exchange = 0.45) was prepared by exchanging the H-ZSM-5 with 1 M $NaNO_3$ solution at 353 K eight times. The first fine exchanges were for 2 h each and next three exchanges were for 4 h each. After the exchange, the zeolite was washed with deionised water, dried at 393 K for 4 h and calcined in air 773 K for 12 h.

2.2.5 Preparation of H-ZSM-8 and H.Na-ZSM-8 Zeolites

H-ZSM-8 : H-ZSM-8 (degree of H^+ exchange = 0.96) was prepared by repeatedly

(eight times) exchanging the calcined zeolite with 0.1 M HCl at 353 K. After the exchange, the zeolite was washed with deionised water, dried in air at 393 K for 12 h and calcined in air at 773 K for 12 h.

H.Na-ZSM-8 : H.Na-ZSM-8 (degree of H^+ exchange = 0.08) was prepared by repeatedly exchanging the calcined ZSM-8 zeolite with 1 M $NaNO_3$ at 353 K. The exchanged zeolite was washed with deionised water, dried at 393 K for 4 h and calcined in air at 773 K for 12 h.

2.2.6 Preparation of Magnesium-, Phosphorous-,and Boron-Modified H-ZSM-8 Zeolites

MgO.H-ZSM-8 : It was prepared by contacting the H-ZSM-8 zeolite (7.1 g) with 25 cm^3 of aqueous magnesium acetate (10%) solution at room temperature for two weeks, while shaking the flask containing the zeolite and the solution occasionally. The zeolite was then filtered using Gooch crucible and washed quickly with about 10 cm^3 of deionised water to remove the magnesium acetate impregnated on the external surface of the zeolite crystals. The zeolite was then dried in vacuum oven at 373 K for 12 h and calcined in air 773 K for 12 h.

P_2O_5.H-ZSM-8 : It was obtained by treating the H-ZSM-8 zeolite (10 g) with 100 cm^3 of 50% ortho phospheric acid solution at room temperature for two weeks by following a procedure similar to that described above for the preparation of MgO.H-ZSM-8 zeolite.

B_2O_3.H-ZSM-8 : It was prepared by contacting the H-ZSM-8 zeolite (7.2 g) with about 25 cm^3 of a saturated aqueous solution of boric acid at room temperature for two weeks by following the procedure described above except that in this case the contacting solution was changed everyday.

All the zeolites (H-ZSM-5, H.Na-ZSM-5, H-ZSM-8, H.Na-ZSM-8 and modified H-ZSM-8) were pressed without any bender and crushed to the particles of about 0.2 mm size.

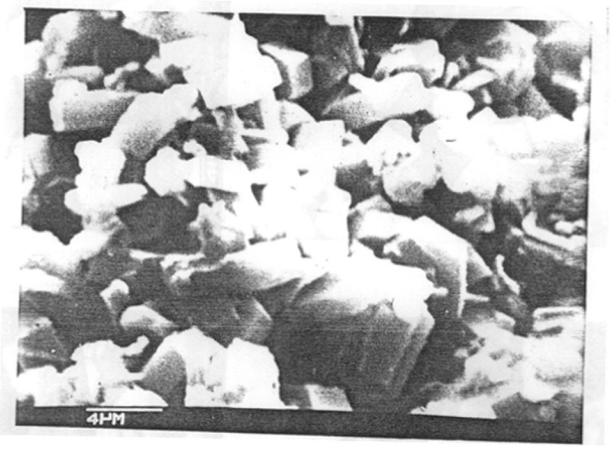

FIG. 2.1 : SCANNING ELECTRON MICROGRAPH OF H-ZSM-5 ZEOLITE

(a) H-ZSM-8

(b) MgO.H-ZSM-8

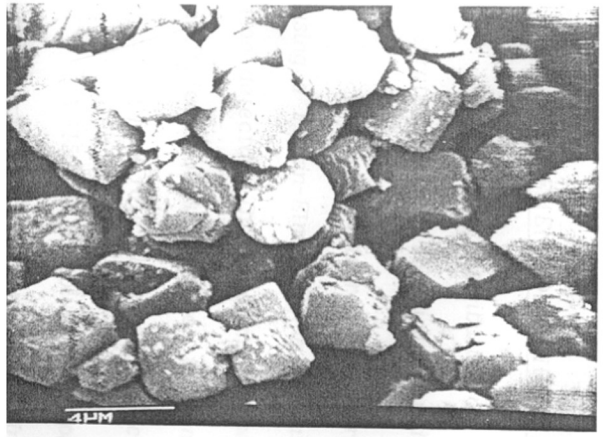

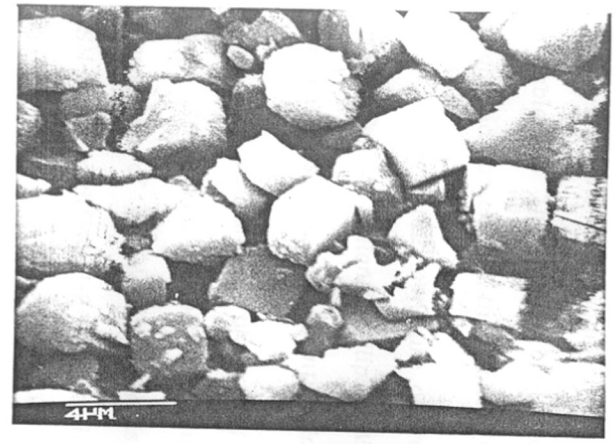

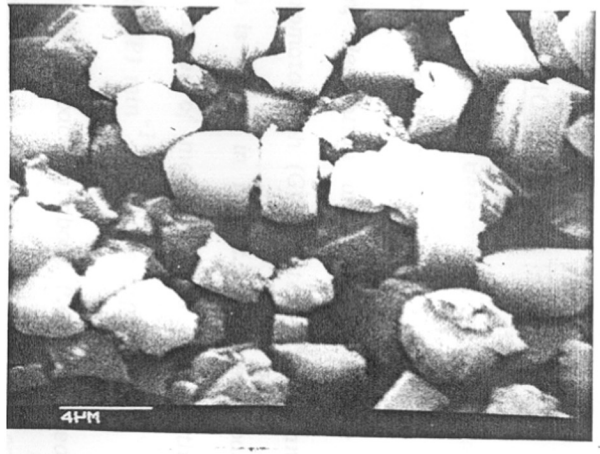

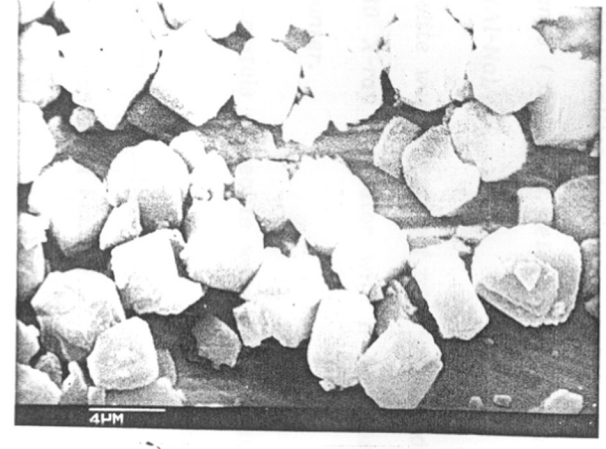

(c) P_2O_5.H-ZSM-8

(d) B_2O_3.H-ZSM-8

FIG. 2.2 : SCANNING ELECTRON MICROGRAPHS OF H-ZSM-8 AND Mg-, P-, AND B- MODIFIED H-ZSM-8 ZEOLITES

2.3 CHARACTERISATION OF ZEOLITES

The chemical compositions of the zeolites (calcined at 773 K) are given in Table-2.1. The degree of H^+ exchange (α) was determined by analyzing the Al and Na contents of the zeolite [α = (Al-Na)/Al].

The crystalline nature of the zeolite was determined by X-ray powder diffraction using a Holland Philips PW 1730 X-ray generator with a Ni-filtered Cu K rediation source and a scintillation counter.

The size and morphology of the crystals of zeolite were studied with a Cambridge Stereoscan model 150 scanning - electron microscope. A scanning electron micrograph of H-ZSM-5 zeolite is shown in Fig. 2.1. The SEM photographs of H-ZSM-8 and modified H-ZSM-8 zeolites are presented in Fig. 2.2.

Detailed characterization of the H-ZSM-5 and H-ZSM-8 zeolites have been given earlier [3,4].

2.4 MEASUREMENT OF ACIDITY DISTRIBUTION

The acidity distribution on the zeolites was determined by the gc adsorption/desorption methods [5,6] using pyridine as an acid probe.

Gas chromatographic adsorption, desorption and TPD data were collected using a Perkin-Elmer Sigma 3B gas chromatograph (GC), fitted with a flame-ionisation detector. The experimental set-up is shown in Fig. 2.3. Nitrogen, passed over activated molecules sieves to remove traces of moisture, was used as the carrier gas. The flow rate was about 10.0 cm^3 (NTP) min^{-1} in all the experiments.

A 15-cm gc column was prepared by packing about 0.42 g of zeolite in a stainless-steel tube (3 mm o.d.). In order to minimise the dead volume, one of the column was directly connected to the detector and the other end to the injector through a 50-cm stainless steel capillary (about 1.5 mm o.d. and 0.7 i.d.), which acted as a pre-heater. The catalyst was calcined in situ by heating it in a flow

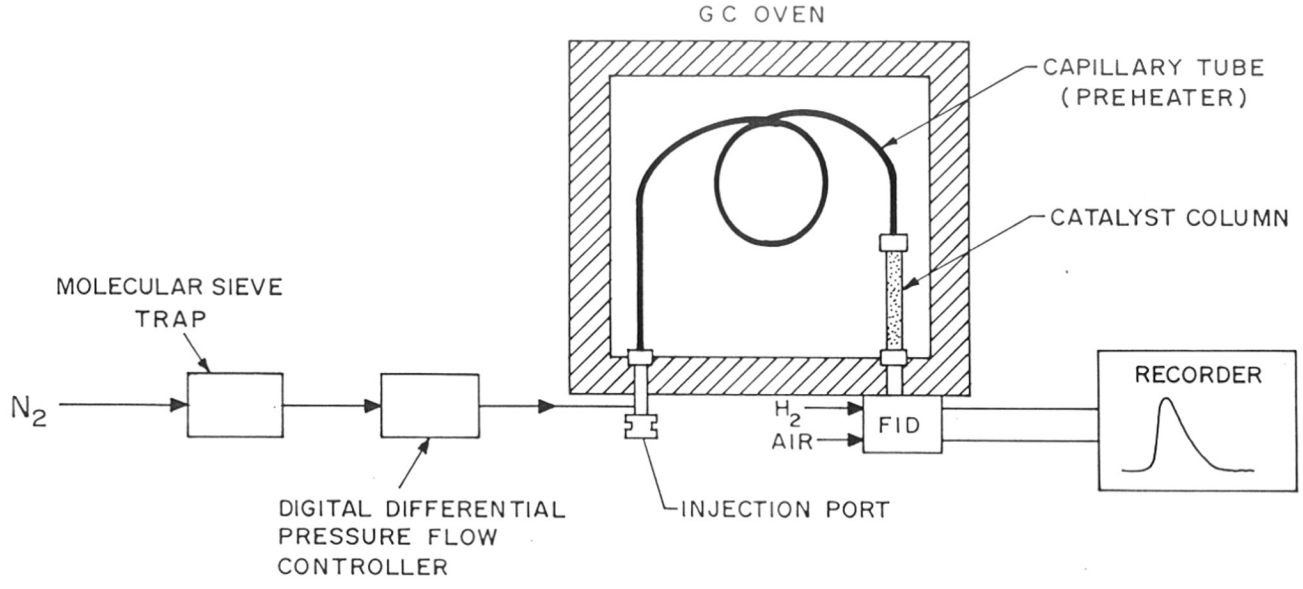

FIG. 2·3: EXPERIMENTAL ARRANGEMENT FOR ACIDITY MEASUREMENT

TABLE-2.1

Composition of ZSM-5 and ZSM-8 Zeolites

Zeolite	Si/Al	Degree of H^+ or NH_4^+ exchange (α)	Concentration (wt.%)		
			MgO	B_2O_3	P_2O_5
H-ZSM-5	31.1	0.99	-	-	-
Na.H-ZSM-5	31.1	0.45	-	-	-
NH_4.H-ZSM-5	31.1	0.99	-	-	-
H-ZSM-8	28.0	0.96	-	-	-
P_2O_5.H-ZSM-8	28.0	0.96	-	-	0.41
MgO.H-ZSM-8	28.0	0.96	0.10	-	-
B_2O_3.H-ZSM-8	28.0	0.96	-	5.4	-

of helium from 353 to 673 K at a linear heating rate of 10 $K.min^{-1}$ and further at 673 K for 2 h.

2.4.1 Measurement of Irreversible Sorption of Pyridine

The irreversible sorption (or chemisorption) of pyridine in the zeolites was measured by the gc pulse method [5] based on TPD under chromatographic conditions.

The initial temperature chosen for the TPD was 353 K. After calcination of the catalyst, the GC oven temperature was decreased to 353 K and a known amount of pyridine was injected into the zeolite column. After allowing 1 min for the redistribution of the sorbed species in the column, the TPD was started at a linear heating rate of 10 $K.min^{-1}$ in the flow of nitrogen. The final temperature chosen for the TPD (or the temperature at which the irreversible sorption of the sorbate was to be measured) was 673 K. After the final temperature was reached, the desorption of the reversibly sorbed species was allowed to continue for a further period of 60 min isothermally at that temperature. At the end of the TPD the zeolite retained only the sorbate irreversibly sorbed at 673 K.

After recording the first TPD chromatogram, the GC oven temperature was reduced to 353 K and the procedure was repeated to obtain the second TPD chromatogram by injecting the same amount of the sorbate.

The amount of pyridine irreversibly sorbed (q_i) was calculated from the expression:

$$q_i = [A^* / S] / M \qquad (1)$$

where, A^* is the difference between the areas of the two chromatograms obtained by the superimposition of the two chromatograms and cutting and weighing; S, the detector sensitivity; and M, the mass of the zeolite.

The irreversible sorption (or chemisorption) in the present study is defined as the amount of sorbate retained by the presaturated zeolite after it was swept with pure nitrogen for a period of 60 min.

2.4.2 Measurement of Stepwise Thermal Desorption (STD) of Pyridine

After calcination, the zeolite was saturated with pyridine at 373 K and the reversibly sorbed pyridine at this temperature was desorbed in the flow of helium. The species sorbed irreversibly at 473 K was thermally desorbed in the flow of nitrogen by heating the zeolite from 473 K to 673 K in a number of steps. The temperature in each step was raised at a linear rate of 10 $K.min^{-1}$. After the maximum temperature of a step was reached, it was maintained for a period of 60 min to desorb the pyridine reversibly sorbed in the zeolite at that temperature. The sorbate desorbed in each step was measured quantitatively by the detector. The amount of sorbate desorbed (q_d) in a step due to increase in the temperature from T_1 to T_2 is given by the expression,

$$[q_d]_{T_1}^{T_2} = A_d / [S.M] \qquad (2)$$

where A_d is the area under the desorption chromatogram.

The amount of pyridine irreversibly sorbed (or chemisorbed) at different temperatures $[q_{i(T)}]$ was calculated from the STD data as follows:

$$q_{i(T)} = q_{i(673K)} + [q_d]_T^{673} \qquad (3)$$

The amount of pyridine irreversibly sorbed at 673 K $[q_{i(673K)}]$ was determined as discussed in the earlier section.

2.5 MEASUREMENT OF CATALYTIC ACTIVITY

The microreactor was made of stainless steel and consisted of a tube [o.d. : 6 mm; i.d. : 4 mm; and length : 22 cm] with the catalyst held between quartz wool plugs, and an injection port. The temperature of the catalyst (measured by a thermocouple kept in the catalyst bed) and that of the injection port could be varied independently. A part of the reactor effluents could be bypassed with the help of needle valve before allowing the effluent to enter the analytical column. The microreactor assembly is shown in Fig. 2.4. The microreactor is connected to the gas chromatograph (Perkin-Elmer Sigma 3B with flame ionization detector).

The catalyst in the microreactor was heated at 673 K in the flow of nitrogen for 1 h. The activity of the catalyst was determined by injecting a known amount of reactant into the microreactor at the desired reaction conditions and analysing the reaction products with the gas chromatograph (provided with flame ionization detector and calculating integrator).

The products of all the reactions were analysed under the following conditions:

Analytical column

Bentone - 34 (5%) and

Dinonyl phthalate (5%)

on Chromosorb - W (3 mm x 9 m)

N_2 flow rate

20 $cm^3.min^{-1}$

Column temperature

Programmed from 323 to 423 K at the heating rate of 10 $K.min^{-1}$,

the initial and final temperatures were held for

10 and 30 min, respectively.

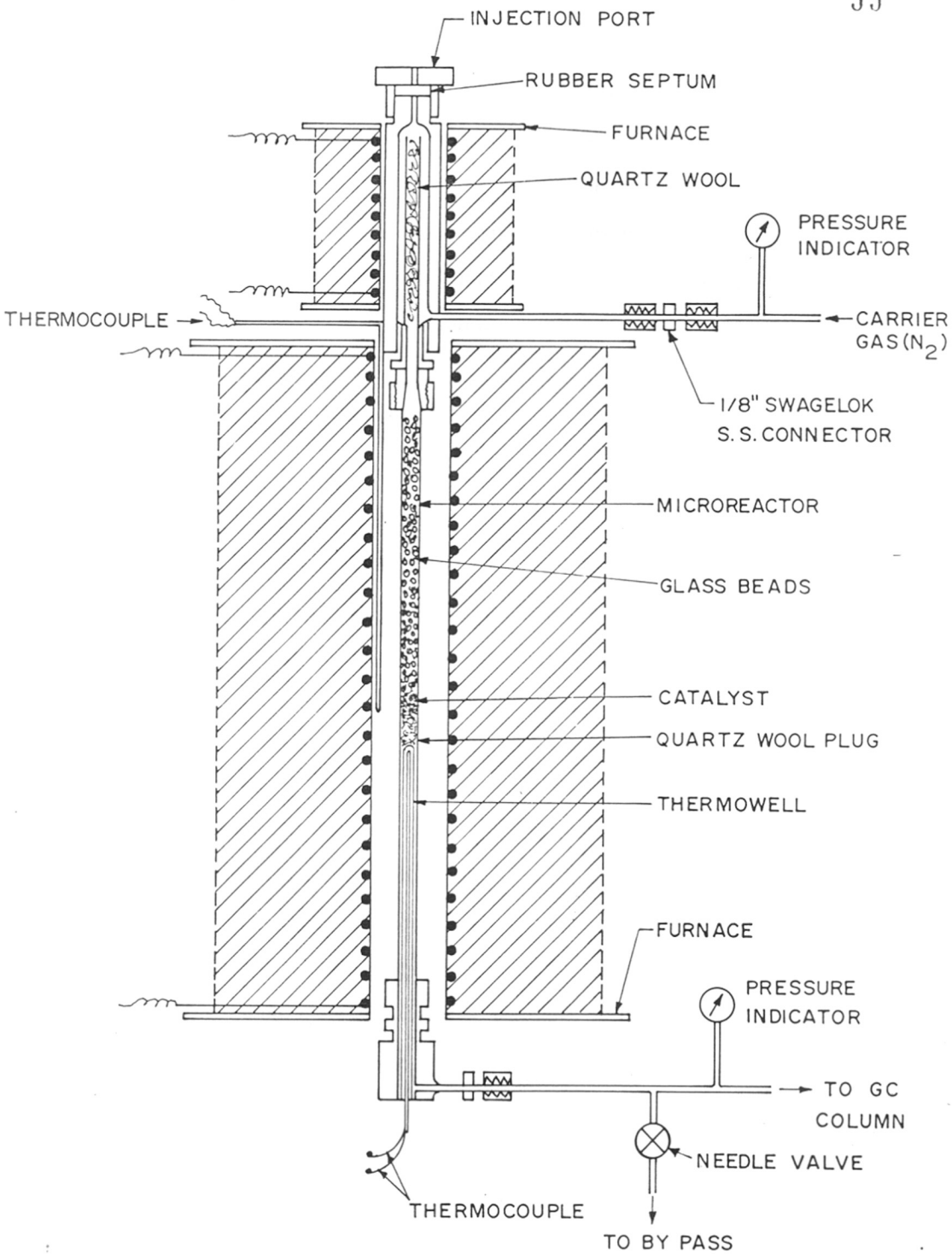

FIG. 2·4: MICRO — REACTOR ASSEMBLY

2.6 MEASUREMENT OF INTRACRYSTALLINE DIFFUSION

Diffusion of liquid cumene in the pentasil zeolites has been investigated by measuring volumetrically the sorption of cumene in the empty channels of the zeolite as a function of time. The volumetric measurements were carried out by contacting the evacuated zeolite with liquid cumene and following the change in the liquid volume using a caliberated capillary.

Satterfield and Cheng [7] used a glass apparatus for investigating single component diffusion of organic liquids in type Y zeolites. Their apparatus is however quite cumbersome and requires fusing and breaking of glass capillary for every sorption experiment. Recently, Choudhary and Nayak [8] have developed a very simple and easy to operate apparatus, which does not require fusing and breaking of glass capillary, for measuring precisely the kinetics of sorption of pure liquid compounds in the zeolites. The latter apparatus has been used in the present investigation for studying diffusion of liquid cumene in the ZSM-5 and ZSM-8 zeolites.

2.6.1 Apparatus and Procedure

The glass apparatus used for measuring diffusion of liquid cumene in the zeolites is shown in Fig. 2.5. It consists of a sample tube (ID = 5 mm and length = 6 cm), a liquid reservoir, a graduated glass capillary (ID = 0·75 mm and length = 30 cm) with an arrangement for liquid overflow over the capillary tip and two rotaflow stopcocks. The liquid reservoir and the capillary are connected to the sample tube as shown in Fig. 2.5. The zeolite in the sample tube could be pretreated under vacuum upto 623 K using a tubular furnace. The whole apparatus is immersed in a constant temperature bath, the temperature of which could be maintained within ± 0.05 K by circulating water through it at a desired temperature.

The apparatus was cleaned thoroughly and dried. The knob (along with plunger) of rotaflow stopcock S1 is removed and zeolite particles (0.5 g) were introduced into the sample tube. The empty space above the zeolite in the sample tube was

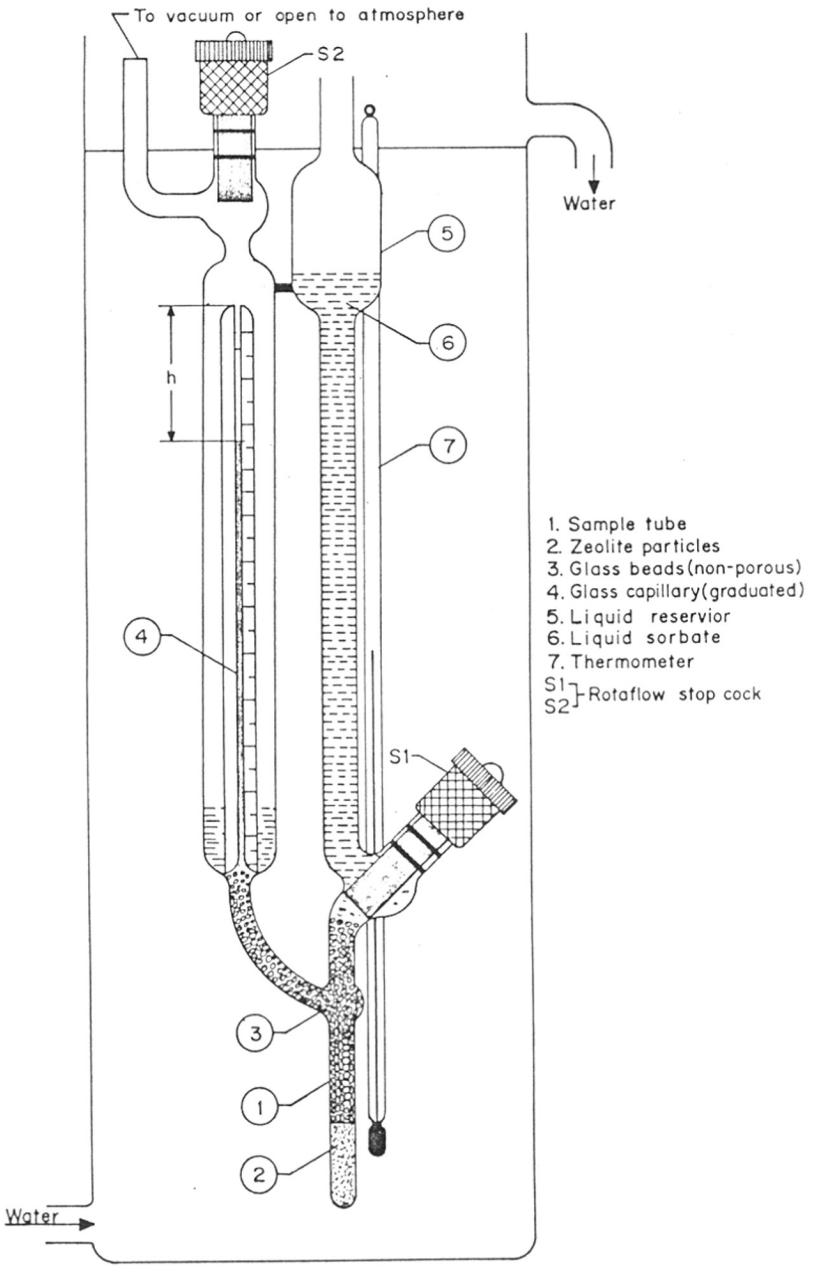

FIG. 2·5 : APPARATUS FOR MEASURING DIFFUSION OF PURE LIQUIDS IN ZEOLITES

then filled with nonporous glass beads (size = 1 mm) and the knob of the stopcock was replaced. Stopcock S1 is closed, the sample tube was kept in a tubular furnace (ID = 1.5 cm and length =8 cm) and the zeolite was pretreated in situ at 623 K (except for the NH_4-ZSM-5 which was treated at 423 K) under vacuum (0.05 torr) for 1 h, while the zeolite was under vacuum the stopcock S2 was closed and the sample tube was cooled down to the room temperature, sorbate liquid cumene was then charged in the liquid reservoir and the apparatus was immersed in the constant temperature bath. A sufficient period (about 1 h) was allowed to attain the thermal equilibrium between the apparatus (and its contents) and the circulating water. The temperature of liquid sorbate in the reservoir was measured by a thermometer.

After a desired temperature is attained, the sorption measurement was started by quickly opening the stopcock S1 (the time of stopcock opening is taken as zero sorption time) allowing the liquid sorbate to flow in the column of zeolite and glass beads and also through the graduated capillary until about 1-2 cm^3 liquid overflowed the capillary tip and collected in the outer jacket (Fig. 2.5). The stopcock S1 was then closed immediately and the stopcock S2 was opened to atmosphere to release the vacuum in the system. After release of vacuum, stopcock S2 was closed. The sorption uptake was then followed by measuring the fall in the height (h) of liquid in the capillary as a function of time until there was no further fall in the height.

The opening of stopcock S1 was the zero sorption time (the zeolite was in contact with the sorbate as soon as the stopcock was opened) and the time of closing of stopcock S1 was the zero reading on the capillary. The time gap between the opening and closing the stopcock was about 5 seconds. hence, correction to the sorption data, similar to that applied by Satterfield and Cheng [7] was also applied, as shown in Fig. 2.6. The correction ($\triangle h$) is obtained by extrapolating the initial h vs. $\sqrt{t}$ plot to zero sorption time. The corrected fall in the liquid height (h^*) could be obtained as follows:

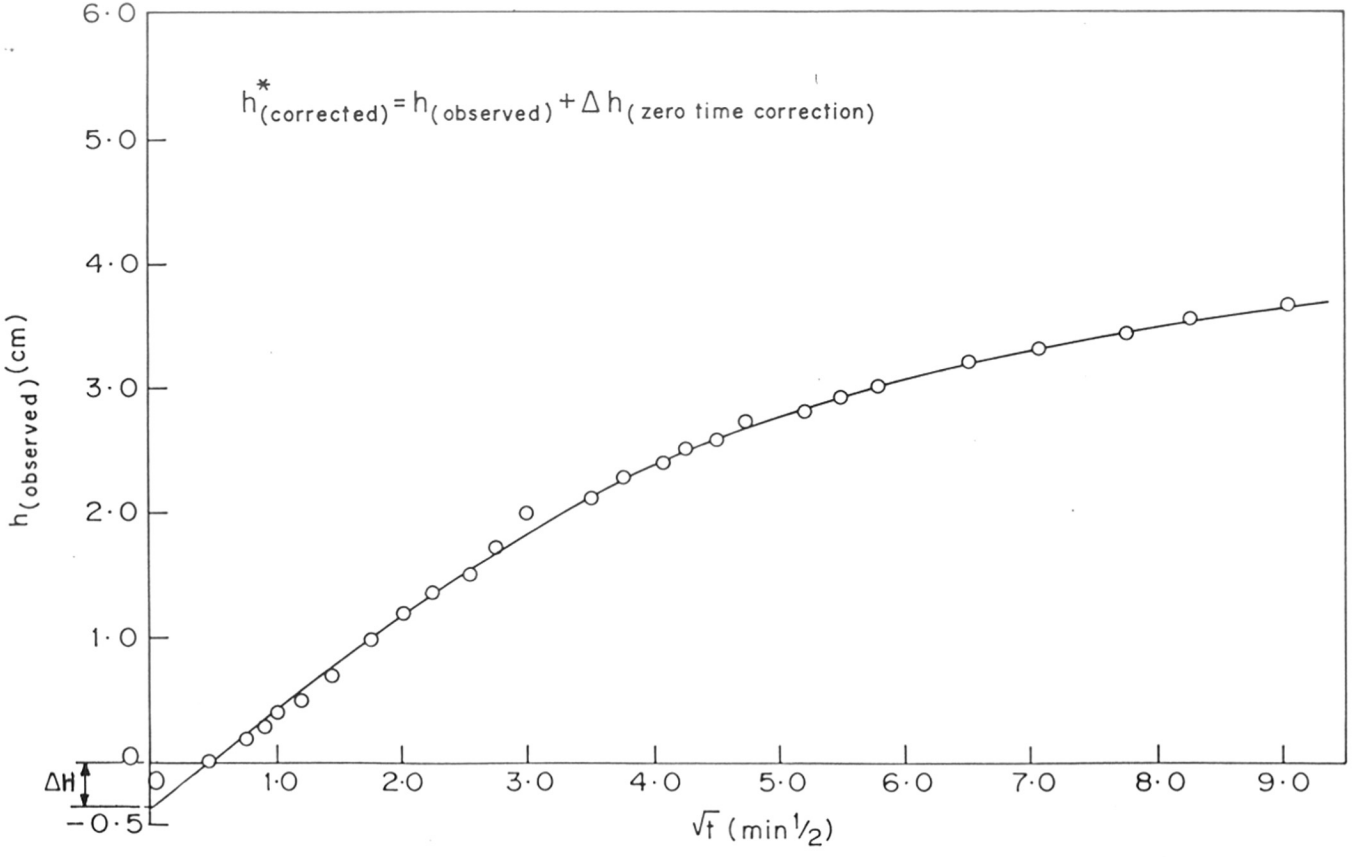

FIG. 2·6 : Ah vs $\sqrt{t}$ PLOT FOR THE SORPTION OF CUMENE IN H-ZSM-5 (AT 288K) SHOWING ZERO TIME CORRECTION.

$$h^{*} = h + \triangle H \qquad (4)$$

where h is the observed fall in liquid height and $\triangle H$, the correction to the fall in liquid height.

The fractional sorption at a particular sorption time, t was obtained as follows:

$$\text{Fractional sorption} = \frac{h^{*}}{h_{(max)}} = \frac{Q_t}{Q_\infty} \qquad (5)$$

where, Q_t and Q_∞ are the amount of liquid cumene sorbed at time t and infinity, respectively.

The liquid sorption data were collected in the temperature range 283-328 K. The sorption data on the zeolites are presented in the Appendices- 1-13.

REFERENCES

1. *Argauer, R.J., and Landolt, G.R., US Patent 3, 702, 886 (1972).*

2. *Mobil Oil Corp., Netherlands Patent, 7, 014, 807 (1971).*

3(a) *Nayak, V.S., and Choudhary, V.R., Appl. Catal. 4, 333 (1982).*

3(b) *Nayak, V.S., Ph.D. Thesis 'Studies on Synthetic Zeolites', University of Poona, Pune (1982).*

4. *Akolekar, D.B., and Choudhary, V.R., J. Catal. 105, 416 (1987).*

5. *Choudhary, V.R., and Nayak, V.S., Appl. Catal. 4, 31 (1982).*

6. *Choudhary, V.R., J. Chromatogr. 268, 207 (1983).*

7. *Satterfield, C.N., and Cheng, C.S., 'Adsorption Technology', AIChE Symp. Ser. (117) 67, 43 (1971).*

8. *Choudhary, V.R., and Nayak, V.S., Chem. Eng. Sci. (to be published).*

Chapter-3 : RESULTS AND DISCUSSION

3. RESULTS AND DISCUSSION

3.1 ACIDITY DISTRIBUTION ON ZEOLITES

The acidity and acid strength distribution on the zeolites have been studied by measuring chemisorption of pyridine at different temperatures and stepwise thermal desorption (STD) of pyridine at temperatures close to those at which catalytic reactions occur, using the gc methods [1,2]. The data on STD and chemisorption of pyridine on the zeolites given in Tables-3.1 and 3.2. In the present study, chemisorption (or irreversible sorption) is defined as the amount of sorbate retained by the presaturated zeolite after it was swept with pure nitrogen for a period of 60 minutes.

3.1.1 Acidity of ZSM-5 Zeolites

Results of the STD of pyridine from the ZSM-5 zeolites are plotted in Fig. 3.1. It may be noted that here the site energy is expressed in terms of a range of temperature in which the base chemisorbed at the lowest temperature of the range is desorbed (T_d is the desorption temperature of the base and T_d^* is the temperature at which the base chemisorbed on the strongest site is desorbed).

The temperature dependence of the chemisorption of pyridine on the zeolites is shown in Fig. 3.2. The q_i (amount of pyridine chemisorbed) vs. T (temperature) curves present a type of site energy distribution in which the number of sites are expressed in terms of the amount of pyridine chemisorbed as a function of chemisorption temperature, which, in turn, is a measure of the strength or energy of sites involved in the chemisorption.

The results in both the figures indicate that the site energy distribution and the number of strong sites (measured in terms of the chemisorption of pyridine at 673 K) on the zeolite are strongly influenced by its calcination temperature and degree of H^+ exchange (α). The number of strong acid sites on the zeolite are increased with the increase in its degree H^+ exchange and are decreased

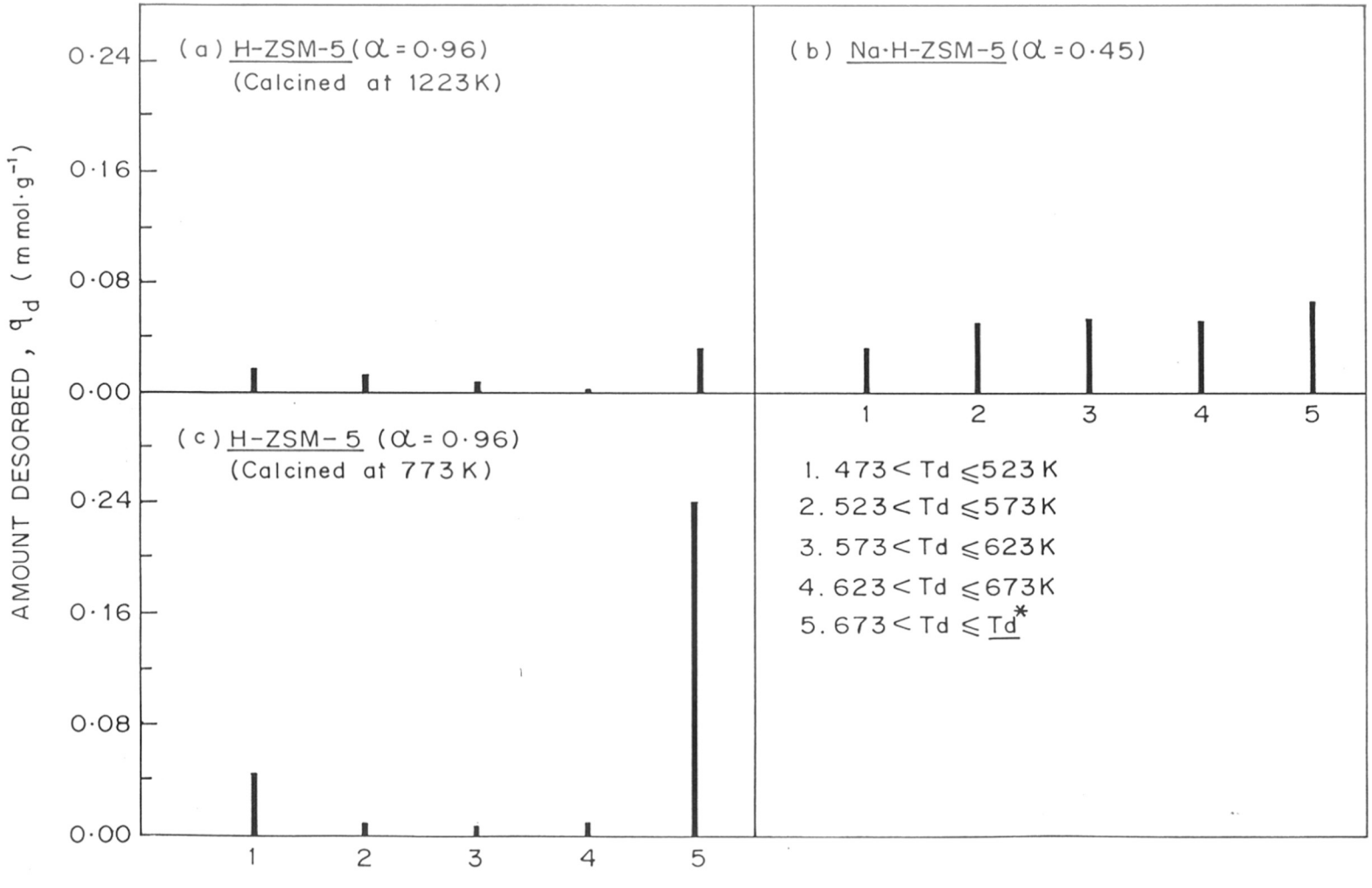

FIG. 3·1: SIDE ENERGY DISTRIBUTION ON ZSM-5 ZEOLITES (OBTAINED BY STD OF PYRIDINE FROM 473 TO 673 K)

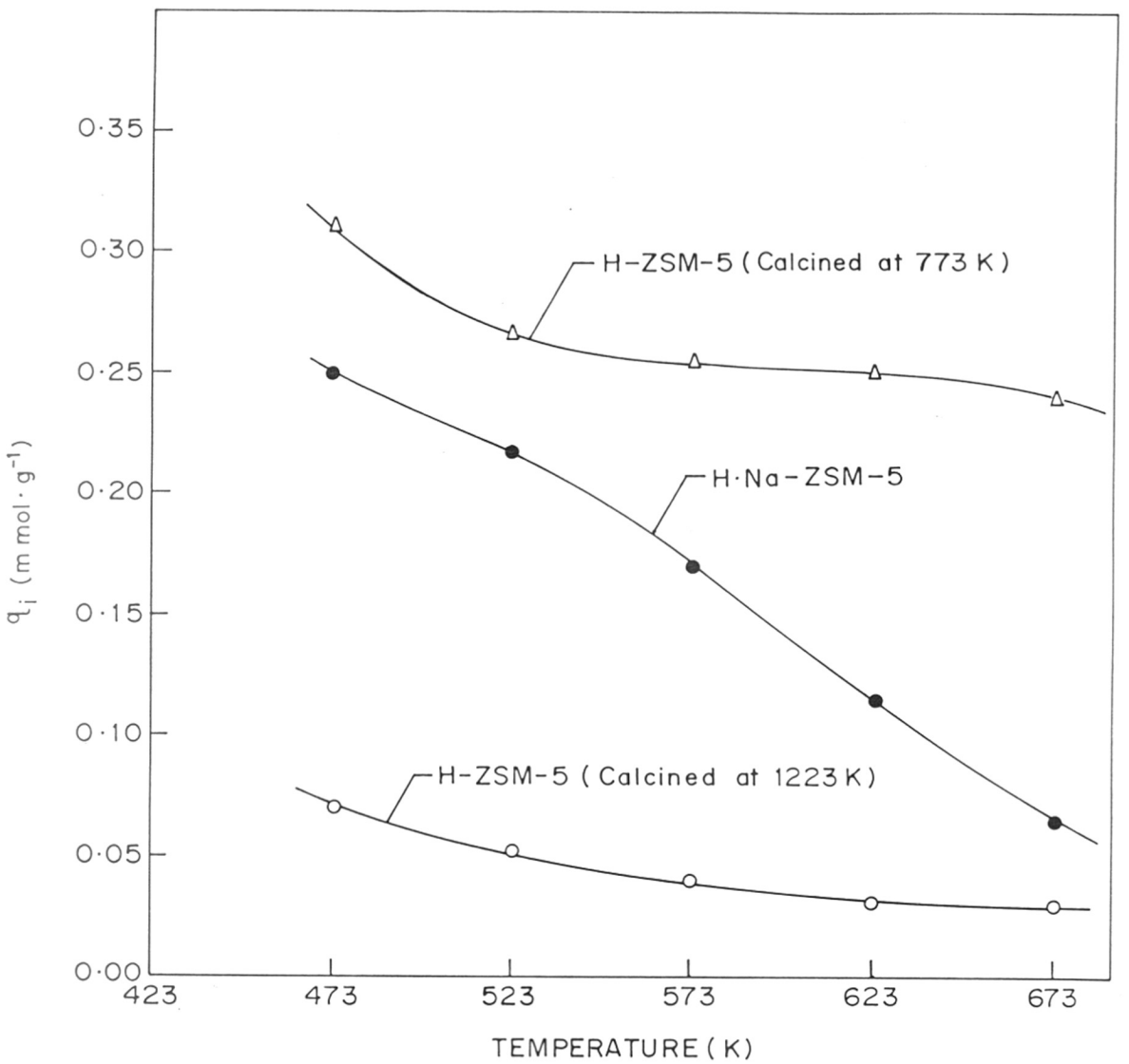

FIG. 3·2 : TEMPERATURE DEPENDENCE OF CHEMISORPTION OF PYRIDINE (q_i) ON ZSM-5 ZEOLITES

TABLE-3.1

Data on the STD and Chemisorption of Pyridine on ZSM-5 Type Zeolites

STD data		Chemisorption data	
Temp. range (K)	q_d $(m.mol.g^{-1})$	*Temperature (K)*	q_i $(m.mol.g^{-1})$
H-ZSM-5 (calcined at 773K)			
473-523	*0.044*	*473*	*0.310*
523-573	*0.010*	*523*	*0.265*
573-623	*0.005*	*573*	*0.255*
623-673	*0.008*	*623*	*0.250*
		673	*0.242*
H-ZSM-5 (calcined at 1223K)			
473-523	*0.019*	*473*	*0.072*
523-573	*0.011*	*523*	*0.053*
573-623	*0.008*	*573*	*0.042*
623-673	*0.002*	*623*	*0.034*
		673	*0.032*
Na·H-ZSM-5 (degree of H^+-exchange : 0.45)			
473-523	*0.032*	*473*	*0.251*
523-573	*0.049*	*523*	*0.219*
573-623	*0.054*	*573*	*0.170*
623-673	*0.051*	*623*	*0.117*
		673	*0.070*

TABLE-3.2

Data on the STD and Chemisorption of Pyridine on H-ZSM-8 and Mg-, P- and B- modified H-ZSM-8

STD data		Chemisorption data	
Temp. range (K)	q_d ($m.mol.g^{-1}$)	Temperature (K)	q_i ($m.mol.g^{-1}$)
H-ZSM-8			
473-523	0.120	473	0.537
523-573	0.070	523	0.420
573-623	0.030	573	0.347
623-673	0.026	623	0.320
		673	0.294
B_2O_3·H-ZSM-8			
473-523	0.089	473	0.353
523-573	0.034	523	0.2635
573-623	0.018	573	0.230
623-673	0.009	623	0.211
		673	0.202
MgO·H-ZSM-8			
473-523	0.075	473	0.333
523-573	0.026	523	0.259
573-623	0.026	573	0.232
623-673	0.026	623	0.232
		673	0.232
P_2O_5·H-ZSM-8			
473-523	0.060	473	0.207
523-573	0.032	523	0.1471
573-623	0.006	573	0.116
623-673	0.003	623	0.110
		673	0.110

with the increase in its calcination temperature because of the dehydroxylation of the zeolite at the higher temperature. These observations are similar to those observed earlier for the case of ZSM-5 zeolite [3-5].

3.1.2 Acidity of ZSM-8 Zeolites

The results of the STD and chemisorption of pyridine on H-ZSM-8 and modified H-ZSM-8 zeolites are shown in Figs. 3.3 and 3.4, respectively. For the site energy distributions shown in Fig. 3.3, the site energy is expressed in terms of a range of temperature in which the base chemisorbed at the lowest temperature of the range is desorbed. Whereas, in the site energy distribution shown by q_i vs. T curves (Fig. 3.4), the number of sites are expressed in terms of the amount of pyridine chemisorbed as a function of temperature and the temperature of chemisorption is a measure of the strength or energy of sites involved in the chemisorption.

A comparison of the acidity distribution of H-ZSM-8 with that of the modified H-ZSM-8 zeolites indicates that the modification of the zeolite with MgO, P_2O_5 or B_2O_3 causes a drastic change in its acidity and acid strength distribution. Both the total number of acid sites (measured in terms of the chemisorption of pyridine at 473 K) and the number of strong acid sites (measured in terms of the chemisorption of pyridine at 673 K) are decreased due to the modification. The zeolites could be arranged in the order of their total and strong acid sites as follows:

For total number of acid sites

H-ZSM-8 $>$ B_2O_3. H-ZSM-8 $>$ MgO. H-ZSM-8 $>$ P_2O_5. H-ZSM-8

For strong acid sites

H-ZSM-8 $>$ MgO. H-ZSM-8 $>>$ B_2O_3. H-ZSM-8 $>$ P_2O_5. H-ZSM-8

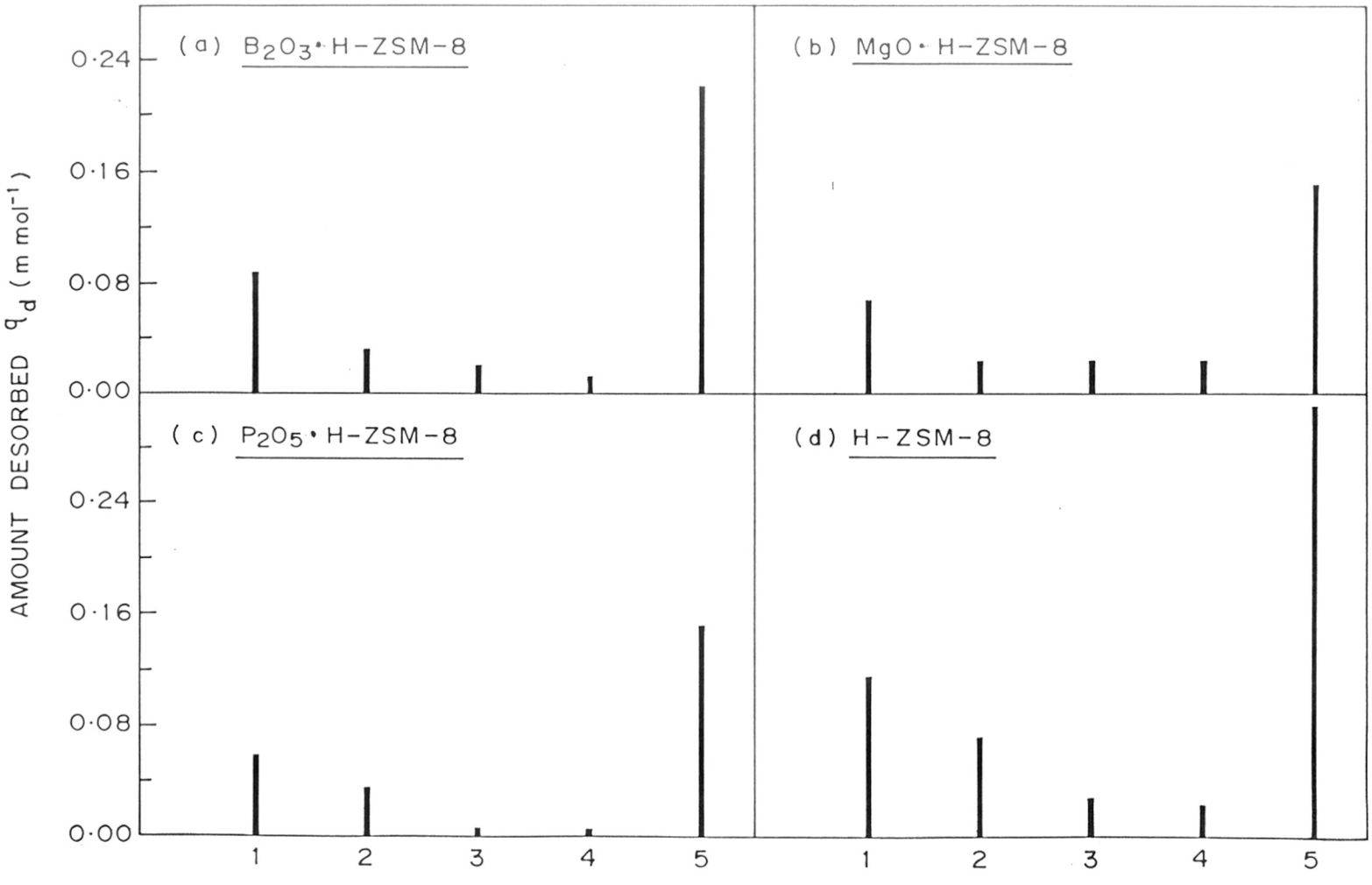

FIG.3·3 : SITE ENERGY DISTRIBUTION ON H-ZSM-8 AND MODIFIED H-ZSM-8 ZEOLITES (OBTAINED BY STD OF PYRIDINE FROM 473 TO 673 K)

1. $473 < T_d \leq 523$ K , 2. $523 < T_d \leq 573$ K , 3. $573 < T_d \leq 623$ K , 4. $623 < T_d \leq 673$ K , 5. $673 < T_d \leq \underline{T_d}^*$

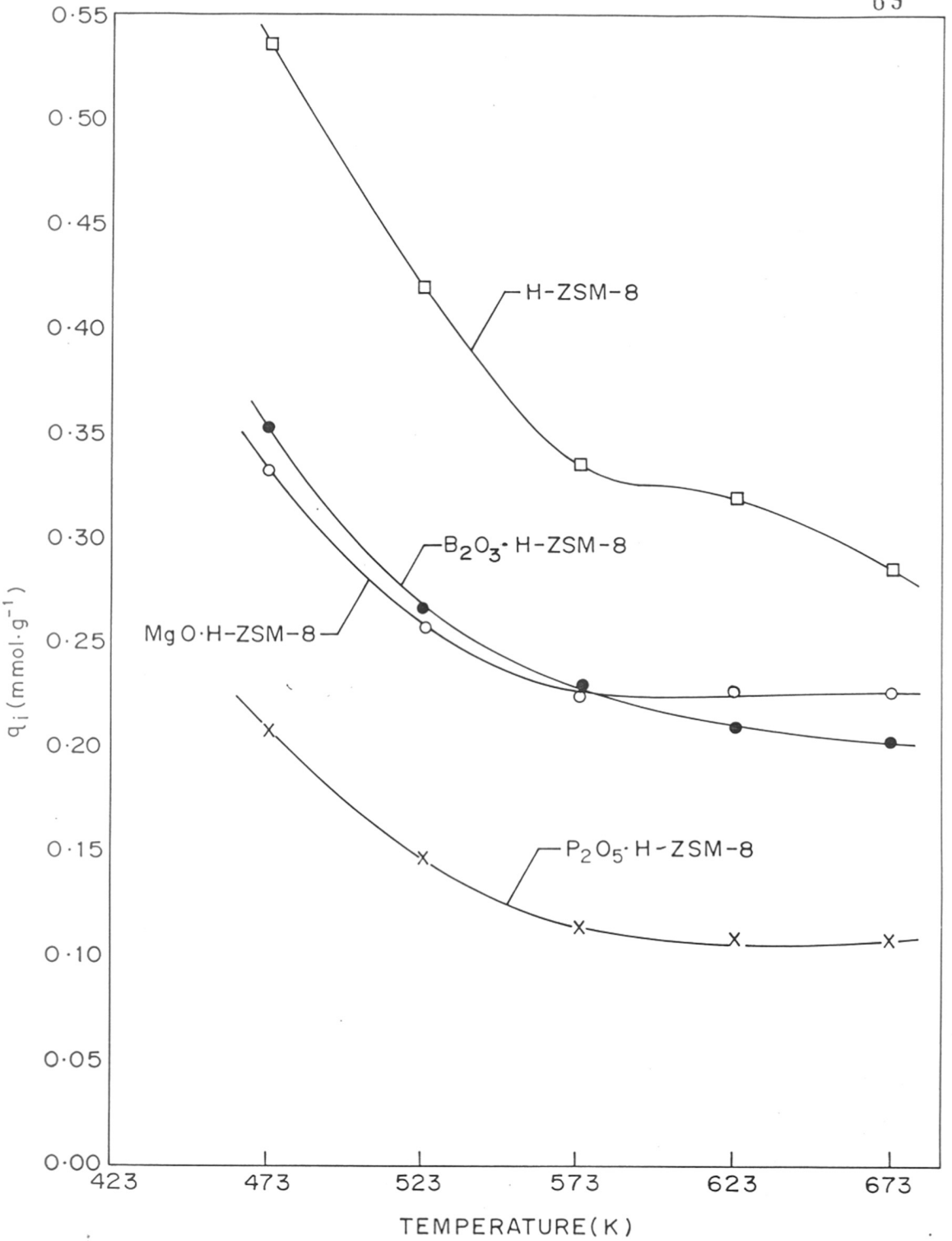

FIG. 3·4: TEMPERATURE DEPENDENCE OF CHEMISORPTION OF PYRIDINE ON H-ZSM-8 AND MODIFIED H-ZSM-8 ZEOLITES

The decrease in the number of acid sites (both weak and strong sites) due to the modification is expected to be because of their blockage by the modifying agent. The deposition of the modifying agent on external surface of zeolite crystals may cause creation of new acid sites (which are expected to be mostly weak ones) on the external surface.

The decrease in the acidity and/or strength of acid sites on H-ZSM-8 due to its modification is consistent with that observed for ZSM-5 zeolite when modified by boron [6-8], phosphorous [9-12] and magnesium [13] oxides.

3.2 DIFFUSION OF CUMENE IN ZEOLITES

The data on sorption kinetics of liquid cumene in the empty channels of the ZSM-5 and ZSM-8 zeolites are given in Appendices 1-13.

Under the present experimental conditions for the sorption of pure cumene from liquid phase into the empty (evacuated) channels of the pentasil zeolites, following two mass transfer processes are involved:

1. Penetration of liquid cumene in the macro (or intercrystalline) pores of the zeolite particles.

2. Diffusion and sorption of cumene in the micro (or intracrystalline) pores of the zeolite.

Since, the sorption may be controlled by the intercrystalline mass transfer or intracrystalline mass transfer or a combination of the two mass transfer processes under a particular set of experimental conditions, it is essential to ensure that the sorption is controlled only by the intracrystalline mass transfer for obtaining intracrystalline diffusivity from sorption kinetics. To achieve this, the effect of zeolite particle size on the sorption kinetics was studied and the absence of intercrystalline mass transfer effect on the sorption kinetics (Appendices 1-13) was established.

The values of intracrystalline diffusion coefficient (D) have been obtained from the sorption kinetics data using the $\sqrt{t}$ - law [14].

$$Q_t / Q_\infty = 6 [D/(\pi r^2)]^{1/2} . t^{1/2} \quad (1)$$

where, D is the diffusion coefficient; r, the radius of zeolite crystals; Q_t and Q_∞, the amount of cumene sorbed at time t and ∞, respectively; and t, the sorption time.

3.2.1 Diffusion in ZSM-5 Zeolites

Figure 3.5 shows that the decrease in the particle size of a ZSM-5 (calcined at 773 K) from 0.2 to 0.1 mm has not resulted in significant change in the sorption kinetics at 328 K, the maximum temperature of the sorption. It is therefore safe to assume that sorption in the ZSM-5 zeolite at 283-328 K is controlled by the intracrystalline mass transfer.

The Q_t/Q_∞ vs. $\sqrt{t}$ plots for the sorption of liquid cumene in the ZSM-5 zeolites are presented in Figs. 3.6-3.9. The values of diffusion coefficient (D) obtained from the slopes of the linear plots for the initial sorption data (Fig. 3.6-3.9) according to the $\sqrt{t}$ - law (Eqn. 1) are given in Table-3.3. The value of activation energy (E) for the diffusion, obtained from the linear log D vs. 1/T plots, shown in Fig. 3.10 according to the Arrhenius type equation,

$$D = A \exp [- E / RT] \quad (2)$$

(where, A is a constant, R, the gas constant and T, the temperature)

are included in Table-3.3.

The results indicate that the diffusion of cumene in ZSM-5 and the activation energy of diffusion are strongly influenced by the calcination temperature, poisoning

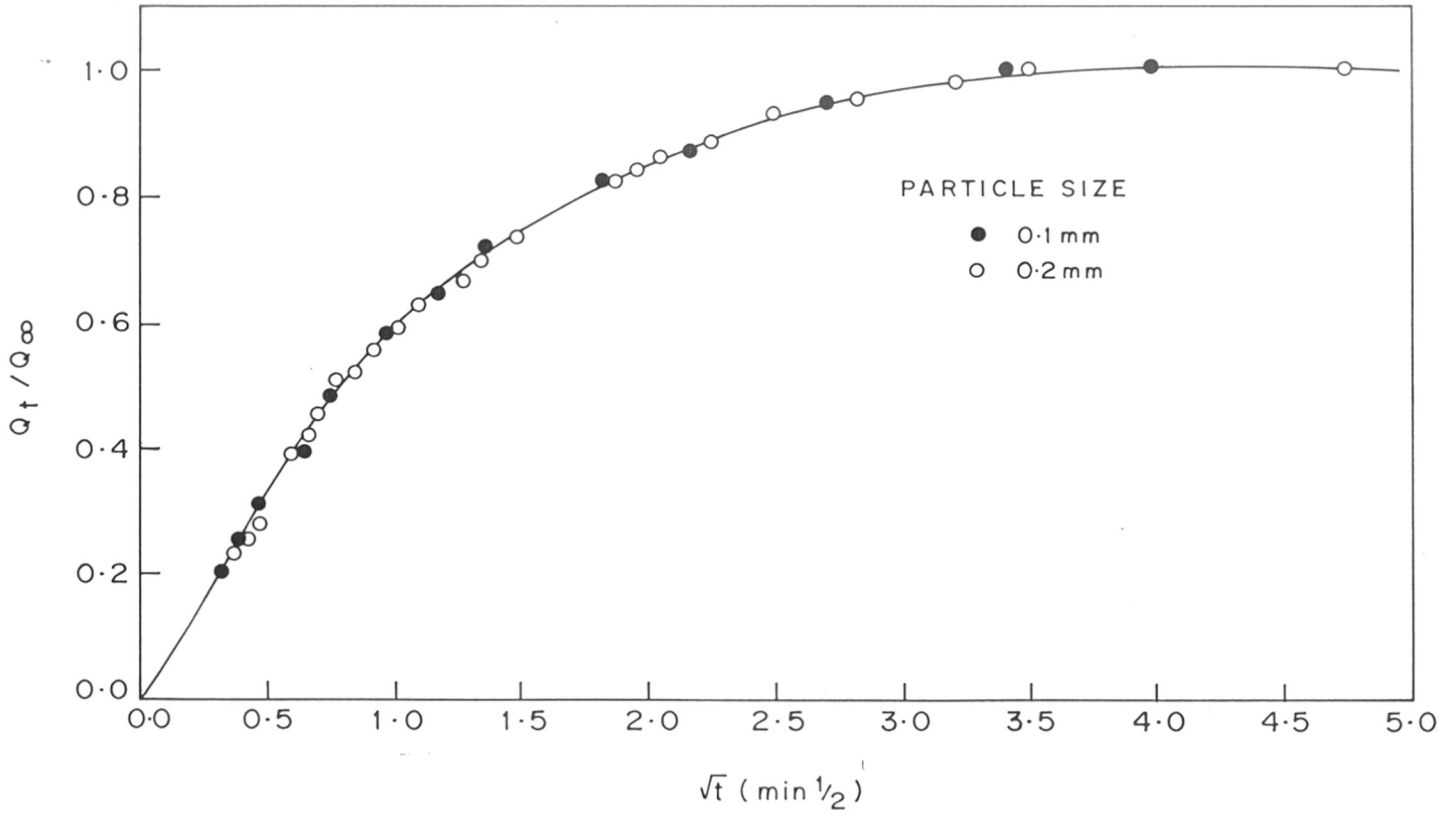

FIG. 3·5: Q_t/Q_∞ vs $\sqrt{t}$ PLOTS SHOWING ABSENCE OF INTERCRYSTALLINE MASS TRANSFER EFFECT IN THE SORPTION OF LIQUID CUMENE IN H-ZSM-5(CALCINED AT 773K) AT 328K

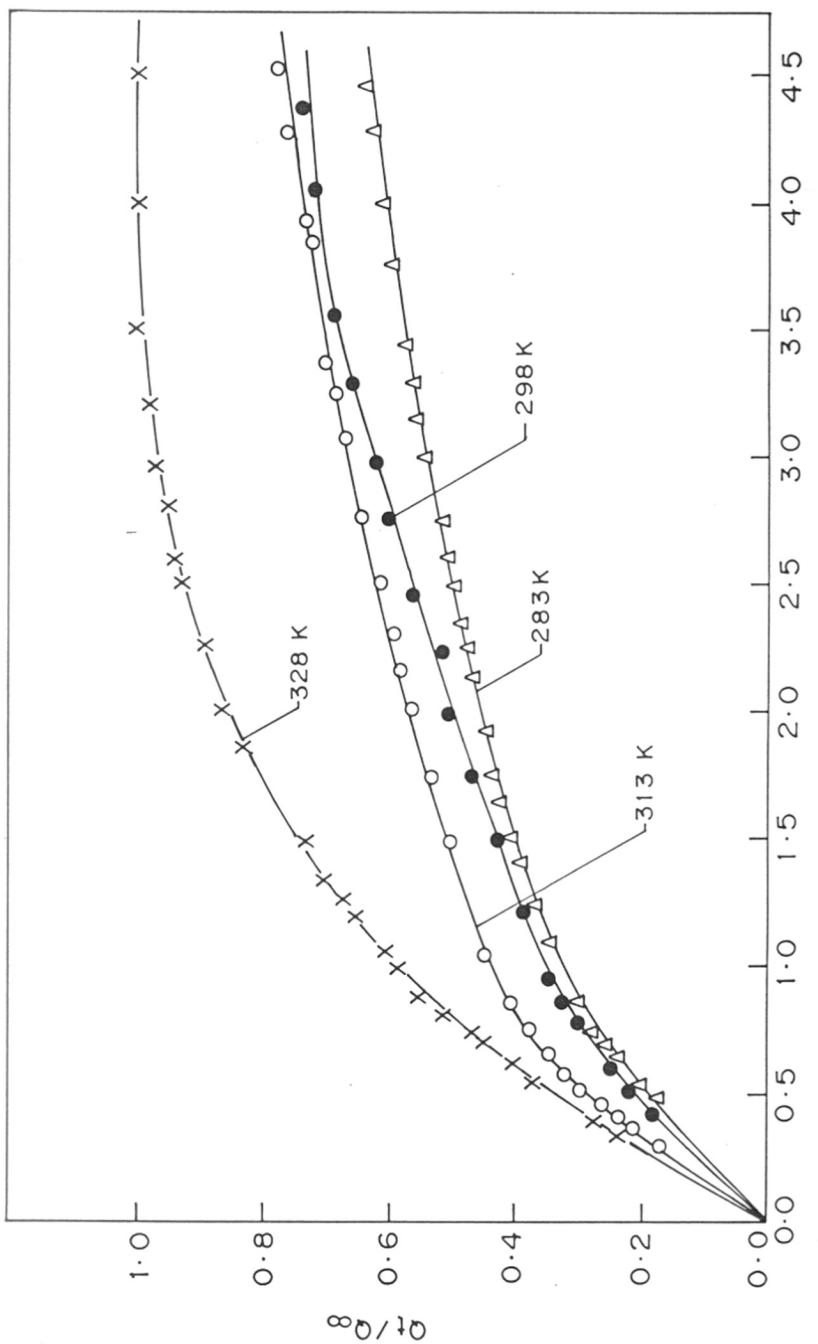

FIG. 3·6: Q_t/Q_∞ vs $\sqrt{t}$ PLOTS FOR THE SORPTION OF CUMENE IN H-ZSM-5 (CALCINED AT 773 K) AT DIFFERENT TEMPERATURES.

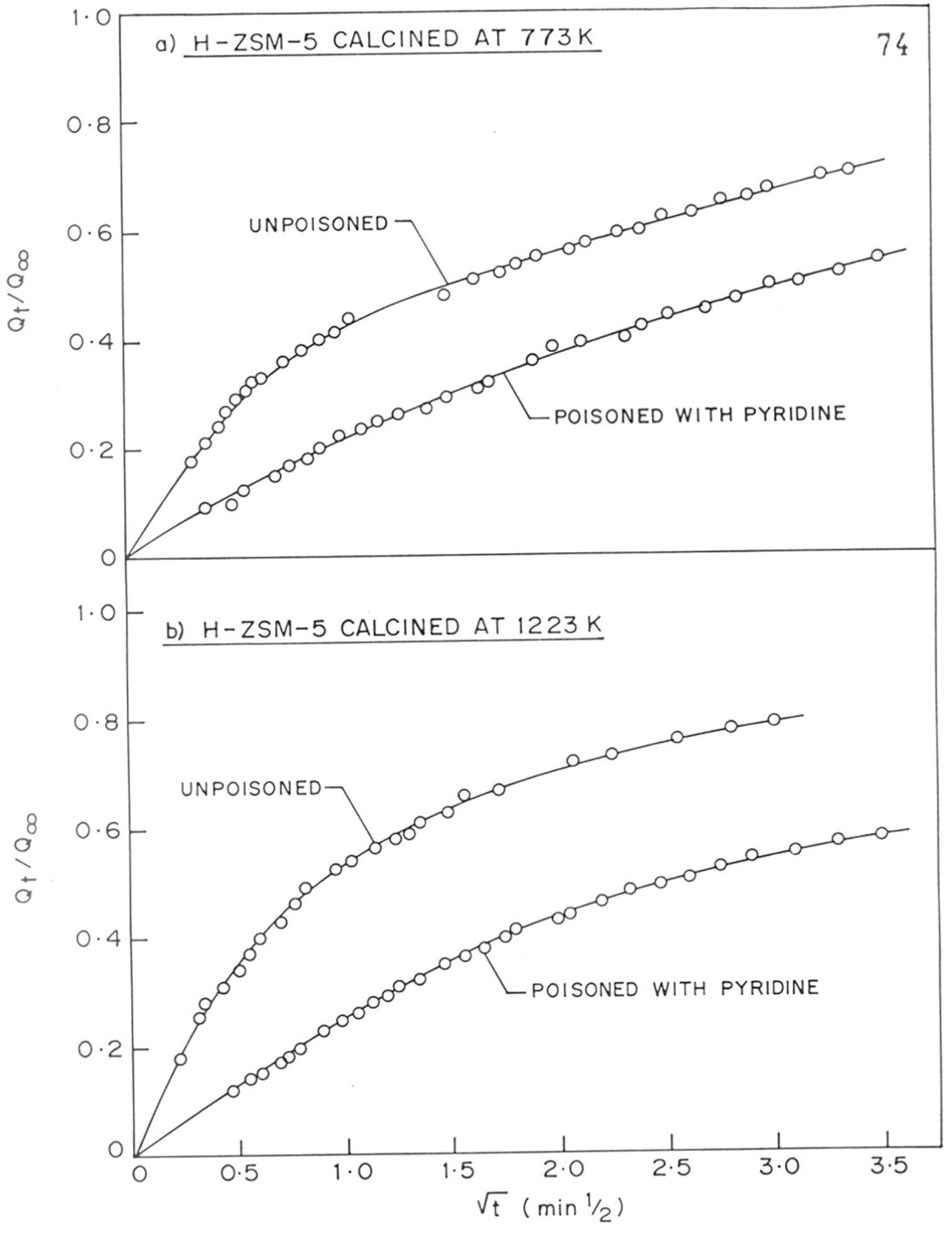

FIG. 3·7: a) Q_t/Q_∞ vs $\sqrt{t}$ PLOTS FOR THE SORPTION OF CUMENE (AT 313 K) IN H-ZSM-5 (CALCINED AT 773K) WITH AND WITHOUT PYRIDINE POISONING
b) Q_t/Q_∞ vs $\sqrt{t}$ PLOTS FOR THE SORPTION OF CUMENE (AT 313 K) IN H-ZSM-5 (CALCINED AT 1223K) WITH AND WITHOUT PYRIDINE POISONING

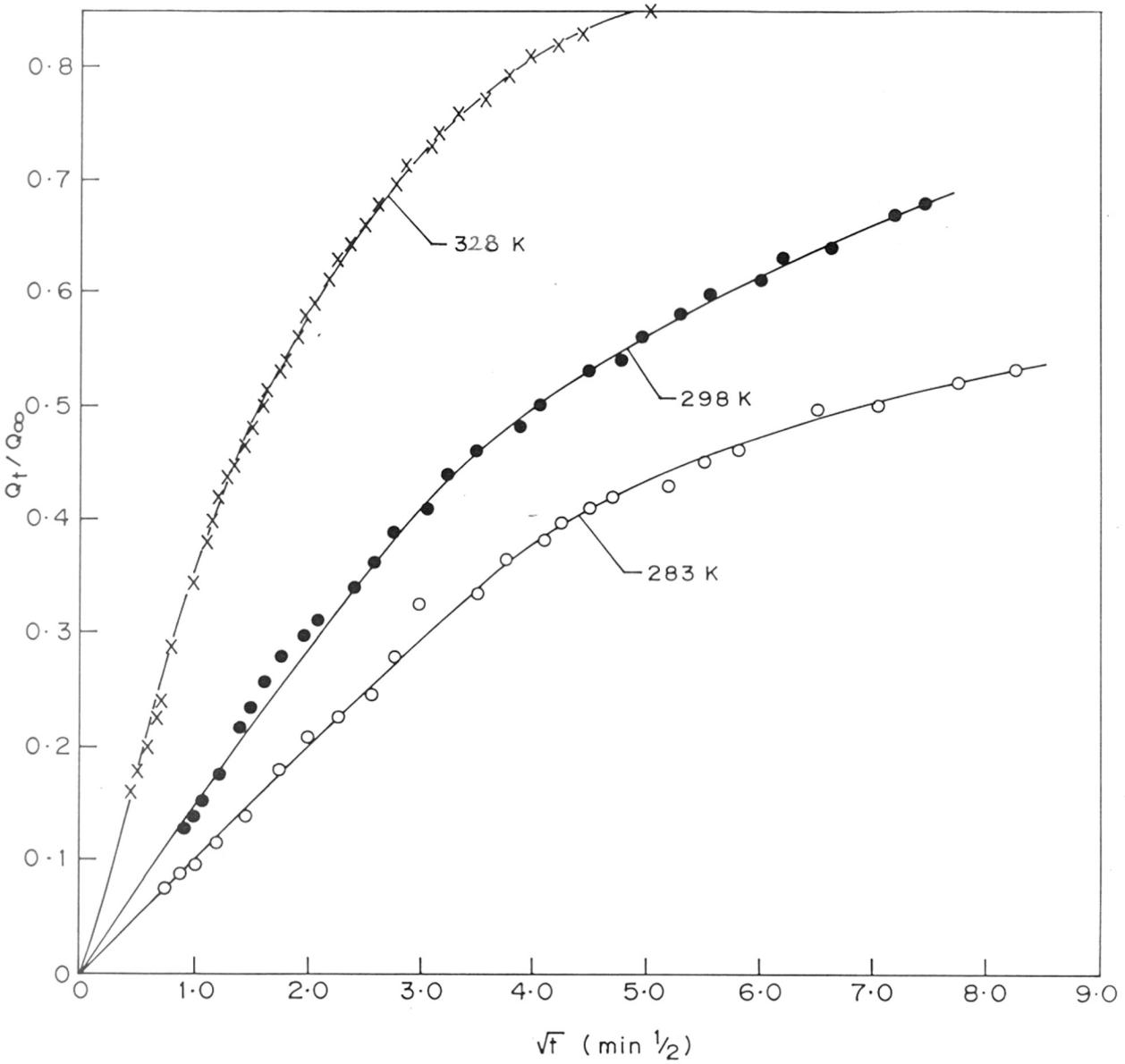

FIG. 3·8 : Q_t / Q_∞ vs $\sqrt{t}$ PLOTS FOR THE SORPTION OF CUMENE IN H·Na-ZSM-5 (α=0·45) AT DIFFERENT TEMPERATURE

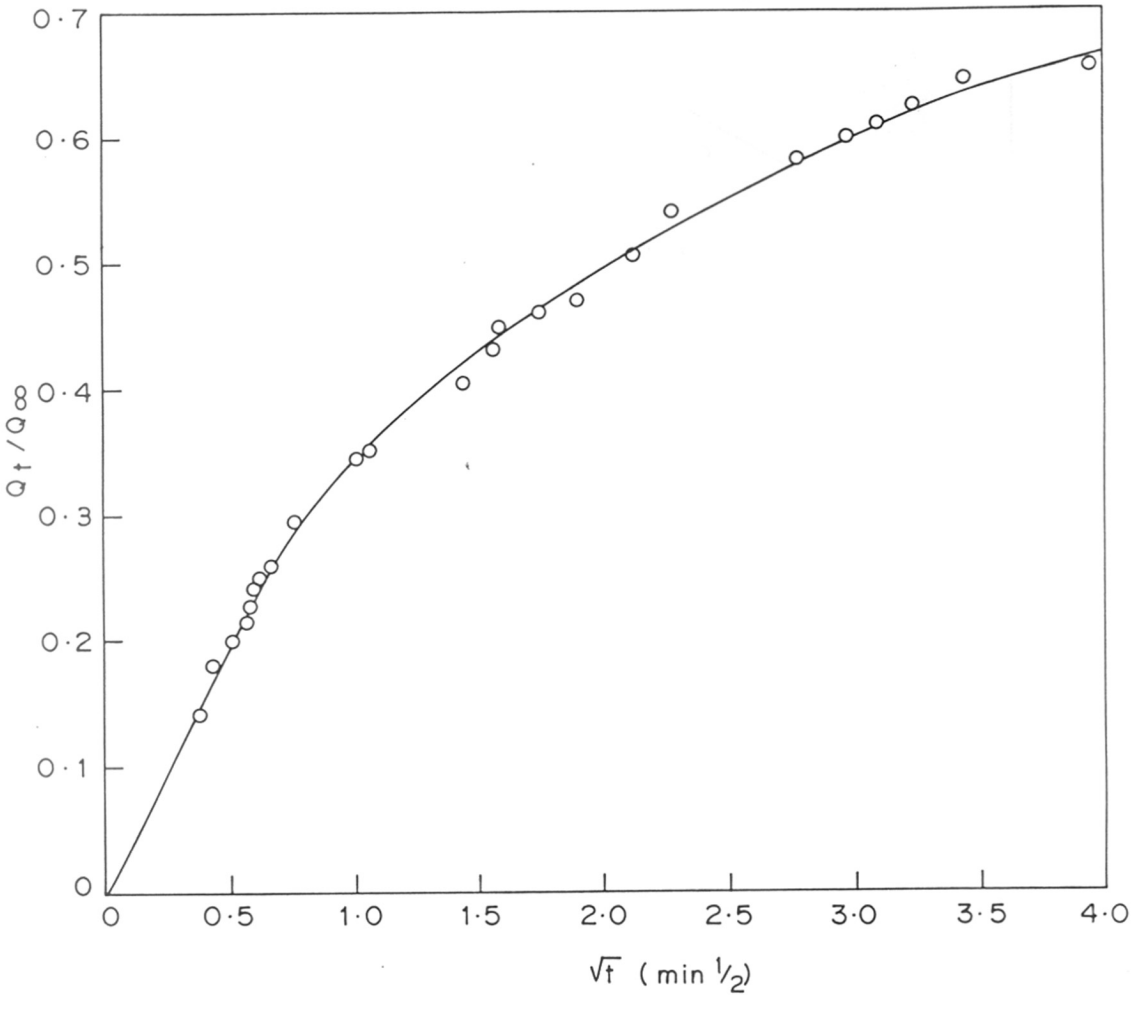

FIG. 3·9 : $Q_t/Q\infty$ vs $\sqrt{t}$ PLOT FOR THE SORPTION OF CUMENE IN NH_4 – ZSM – 5 AT 313 K

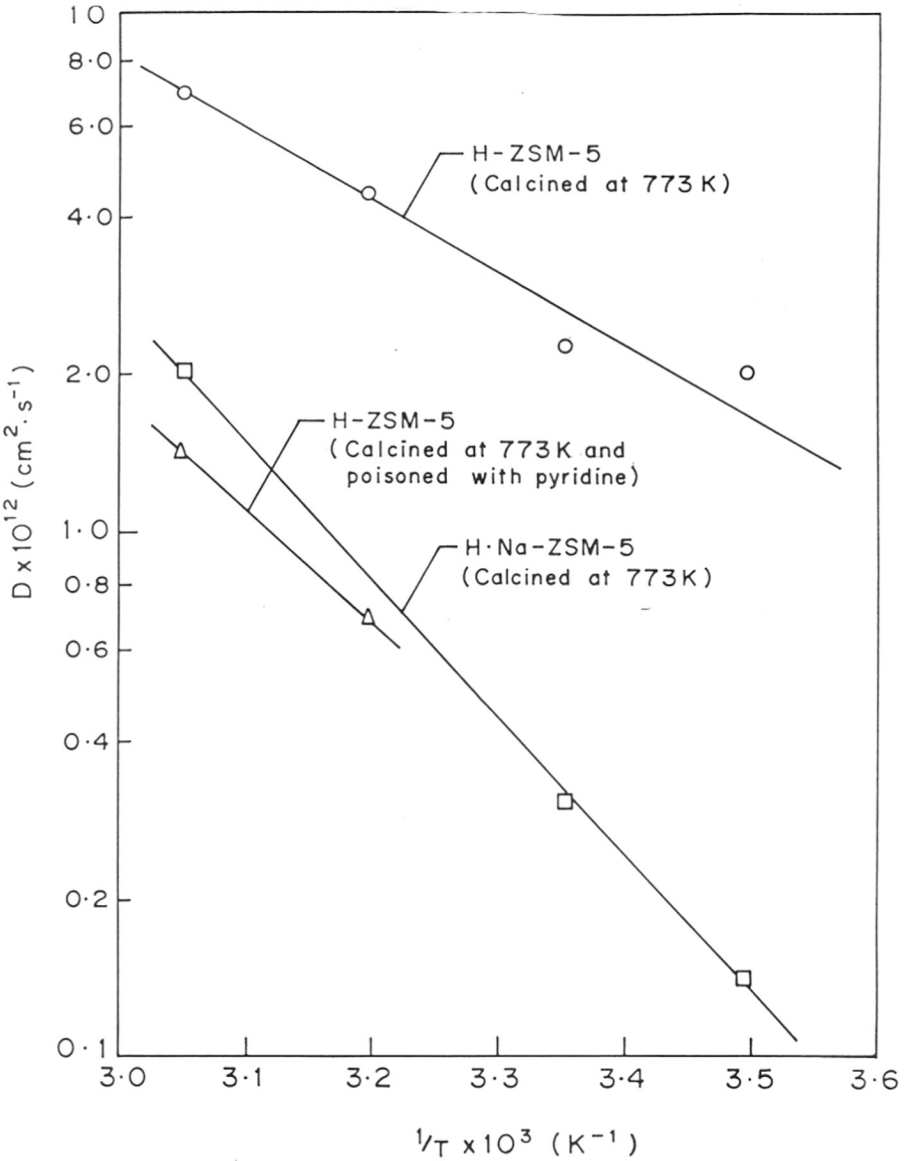

FIG. 3·10 : TEMPERATURE DEPENDENCE OF DIFFUSION OF CUMENE IN ZSM-5 ZEOLITES

and by the type of cation/or degree of its exchange of the zeolite.

(a) Influence of dehydroxylation

The dehydroxylation has resulted in a large decrease in the protonic acidity of H-ZSM-5 (Fig. 3.2) and a very significant increase in the diffusion in the zeolite (Table-3.3). This reveals that the diffusion is strongly influenced by the introduction of protonic acid sites with the cumene molecules; stronger and/or larger interactions result in the lower diffusivity.

(b) Influence of cation or degree of cation exchange

The diffusivity of cumene in ZSM-5 having different cations is in the following order:

H-ZSM-5 $>$ NH_4-ZSM-5 $>$ H.Na-ZSM-5

Also the activation energy for the diffusion in H.Na-ZSM-5 is much higher than in H-ZSM-5. The lower diffusivity in the NH_4-ZSM-5 is mostly due to a reduction in effective channel diameter when H^+ (with negligible ionic diameter) is replaced by a larger diameter NH_4^+ (- 0.4 nm) which is expected to be located at the channel intersections as shown in Fig. 3.11. Whereas, the very strong influence of Na^+-content on the diffusion and its activation energy is expected to be mostly due to the stronger interaction of cumene with Na^+ cations than with protons in the zeolites. The higher size of Na^+ cation (0.19 nm) may also have some effect on the diffusion.

(c) Influence of strongly sorbed foreign molecules/poisons

The poisoning of H-ZSM-5 (calcined at 773 or 1223 K) with pyridine results in a drastic reduction in the diffusion in the zeolite. The activation energy for the diffusion is also increased markedly (Table-3.3). This is mostly due to the reduction

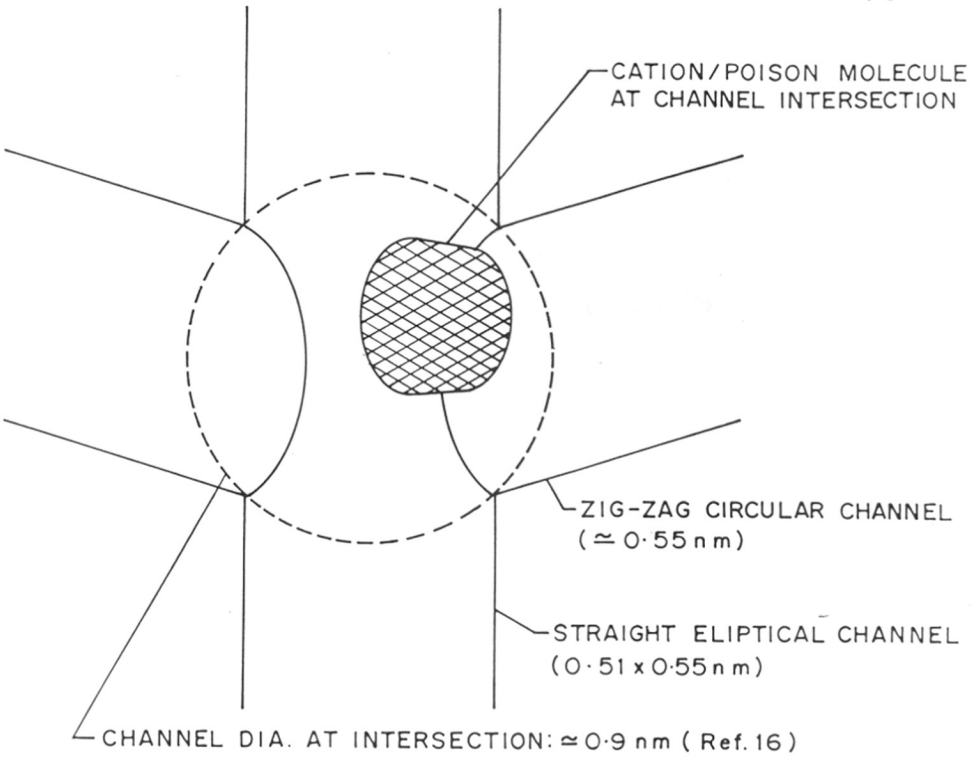

CHANNEL INTERSECTION IN ZSM-5

CATION / POISON MOLECULE		SIZE (or dimension) (nm)
H^+	——	NEGLIGIBLE SMALL
Na^+	——	0·19 (spherical)
NH_4^+	——	≃0·4 (spherical)
 (Pyridinium ion)	——	≃0·68 x 0·74 x 0·17 (flat plate)

FIG. 3·11 : INFLUENCE OF CATION OR POISON MOLECULE ON THE FREE VOLUME AVAILABLE AT CHANNEL INTERSECTIONS IN ZSM-5 ZEOLITE

TABLE-3.3

Results on Diffusion of Cumene - in ZSM-5 Zeolites Si/Al = 31.1 and Crystal Size (Average) = 2.08 um

S.No.	Zeolite	Degree of H^+ or NH_4 exchange (α)	Temp. (K)	Diffusion coefficient		Activation energy, $E(kJ.mol^{-1})$
				$D/r^2 \times 10^4$ (s^{-1})	$D \times 10^{12}$ $(cm^2.sec^{-1})$	
1.	H-ZSM-5 (calcined at 773K) (N_A=0.24 m.mol.g^{-1})	0.99	283 298 313 328	1.94 2.10 4.14 6.34	2.10 2.27 4.48 6.86	27.45
2.	H-ZSM-5 (calcined at 773K and poisoned with pyridine) (q_{py}=0.24 m.mol.g^{-1})	0.99	313 328	0.63 1.31	0.68 1.42	41.59
3.	H-ZSM-5 (calcined at 1223K) (N_A=0.032 m.mol.g^{-1})	0.99	313	9.31	10.01	-
4.	H-ZSM-5 (calcined at 1223K and poisoned with pyridine) (q_{py}=0.032 m.mol.g^{-1})	0.99	313	0.89	0.97	-
5.	H.Na-ZSM-5 (calcined at 773K) (N_A=0.07 m.mol.g^{-1})	0.45	283 298 328	0.13 0.29 1.89	0.14 0.31 2.04	50.24
6.	NH_4-ZSM-5 (dried at 423K)	0.99	313	2.29	2.48	-

(* Zeolite poisoned with the pyridine chemisorbed at 673K)

N_A = Number of strong protonic acid sites in the zeolite measured in terms of pyridine chemisorbed irreversibly at 673K.

q_{py} = Amount of pyridine (poison) in the zeolite channels.

in zeolite channel size at the channel intersections, where the pyridine molecules (as pyridinium ions) chemisorb on the protonic acid sites are expected to be located. The results on NH_4-ZSM-5 are much consistent with this. The diffusion in the zeolites is in the order - H-ZSM-5 > NH_4-ZSM-5 > pyridine poisoned H-ZSM-5, as the size of NH_4^+ is smaller than that of pyridinium ion (Fig. 3.11).

The observed influence of degree of cation exchange and calcination temperature on the diffusion is very much consistent with that observed for the desorptive diffusion of benzene in ZSM-5 zeolite [15] at higher temperature (523 K).

(d) Resistances for intracrystalline mass transfer in ZSM-5

The critical diameter of cumene molecule is 0.68 nm, which is the same as that of benzene molecule. However, the presence of isopropyl group (d = 0.56 nm) is expected to impart steric hindrance for the diffusion of cumene in the channels of ZSM-5, as shown schematically in Fig. 3.12. The diffusion of cumene in the direction of its isopropyl group is expected to be more sterically hindered than that in the direction of its benzene nucleus. This is because of the fact that the isopropyl group tends to expand in former case but tends to compress in the latter case, similar to a shuttle cock in shuttle box [17].

In the sorption of cumene in ZSM-5, apart from the diffusion of cumene inside the zeolite channels, the entrance of cumene into the zeolite channels is also expected to play an important role in controlling the overall intracrystalline mass transfer in the zeolite. Because of the reason discussed above, the entrance of cumene molecule in the direction of its benzene nucleus (eventhough the critical size of the benzene nucleus is somewhat higher than that of isopropyl group) is expected to be favoured.

The influence of the size of cation or strongly sorbed poison (which is expected to be located at the channel intersections) on the free space available (or resistance) for diffusion at channel intersections is illustrated in Fig. 3.11. The

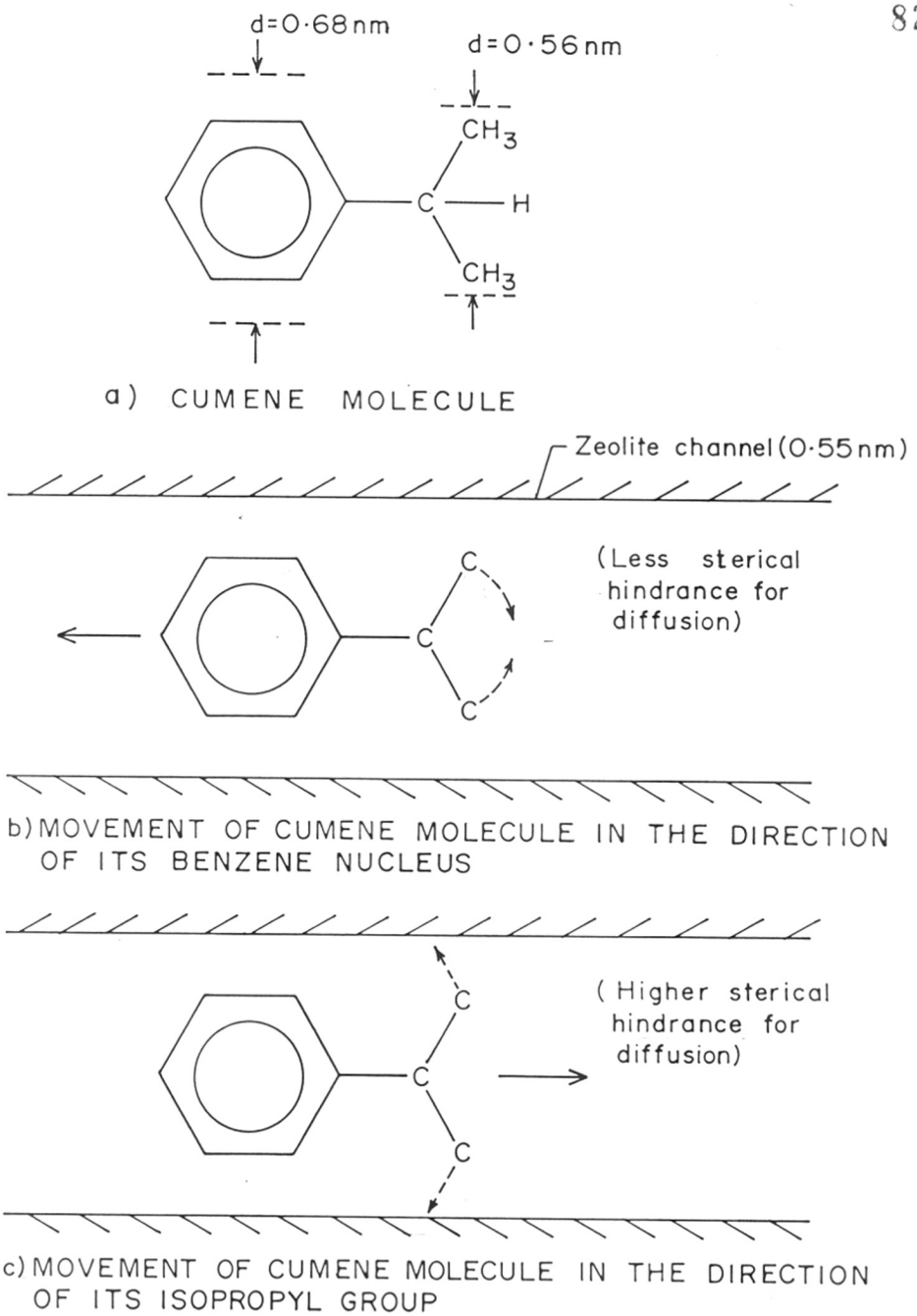

FIG. 3·12 STERICAL HINDRANCE FOR DIFFUSION OF CUMENE MOLECULE IN THE CHANNELS OF ZSM-5 ZEOLITE

diameter of space available at the channel intersections in ZSM-5 has been estimated to be about 0.9 nm [16], which is larger than the channel diameter (- 0.55 nm). The cations and/or acid sites and therefore, also poison molecules, are expected to be located at the channel intersections. The available space at the intersections is therefore,reduced depending upon the size of the located cations or poison molecules. The large decrease in the diffusivity of cumene due to the pyridine poisoning of H-ZSM-5 (Table-3.3) is a result of an increase in the steric hindrance for the diffusion at the channel intersections caused by reduction in channel diameter at the channel intersections and/or partial or complete blockage of some of the channels opening at the intersections. The partial and complete blockage of channel opening, which does not allow the diffusion to occur; causes decrease in the diffusivity due to increase in the tortuous path for the diffusion [18].

3.2.2 Diffusion in ZSM-8 Zeolites

A number of studies on the diffusion of various organic species in ZSM-5 zeolites have been reported (Table-1.3 in Chapter 1). However, so far only the diffusion of cyclohexane in H-ZSM-8 at 386 K has been reported [19].

The Q_t/Q_∞ vs. $\sqrt{t}$ plots for the sorption of pure cumene from the liquid phase in H-ZSM-8 and H.Na-ZSM-8 zeolites are shown in Fig. 3.13. Whereas, the sorption kinetics plots for the MgO.H-ZSM-8, P_2O_5.H-ZSM-8 and B_2O_3.H-ZSM-8 zeolites are presented in Figs. 3.14, 3.15 and 3.16, respectively. Values of the coefficient of diffusion of cumene in the ZSM-8 zeolites have been obtained using the $\sqrt{t}$ - law from the slopes of the initial linear section of the Q_t/Q_∞ vs. $\sqrt{t}$ plots. The values of diffusion coefficient (D) and energy of activation for the diffusion are given in Table-3.4. The activation energy for diffusion has been estimated from the temperature dependence of the diffusion (Fig. 3.17), according to the Arrhenius type expression (Eqn. 2).

In the present case, the sorption is expected to be controlled only by the intracrystalline mass transfer because the reduction in the zeolite particle size

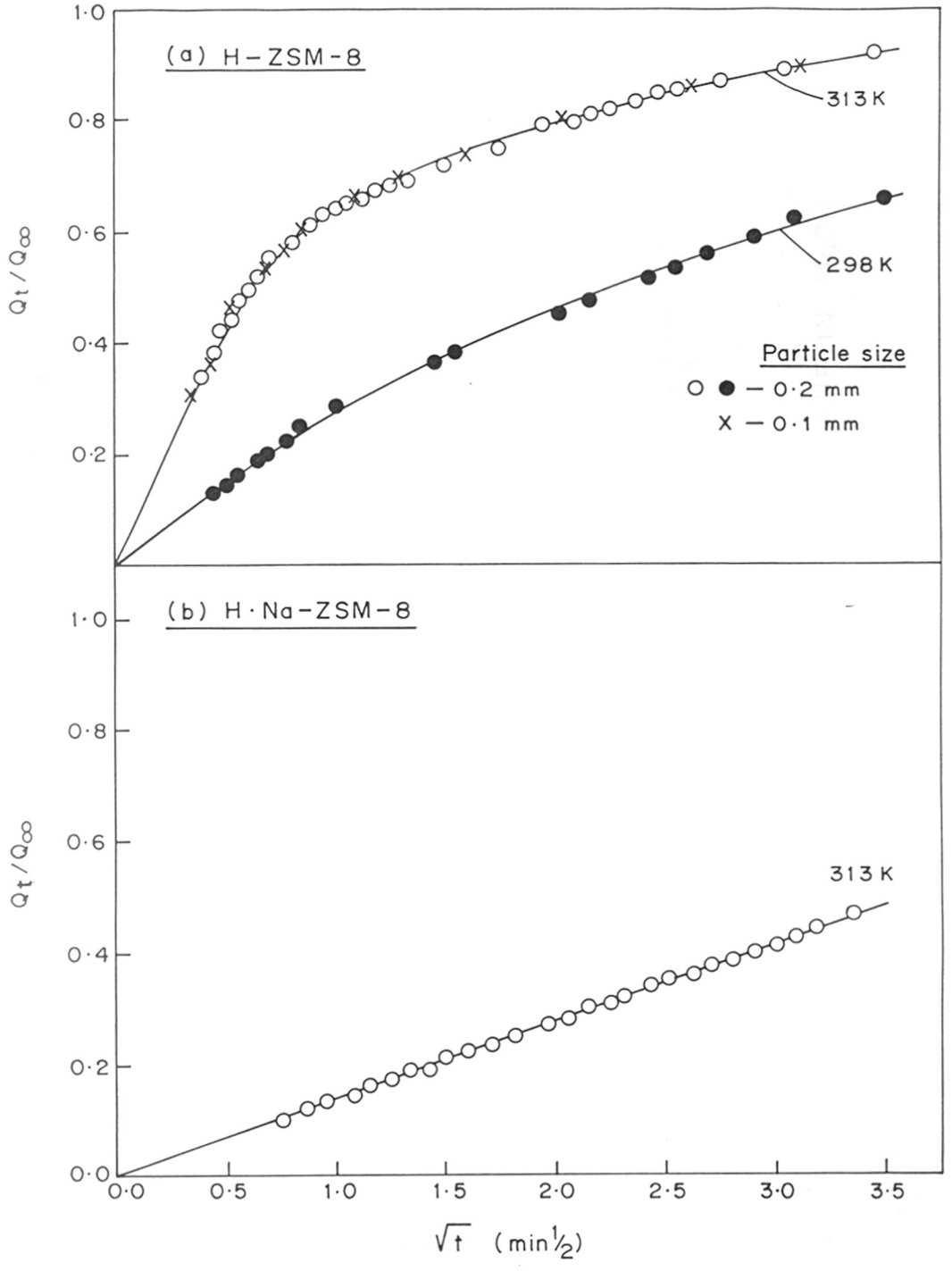

FIG. 3·13 : (a) Q_t/Q_∞ vs $\sqrt{t}$ PLOTS FOR THE SORPTION OF CUMENE IN H-ZSM-8
(b) Q_t/Q_∞ vs $\sqrt{t}$ PLOTS FOR THE SORPTION OF CUMENE IN H·Na-ZSM-8

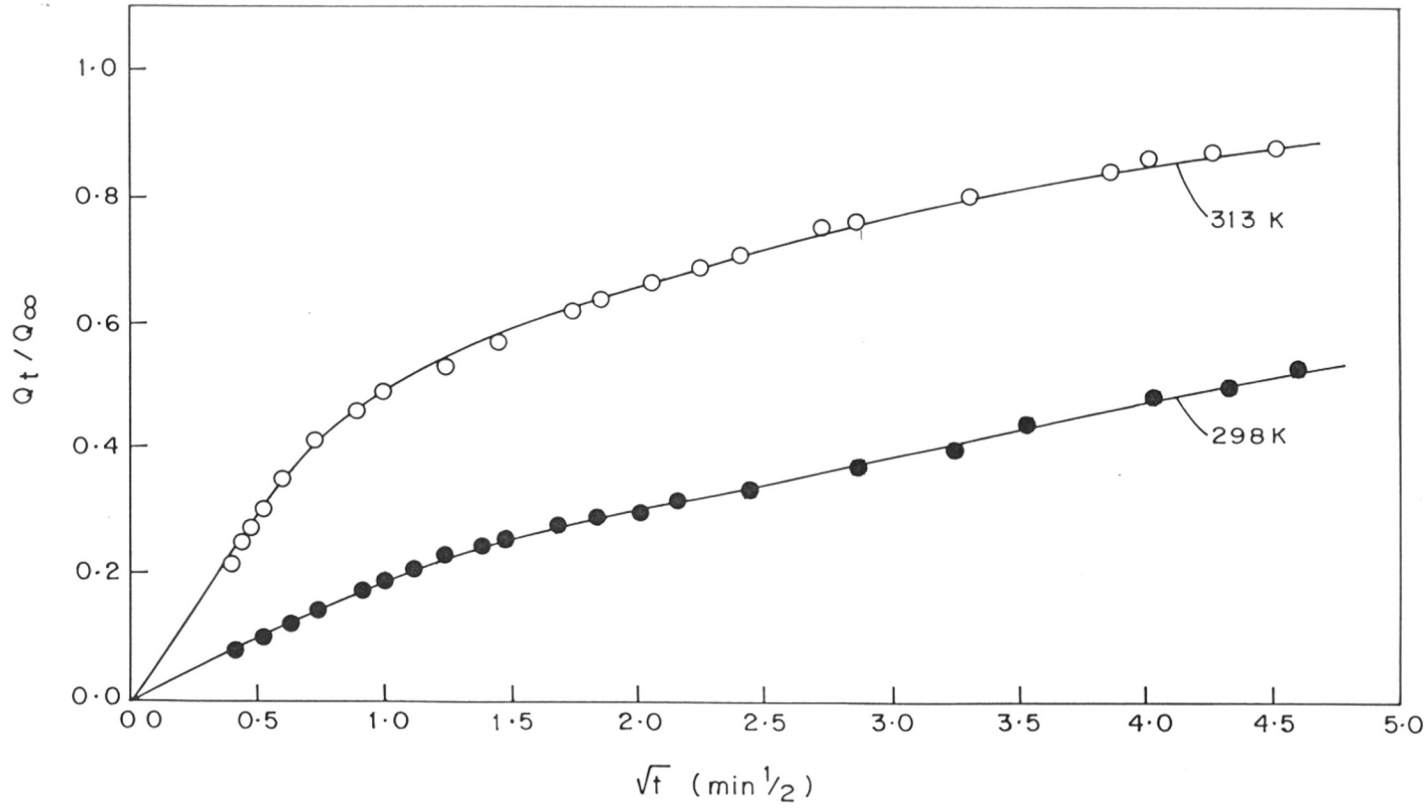

FIG. 3·14 : $Q_t/Q\infty$ vs $\sqrt{t}$ PLOTS FOR THE SORPTION OF CUMENE IN MgO-H-ZSM-8 AT DIFFERENT TEMPARATURES

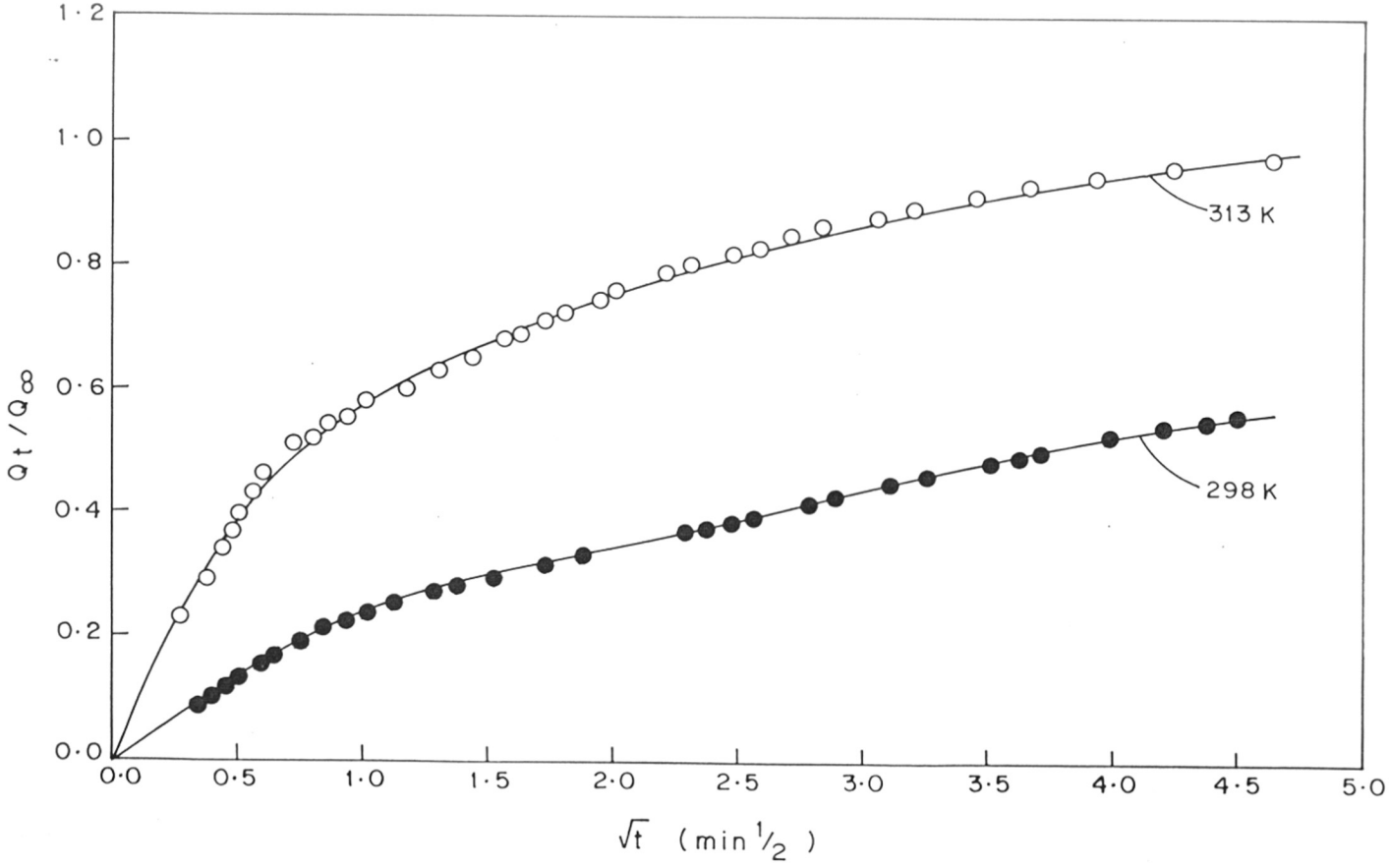

FIG. 3·15: $Q_t / Q\infty$ vs $\sqrt{t}$ PLOTS FOR THE SORPTION OF CUMENE IN P_2O·H-ZSM-8 AT DIFFERENT TEMPERATURES

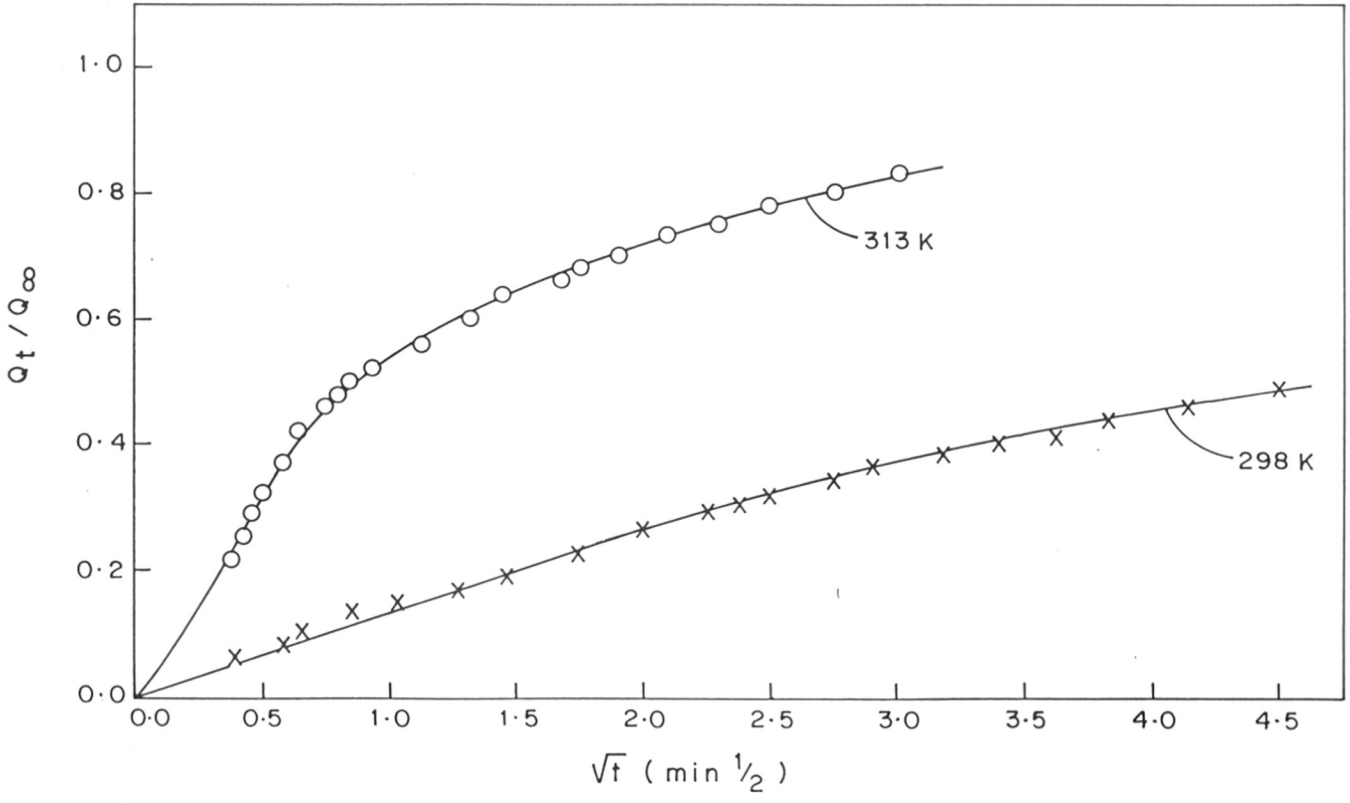

FIG. 3·16 : Q_t / Q_∞ vs $\sqrt{t}$ PLOT FOR THE SORPTION OF CUMENE IN B_2O_3·H-ZSM-8 AT DIFFERENT TEMPERATURES

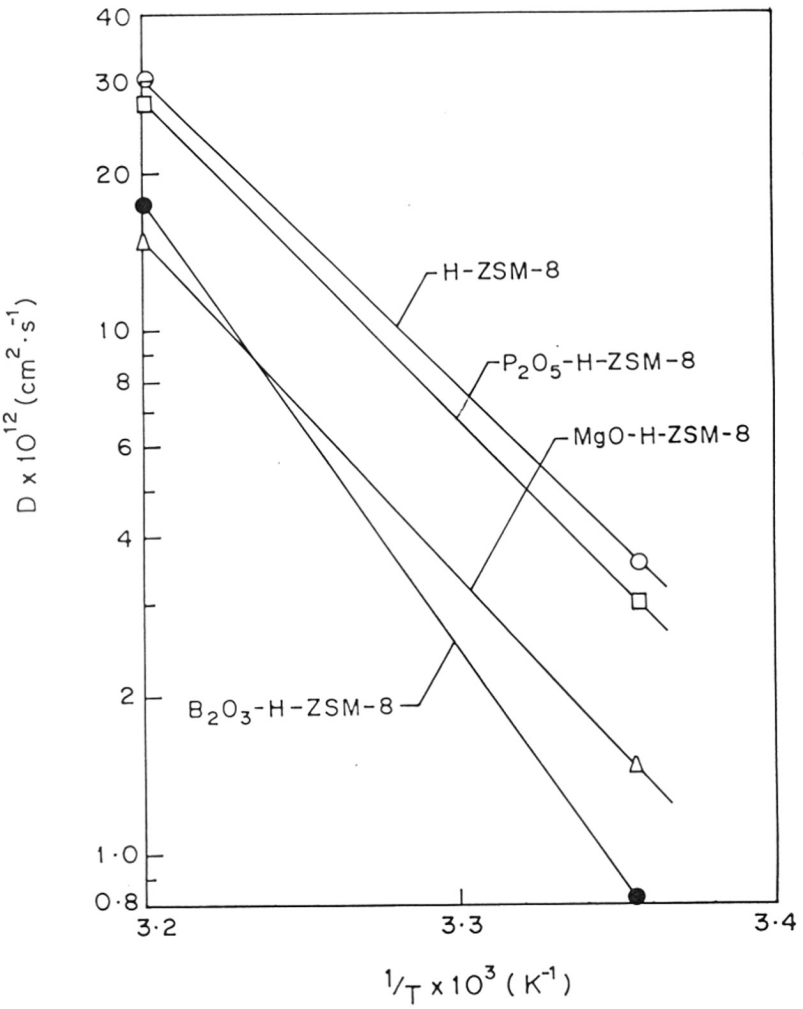

FIG. 3·17 : TEMPERATURE DEPENDENCE OF DIFFUSION OF CUMENE IN H-ZSM-8 AND MODIFIED H-ZSM-8 ZEOLITES

from 0.2 to 0.1 mm showed no significant effect on the sorption kinetics (Fig. 3.13(a)). Thus, there was no influence of intercrystalline (macropore diffusional) mass transfer on the sorption process.

The results (Table-3.4) reveal that the diffusion of cumene in H-ZSM-8 and modified H-ZSM-8 zeolites is highly activated one and it is strongly influenced by the degree of H^+ exchange (α) of H.Na-ZSM-8 and also by the modification of H-ZSM-8 zeolite.

(a) Influence of cation exchange

A comparison of the diffusion data (Table-3.4) for H-ZSM-8 (α = 0.96) and H.Na-ZSM-8 (α = 0.08) shows that the diffusion in the latter zeolite is very much slower. The large decrease in the diffusivity due to increase in the Na^+ content of the zeolite is expected to be mostly due to stronger interaction of π electrons of the benzene nucleus of cumene with the Na^+ cations than with H^+ cations in the zeolite. Earlier studies have indicated that aromatics are sorbed more strongly on Na-ZSM-5 [15,20] and Na-ZSM-8 [17] than on the zeolites in their H-form. The larger size of Na^+ cation (size of H^+ is negligible) may also cause a small but significant reduction in the channel size and consequently reduce the diffusivity to some extent.

(b) Influence of modification

The results (Table-3.4) clearly show that the modification of H-ZSM-8 by MgO, P_2O_5 or B_2O_3 causes reduction in the diffusivity and increase in the activation energy for the diffusion.

In the process of the modification of zeolite, the deposition of extrazeolitic material (viz. MgO, P_2O_5 or B_2O_3) is expected to occur on both the external and internal surface of the zeolite crystals. The deposition on the external surface may cause a complete and/or partial blockage of some of the channel openings. Whereas, the deposition on the internal surface may result in a complete and/or partial blockage of some of the zeolite channels and also cause a reduction in channel size,

TABLE-3.4

Data on the Diffusion of Liquid Cumene in ZSM-8 and Modified ZSM-8 Zeolites

(Si/Al = 29.6, Degree of H^+-exchange = 0.96, precalcination temperature = 773K, Crystal size : 3.5 um)

Zeolite	Concentration of MgO, P_2O_5 or B_2O_3 (wt.%)	No. of strong acid sites, NA ($m.mol.g^{-1}$)	Diffusion data			Activation energy, E ($kJ.mol^{-1}$)
			Temperature (K)	$(D/r^2)x\ 10^4$ (s^{-1})	$D\ x\ 10^{12}$ ($cm^2.s^{-1}$)	
H-ZSM-8 (α = 0.96)	-	0.29	298	1.19	3.63	113.4
			313	10.10	30.1	
H.Na-ZSM-8 (α = 0.08)	-	0.07	313	0.38	1.17	-
MgO.H-ZSM-8	0.10	0.23	298	0.69	1.44	123.8
			313	4.81	14.73	
P_2O_5.H-ZSM-8	0.41	0.11	298	0.98	3.01	116.9
			313	9.08	27.81	
B_2O_3.H-ZSM-8	5.4	0.20	298	0.27	0.83	163.2
			313	5.60	17.13	

particularly at channel intersections. These changes in the zeolite resulting from its modification are responsible for the observed decrease in the diffusivity and the increase in the activation energy of the diffusion. The extent to which the diffusion in the zeolite is influenced by its modification may depend on a number of factors such as - (1) concentration of modifying agent and the procedure of its deposition, (2) location of the deposition (viz. external surface, channel walls, channel intersections), (3) distribution of modifying agent in the zeolite crystals (i.e. uniform distribution or concentration changing from external surface to the centre of zeolite crystals), (4) dispersion of modifying agent (or its average crystal size), and other unknown factors.

For the diffusion of cumene in the zeolite, the isopropyl group of the sorbate is expected to impart larger steric hindrance when the channel diameter and/or the size of channel opening are decreased even to a small extent due to the modification. Hence, the modification causes an increase in the activation energy for the diffusion.

(c) Comparison of diffusion in H-ZSM-5 and H-ZSM-8 zeolites

The Si/Al ratio and degree of H^+ exchange of H-ZSM-8 (Si/Al = 29.6; α = 0.96) and H-ZSM-5 (Si/Al = 31.1; α = 0.99) are more or less the same. Therefore it would be interesting to compare the diffusion of cumene in the two zeolites.

A comparison of the data on diffusion (Tables-3.3 and 3.4) shows that the diffusion of cumene in H-ZSM-8 is much faster than that in H-ZSM-5. Also, the diffusion in H-ZSM-8 is highly activated one as compared to that in H-ZSM-5. This reveals that there is a significant difference in the channel structure of the two zeolites. A similar conclusion was drawn earlier from the studies on sorbate selectivity [17] and acidic and catalytic properties [21] of the two zeolites.

It may be noted that the observed higher diffusivity of cumene in H-ZSM-8 is consistent with that observed for cyclohexane (at 368 K) in H-ZSM-8 (D = 2 x

10^{-12} cm^2 s^{-1}) and in H-ZSM-5 ($D = 0.6 \times 10^{-12}$ cm^2 s^{-1}) by Chou et al. [19].

3.3 CATALYTIC ACTIVITY OF MODIFIED H-ZSM-8 ZEOLITES

Catalytic activity of H-ZSM-8 and MgO-, P_2O_5- and B_2O_3- modified H-ZSM-8 zeolites in hydrocarbon conversion (viz. cumene cracking and o- and m- xylene isomerisation) and alcohol (viz. methanol and ethanol) conversion reactions has been investigated using a pulse microreactor attached to a gas chromatograph. For the purpose of comparison, the catalytic properties of the zeolites have been determined under identical experimental conditions.

3.3.1 Cracking of Cumene

Cumene cracking on the zeolites was studied at the following experimental conditions:

Reaction temperature	673 K
Amount of catalyst	50 mg
N_2 flow rate	1 $dm^3.min^{-1}$
Pressure	180 kPa
Pulse size	8 ul

Results of the cumene cracking on the ZSM-8 zeolites are given in Table-3.5. The cumene cracking activity of the zeolites is found to be in the following order:

B_2O_3.H-ZSM-8 > P_2O_5-ZSM-8 > H-ZSM-8 > MgO.H-ZSM-8

The lower activity of MgO.H-ZSM-8 is consistent with the decrease in the acidity (both weak and strong acid sites) of H-ZSM-8 by the addition of MgO. However, the higher observed activity for P_2O_5.H-ZSM-8 and B_2O_3.H-ZSM-8 is not at all consistent with their lower acidity (Table-3.2 and Fig. 3.4).

It may be noted that the formation of side products (viz. toluene and C_{9+} - aromatics) are greatly reduced after the modification of the zeolite. This is mostly due to the reduction in the number of strong acid sites on the zeolite after its

TABLE-3.5

Distribution of Hydrocarbons in the Conversion of Cumene on H-ZSM-8 and Modified H-ZSM-8 Zeolites

(Reaction conditions: Amount of catalyst - 50 mg; N_2-flow rate - 1.0 $dm^3.min^{-1}$; Pressure - 180 kPa; Temperature - 673K; Pulse size - 8 ul)

	H-ZSM-8	MgO.H-ZSM-8	B_2O_3-H-ZSM-8	P_2O_5.H-ZSM-8
Conversion of cumene (%)	17.57	15.72	34.80	27.40
Distribution of hydrocarbons (wt.%)				
Aliphatics	3.44	3.66	8.85	7.70
Benzene	7.38	9.16	22.73	16.73
Toluene	1.37	0.15	0.35	0.14
Cumene	82.43	84.28	65.20	72.60
C_{9+} - aromatics	5.38	2.75	2.87	2.83
Total	100.00	100.00	100.00	100.00

modification.

3.3.2 Isomerisation of O-xylene

O-xylene isomerisation on the zeolites was carried out at the following conditions:

Reaction temperature	*673 K*
Amount of catalyst	*50 mg*
N_2 *flow rate*	*200 ml. min*$^{-1}$
Pressure	*180 kPa*
Pulse size	*6 ul*

Product distribution in the conversion of o-xylene on the ZSM-8 zeolites is shown in Table-3.6. A comparison of the results (Table-3.6) on the zeolites indicates the following:

1. The zeolite modification by MgO, P_2O_5 *and* B_2O_3 *causes a significant change in the product distribution.*

2. The conversion of xylene (or xylene isomerisation activity) on the zeolites is in the following order:

$$B_2O_3.H\text{-}ZSM\text{-}8 > P_2O_5.H\text{-}ZSM\text{-}8 > H\text{-}ZSM\text{-}8 > MgO.H\text{-}ZSM\text{-}8$$

which is the same as that for the case of cumene cracking. The observed xylene isomerisation activity of the modified zeolites (except MgO.H-ZSM-8) is not consistent with their acidity.

3. The selectivity for o-xylene isomerisation is higher (or the xylene loss is lower) for the modified zeolites than that for H-ZSM-8. This is mostly because of the reduction in the number of strong acid sites (which are required for the cracking/dealkylation and disproportionation reactions) on the zeolite after its modification.

TABLE-3.6

Distribution of Hydrocarbons in the Conversion o-Xylene on H-ZSM-8 and Modified H-ZSM-8 Zeolites

(Reaction conditions : Amount of catalyst - 50 mg; N_2-flow rate - 200 $cm^3.min^{-1}$; Pressure = 180 kPa ; Temperature - 673 K ; Pulse size - 6 ul)

	H-ZSM-8	MgO.H-ZSM-8	B_2O_3.H-ZSM-8	P_2O_5.H-ZSM-8
Conversion of o-xylene (%)	9.85	8.41	15.67	11.25
Distribution of hydrocarbons (wt.%)				
Aliphatics	0.37	0.41	0.14	0.10
Benzene	0.18	-	0.07	-
Toluene	0.63	0.28	0.54	0.33
p-Xylene	4.46	5.70	5.37	6.72
m-Xylene	4.17	2.02	9.46	4.10
o-Xylene	90.15	91.59	84.33	88.75
C_{9+}.... Aromatics	0.04	-	0.09	-
Total	100.00	100.00	100.00	100.00
p-X/m-X ratio	1.07	2.82	0.56	1.64
Selectivity for m- & p-xylenes	87.6	91.80	94.64	96.17

4. The distribution of xylenes (i.e. p-X/m-X ratio) indicates that the para selectivity of the zeolites is in the following order:

$$MgO.H\text{-}ZSM\text{-}8 > P_2O_5.H\text{-}ZSM\text{-}8 > H\text{-}ZSM\text{-}8 > B_2O_5.H\text{-}ZSM\text{-}8$$

This indicates that the modification of H-ZSM-8 by MgO and P_2O_5 has resulted in the increase in the shape-selectivity of the zeolite. Whereas, the modification by B_2O_3 has opposite effect.

3.3.3 Isomerisation of m-xylene

m-Xylene isomerisation on the ZSM-8 zeolites was investigated at the following conditions:

Reaction temperature	673 K
Amount of catalyst	50 mg
N_2 flow rate	300 $ml.min^{-1}$
Pressure	180 kPa
Pulse size	6 ul

The results of the m-xylene isomerisation on the zeolites are presented in Table-3.7. The observations made from the results (Table-3.7) are quite similar to those for the o-xylene isomerisation. The results are summarised below.

1. The conversion of m-xylene on the zeolites is in the following order:

$$B_2O_3.H\text{-}ZSM\text{-}8 > P_2O_5.H\text{-}ZSM\text{-}8 > H\text{-}ZSM\text{-}8 > MgO.H\text{-}ZSM\text{-}8$$

which is the same as that observed in case of the cumene cracking and o-xylene isomerisation. The higher activity of B_2O_3 and P_2O_5 modified zeolites is not consistent with the lower acidity of the zeolite.

2. The selectivity for the o-xylene isomerisation is higher for the modified zeolites. This is consistent with that observed for the o-xylene isomerisation on

TABLE-3.7

Distribution of Hydrocarbons in the Conversion of m-Xylene on H-ZSM-8 and Modified H-ZSM-8 Zeolites

(Reaction conditions : Amount of Catalyst - 50 mg; N_2-flow rate - 300 $cm^3.min^{-1}$; Pressure - 180 kPa ; Temperature - 673 K ; Pulse size - 6 ul)

	H-ZSM-8	MgO.H-ZSM-8	B_2O_3.H-ZSM-8	P_2O_5.H-ZSM-8
Conversion of m-xylene (%)	9.14	7.41	28.14	17.82
Distribution of hydrocarbons (wt.%)				
Aliphatics	0.09	0.05	0.05	0.16
Benzene	0.12	0.05	0.03	0.32
Toluene	0.89	0.65	1.02	0.86
p-Xylene	4.48	3.91	8.24	12.96
m-Xylene	90.86	92.59	78.86	82.18
o-Xylene	3.26	2.67	11.71	3.40
C_{9+} .... Aromatics	0.30	0.08	0.09	0.12
Total	100.00	100.00	100.00	100.00
p-X/o-X ratio	1.37	1.46	0.70	3.81
Selectivity for p- and m- xylenes	84.6	88.7	94.37	91.80

the zeolites.

3. The para shape-selectivity of the zeolites is in the following order:

$$P_2O_5.H\text{-}ZSM\text{-}8 > MgO.H\text{-}ZSM\text{-}8 > H\text{-}ZSM\text{-}8 > B_2O_3.H\text{-}ZSM\text{-}8$$

3.3.4 Methanol-to-Aromatics Conversions

The methanol conversion on the zeolites was carried out at the following reaction conditions:

Reaction temperature	*673 K*
Amount of catalyst	*50 mg*
N_2 *flow rate*	*30* $ml.min^{-1}$
Pressure	*180 kPa*
Pulse size	*1.0 ul*

The distribution of hydrocarbons formed in the methanol conversion on the zeolites is given in Table-3.8. The dependence of the aromatization in the methanol conversion over the zeolites on their strong acid sites (measured in terms of pyridine chemisorbed at 673 K) is shown in Fig. 3.18. The results (Table-3.8 and Fig. 3.18) reveal the following information.

1. The conversion of methanol to hydrocarbons on the zeolites is complete (i.e. 100%).

2. The extent of aromatization on the zeolites is in the following order:

$$H\text{-}ZSM\text{-}8 > MgO.H\text{-}ZSM\text{-}8 > B_2O_3.H\text{-}ZSM\text{-}8 > P_2O_5.H\text{-}ZSM\text{-}8$$

Thus the aromatization activity of ZSM-8 zeolite increases with the number of strong acid sites on the zeolite, as shown in Fig. 3.18. This is very much consistent with that observed earlier in the conversion of methanol on ZSM-8 [21] and ZSM-5 [4,22,23] zeolites.

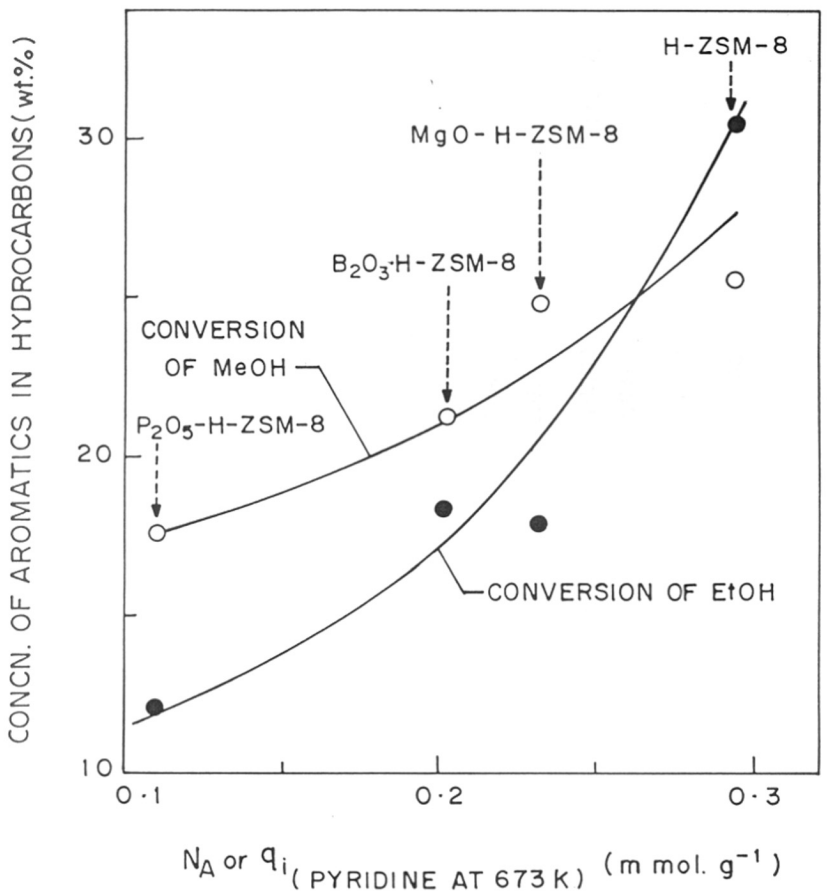

FIG. 3·18: DEPENDENCE OF AROMATIZATION ACTIVITY OF ZSM-8 ZEOLITES (IN METHANOL AND ETHANOL CONVERSIONS) ON THEIR ACIDITY (STRONG ACID SITES)

TABLE-3.8

Distribution of Hydrocarbons in the Conversion of Methanol on H-ZSM-8 and Modified H-ZSM-8 Zeolites

(Reaction conditions : Amount of catalyst - 50 mg; N_2-flow rate - $30 cm^3.min^{-1}$; Pressure - 180 kPa ; Temperature - 673 K ; Pulse size - 1.0 ul)

	H-ZSM-8	MgO.H-ZSM-8	B_2O_3.H-ZSM-8	P_2O_5.H-ZSM-8
Conversion of methanol to hydrocarbons (%)	100.00	100.00	100.00	100.00
Distribution of hydrocarbons (wt.%)				
Aliphatics	74.42	75.31	78.79	82.43
Benzene	2.22	1.87	1.64	2.18
Toluene	8.92	7.91	6.19	6.53
Ethyl benzene	1.27	0.55	0.08	0.30
p-Xylene	3.31	3.76	2.39	1.44
m-Xylene	5.61	5.15	6.81	3.69
o-Xylene	1.69	1.61	2.97	1.78
(Total xylenes)	(10.61)	(10.52)	(12.17)	(6.91)
C_{9+} .... Aromatics	2.55	3.84	3.13	1.67
(Total aromatics)	(25.58)	(24.69)	(21.21)	(17.57)
Total	100.00	100.00	100.00	100.00
Distribution of xylenes				
p-X/m-X	0.59	0.73	0.35	0.39
p-X/o-X	1.96	2.33	0.80	0.80

3. *From the distribution of xylenes (i.e. from p-X/m-X and p-X/o-X ratios), the para selectivity of the zeolites is found to be in the following order:*

$MgO.H\text{-}ZSM\text{-}8 > H\text{-}ZSM\text{-}8 > P_2O_5.H\text{-}ZSM\text{-}8 > B_2O_3.H\text{-}ZSM\text{-}8$

It is interesting to note that the shape-selectivity of H-ZSM-8 is increased by its modification with MgO but not with P_2O_5 *and* B_2O_3.

3.3.5 Ethanol-to-Aromatics Conversion

The ethanol conversion on the zeolites was studied at the following reaction conditions:

Reaction temperature	*673 K*
Amount of catalyst	*50 mg*
N_2 *flow rate*	$30\ ml.min^{-1}$
Pressure	*180 kPa*
Pulse size	*1.0 ul*

The product distribution in the ethanol conversion on the ZSM-8 zeolite is presented in Table-3.9 and the variation in the aromatization with the strong acid sites of the zeolite is shown in Fig. 3.18. The main observations are summarised below.

1. *The conversion of ethanol to hydrocarbons on all the zeolites is complete (i.e. 100%).*

2. *The aromatisation activity of the zeolites is in the following order:*

$H\text{-}ZSM\text{-}8 > B_2O_3.H\text{-}ZSM\text{-}8 \gg MgO.H\text{-}ZSM\text{-}8 > P_2O_5.H\text{-}ZSM\text{-}8$

The increase in the extent of aromatization with the strong acid sites on the ZSM-8 zeolites (Fig. 3.18) is quite consistent with the observation made earlier in the ethanol conversion on ZSM-5 zeolites [4,22,23].

3. *The distribution of xylenes (p-X/m-X and p-X/o-X ratios) in the products*

TABLE-3.9

Distribution of Hydrocarbons in the Conversion of Ethanol on H-ZSM-8 and Modified H-ZSM-8 Zeolites

(Reaction conditions : Amount of catalyst - 50 mg ; N_2-flow rate - 30 $cm^3.min^{-1}$; Pressure - 180 kPa ; Temperature - 673 K ; Pulse size - 1.0 ul)

	H-ZSM-8	MgO.H-ZSM-8	B_2O_3.H-ZSM-8	P_2O_5.H-ZSM-8
Conversion of ethanol to hydrocarbons (%)	100.00	100.00	100.00	100.00
Distribution of hydrocarbons (wt.%)				
Aliphatics	69.49	82.03	81.59	88.08
Benzene	3.94	3.24	2.65	2.68
Toluene	11.46	6.75	7.55	5.35
Ethyl benzene	3.41	0.92	0.74	0.14
p-Xylene	1.52	3.17	1.67	0.78
m-Xylene	3.89	2.11	3.39	1.92
o-Xylene	2.69	0.23	1.63	0.82
(Total xylenes)	(8.10)	(5.51)	(6.68)	(3.52)
C_{9+} .... aromatics	3.60	1.55	0.78	0.23
(Total aromatics)	(30.51)	(17.97)	(18.41)	(11.92)
Total	100.00	100.00	100.00	100.00
Distribution of xylenes				
p-X/m-X ratio	0.39	1.50	0.49	0.40
p-X/o-X ratio	0.56	13.78	1.02	0.95

indicates that the para selectivity of the zeolites is in the following order:

$$MgO.H\text{-}ZSM\text{-}8 \gg B_2O_3.H\text{-}ZSM\text{-}8 > P_2O_5.H\text{-}ZSM\text{-}8 > H\text{-}ZSM\text{-}8$$

Thus, in case of the ethanol conversion, para selectivity of H-ZSM-8 is increased due to the modification by MgO to a very significant extent and also by P_2O_5 and B_2O_3 but to a smaller extent.

3.4 INFLUENCE OF MODIFICATION

3.4.1 Modification of H-ZSM-8 with MgO

The modification of H-ZSM-8 with MgO has resulted in the decrease in the acidity (both the total and strong acid sites), the intracrystalline diffusivity of cumene, and in the catalytic activity (in the cumene cracking, o- and m- xylene isomerisation and aromatization in methanol and ethanol conversion reactions) of the zeolite. Whereas, the shape-selectivity or para selectivity of the zeolite is increased markedly after the modification eventhough the concentration of MgO in the zeolite is quite low (0.1%).

The decrease in the acidity after the modification of the zeolite is mostly because of blocking the intracrystalline acid sites located at the channel intersections by MgO. The decrease in the diffusivity of cumene is attributed to the presence of MgO in the zeolite channels, particularly at channel intersections. This is expected to result in a reduction in the effective channel diameter. The reduction in the effective channel diameter is also responsible for the observed higher para selectivity in the xylene isomerisations and the alcohol conversion reactions. The decrease in catalytic activity (in the hydrocarbon and alcohol conversion reactions) of H-ZSM-8 after the modification is consistent with the decrease of the acidity of the zeolite. All this results point to the fact that the deposition of MgO in the modified zeolite was mostly in the zeolite channels.

3.4.2 Modification of H-ZSM-8 with P_2O_5

The modification of H-ZSM-8 with P_2O_5 has resulted in the decrease in the acidity (both the total and strong acid sites), the intracrystalline diffusivity of cumene and in the aromatisation activity (in both the alcohol conversion reactions) of the zeolite. However, the cumene cracking and o- and m- xylene isomerisation activity of the zeolite is increased and also the para selectivity in the xylene isomerisation and ethanol conversion is increased after the modification.

The decrease in acidity after the modification is because of the blockage of intracrystalline acid sites by P_2O_5. The decrease in the cumene diffusivity and the increase in the para selectivity in the above reaction are attributed to the reduction in the effective channel diameter due to deposition of P_2O_5 in the zeolite channel and also may be due to partial blocking of the channel opening due to the deposition of P_2O_5 on the external surface of the zeolite crystals.

The higher activity in cumene cracking and xylene isomerisation after the modification is expected to be mostly due to the occurrence of the catalytic reactions on the external acid sites created due to the deposition of P_2O_5 on the external surface of zeolite crystals. This is supported by the fact that the aromatization activity [which requires strong acid sites [4,21,25]] in the alcohol conversions is greatly reduced after the modification. The strong acid sites are present only on the internal surface of the zeolite crystals and hence, there is no possibility of aromatization on the external surface. The decrease in the aromatization activity of the zeolite after modification is therefore consistent with the decrease in the strong acidity.

The intracrystalline mass transfer limitation on the methanol or ethanol conversion is expected to be less severe as compared to that on the cumene cracking and o-X and m-X isomerisation reactions. This is because of the fact that the critical molecular size of methanol and ethanol is much smaller and their intracrystalline diffusivity is expected to be much higher than that of the cumene, o-xylene and

p-xylene molecules. The observed higher cumene cracking and xylene isomerisation activity of the modified zeolite (with lower acidity than that possessed by the unmodified zeolite i.e. H-ZSM-8) is therefore because of the fact that the reaction occurs partly on the zeolite external surface and partly in the zeolite channels. There is little or no mass transfer limitation on the former but the latter is severely limited by the intracrystalline mass transfer. In case of the unmodified zeolite, the reaction which occurs mostly on the zeolite internal surface, is severely limited by the intracrystalline mass transfer, resulting in the lower conversion of reactant, inspite of the higher acidity of the zeolite. However, since the strong acid sites require for the aromatization in alcohol conversion are present only in the zeolite channels, the catalytic process is expected to be influenced by intracrystalline mass transfer to a larger extent on the modified zeolite than on the unmodified one. Therefore, the aromatization activity of H-ZSM-8 is much higher than that of the modified zeolite and is also consistent with the acidity (strong acid sites) of the zeolites.

3.4.3 Modification of H-ZSM-8 with B_2O_3

The modification of H-ZSM-8 with B_2O_3 has resulted in the decrease in the acidity (both the total and strong acid sites), the intracrystalline diffusivity of cumene and in the aromatization activity (in both the alcohol conversion reactions) of the zeolite but in the large increase in the conversion of cumene, o-xylene and m-xylene. In general, the shape-selectivity (or para selectivity) of H-ZSM-8 in the above reactions is reduced after the modification. These observations indicate that a large part of the cumene cracking and xylene isomerisation reactions occurs on the external surface of the zeolite crystals. Because of the high concentration of B_2O_3 in the modified zeolite, the deposition of B_2O_3 on the external surface of the zeolite crystals is expected to be very high resulting in the creation of a large number of active sites on the external surface. These external active sites are responsible for the observed higher activity of the modified zeolite in the cumene cracking

and xylene isomerisation reactions. Detailed explanation for this and influence of intracrystalline mass transfer on the catalytic reactions have been given earlier for the case of P_2O_5 modified zeolite. It may be noted that the lower shape-selectivity of the B_2O_3 modified zeolite even in the alcohol conversion reactions is mostly due to the interconversion (i.e. isomerisation) of xylenes formed in the zeolite channels on the external sites leading to almost an equilibrium mixture of xylenes.

REFERENCES

1. *Choudhary, V.R., and Nayak, V.S., Appl. Catal. 4, 31 (1982).*

2. *Choudhary, V.R., J. Chromatogr., 268, 207 (1983).*

3. *Nayak, V.S., and Choudhary, V.R., Appl. Catal. 4, 333 (1982).*

4. *Nayak, V.S., and Choudhary, V.R., J. Catal., 81, 26 (1983).*

5. *Choudhary, V.R., and Nayak, V.S., Zeolites, 5, 15 (1985).*

6. *Auroux, A., Sayed, M.B., Vedrine, J.C., Thermochim. Acta. 93, 557 (1985).*

7. *Sayed, M.B., Auroux, A., Vedrine, J.C., Appl. Catal. 23(1), 49 (1986).*

8. *Auroux, A., Sayed, M.B., Vedrine, J.C., Thermochim. Acta. 93, 557 (1985).*

9. *Lercher, J.A., Rumplmyr, G., Noller, H., Acta. Phys. Chem., 31, 71 (1985).*

10. *Derewenski, M., Haber, J., Pataszynski, J., Shiralkar, V.P., Dzwigaj, S., Stud. Surf. Sci. Catal. 18, 209 (1984).*

11. *Lercher, J.A., and Rumplmyr, G., Appl. Catal., 25, 215 (1986).*

12. *Chen, L., Sun, D., Wang, J., Wang, X., Dalian Gongxueyum Xuebao, 25(3), 33 (1986).*

13. *Musa, M., Goidea, D., Blum, J., Mihilescu, M., Goidea, N., Georghe, G., Russu, R., Manoiu, D., Stud. Surf. Sci. Catal. 23, 205 (1985).*

14. *Barrer, R.M., Adv. Chem. Ser., 102, 21 (1971).*

15. *Choudhary, V.R., and Srinivasan, K.R., J. Catal. 102, 328 (1986).*

16. *Derouane, E.G., and Gabelica, Z., J. Catal., 65, 486 (1980).*

17. *Choudhary, V.R., and Akolekar, D.B., J. Catal. (communicated).*

18. *Theodorou, D., and Wei, J., J. Catal. 83, 205 (1983).*

19. *Chou, H., Ahu, B.J., Park, S.E., Int. Congr. Catal. (Proc.), 8th 4, IV-555, (1984).*

.....

20. Choudhary, V.R., Srinivasan, K.R., and Singh, A.P., J. Catal. (communicated).

21. Akolekar, D.B., and Choudhary, V.R., J. Catal. 105, 416 (1987).

22. Nayak, V.S., and Choudhary, V.R., Appl. Catal. 10, 137 (1984).

23. Choudhary, V.R., and Nayak, V.S., Zeolites, 5, 325 (1985).

24. Nayak, V.S., and Choudhary, V.R., Appl. Catal., 9, 251 (1984).

APPENDICES

APPENDIX-1

Data on Kinetics of Cumene (Liquid) Sorption in H-ZSM-5 (calcined at 773K at 283 and 298K

T = 283 K		T = 298 K	
Time, t (min.)	$\frac{h^*}{h^*(max.)}$	Time, t (min.)	$\frac{h^*}{h^*(max.)}$
1	2	3	4
0.00	0.00	0.00	0.00
0.13	0.162	0.20	0.128
0.18	0.183	0.27	0.143
0.22	0.204	0.37	0.158
0.25	0.215	0.40	0.173
0.30	0.225	0.43	0.188
0.38	0.246	0.48	0.203
0.42	0.256	0.53	0.218
0.45	0.267	0.63	0.233
0.53	0.278	0.80	0.248
0.57	0.288	0.92	0.263
0.65	0.298	1.03	0.278
0.73	0.309	1.22	0.293
0.83	0.319	1.72	0.308
0.92	0.330	1.87	0.323
1.07	0.340	2.22	0.353
1.22	0.350	2.48	0.369
1.35	0.361	3.37	0.413
1.53	0.372	3.80	0.428
1.73	0.382	4.23	0.443
1.93	0.393	4.58	0.459
2.25	0.403	5.42	0.473
2.78	0.424	6.08	0.519
3.10	0.434	6.52	0.533
3.75	0.445	7.33	0.564
4.18	0.471	8.57	0.594
4.57	0.466	9.62	0.624
5.08	0.476	11.7	0.639
5.58	0.487	12.28	0.654
6.17	0.497	14.78	0.669
6.88	0.508	17.92	0.691
7.57	0.518	18.75	0.699
8.33	0.529	20.30	0.706
9.08	0.540	21.08	0.714
9.97	0.550	23.50	0.729
10.83	0.560	24.52	0.744
11.87	0.570	26.43	0.760
12.88	0.581	28.63	0.774
14.05	0.591	29.78	0.790
15.30	0.602	32.03	0.804

.....

Appendix-1 contd...

1	2	3	4
16.73	0.612	35.07	0.820
18.30	0.623	38.08	0.834
19.75	0.633	41.75	0.850
21.48	0.644	45.15	0.864
23.12	0.654	49.87	0.880
24.93	0.665	55.20	0.895
27.10	0.675	62.06	0.910
29.25	0.686	70.03	0.925
31.43	0.696	80.97	0.940
34.10	0.707	99.45	0.955
37.07	0.717	116.22	0.970
40.50	0.728	1227.25	1.0
43.18	0.738	1320.50	1.0
46.50	0.749		
50.12	0.756		
54.12	0.770		
58.13	0.780		
62.10	0.790		
66.17	0.801		
71.73	0.811		
77.83	0.822		
84.13	0.832		
90.42	0.843		
98.25	0.853		
107.77	0.863		
114.28	0.874		
1170.25	1.0		
1278.00	1.0		

APPENDIX-2

Data on Kinetics of Cumene (Liquid) Sorption in H-ZSM-5 (calcined at 773 K) at 313 and 328 K

313 K		328 K	
Time, t (min.)	$\frac{h^*}{h^* max.}$	Time, t (min.)	$\frac{h^*}{h^* max.}$
1	2	3	4
0.0	0.0	0.0	0.0
0.10	0.170	0.13	0.230
0.15	0.210	0.15	0.245
0.18	0.238	0.17	0.259
0.23	0.265	0.18	0.273
0.27	0.278	0.22	0.287
0.28	0.292	0.25	0.300
0.32	0.306	0.30	0.370
0.33	0.319	0.35	0.399
0.42	0.333	0.40	0.427
0.45	0.346	0.46	0.454
0.57	0.360	0.53	0.469
0.63	0.374	0.58	0.510
0.70	0.387	0.65	0.522
0.75	0.401	0.72	0.539
0.88	0.414	0.75	0.552
0.95	0.428	0.83	0.567
1.10	0.442	0.98	0.580
2.25	0.482	1.05	0.600
2.67	0.510	1.12	0.608
3.00	0.523	1.20	0.637
3.33	0.537	1.42	0.650
3.75	0.557	1.52	0.664
4.33	0.564	1.58	0.679
4.66	0.587	1.67	0.692
5.33	0.597	1.78	0.706
5.83	0.605	1.92	0.720
6.33	0.619	2.20	0.734
7.00	0.632	3.53	0.832
7.75	0.646	3.82	0.846
8.50	0.660	4.18	0.860
9.58	0.673	5.00	0.888
10.67	0.687	5.83	0.916
11.42	0.700	6.23	0.930
14.75	0.727	6.87	0.944
15.50	0.741	7.87	0.958
18.42	0.768	8.70	0.972
20.50	0.782	10.28	0.986
22.58	0.795	12.15	1.00

.....

Appendix-2 contd...

1	*2*	*3*	*4*
25.50	*0.809*	*22.50*	*1.00*
28.25	*0.823*	*30.33*	*1.00*
32.92	*0.836*		
36.92	*0.850*		
40.50	*0.863*		
45.75	*0.877*		
52.58	*0.891*		
64.75	*0.904*		
101.17	*0.931*		
188.42	*0.945*		
222.33	*0.959*		
243.75	*0.959*		
269.08	*0.959*		
1353.50	*0.972*		
2449.50	*0.972*		
1490.50	*1.0*		
1500.00	*1.0*		
1520.00	*1.0*		

APPENDIX-3

Data on Kinetics of Cumene (Liquid) Sorption in H-ZSM-5 Calcined at 773K and Poisoned with Pyridine

313 K		328 K	
Time, t (min.)	h^*/h^*_{max}	Time, t (min.)	h^*/h^*_{max}
1	2	3	4
0.0	0.0	0.0	0.0
0.15	0.088	0.10	0.107
0.25	0.104	0.17	0.124
0.32	0.120	0.20	0.140
0.40	0.136	0.25	0.150
0.48	0.152	0.317	0.173
0.58	0.168	0.38	0.190
0.72	0.184	0.48	0.207
0.87	0.200	0.58	0.273
1.02	0.216	0.70	0.240
1.22	0.232	0.80	0.257
1.38	0.248	0.93	0.272
1.65	0.264	1.27	0.305
1.95	0.280	1.58	0.339
2.25	0.293	1.80	0.355
2.50	0.312	1.98	0.372
2.83	0.328	2.22	0.389
3.17	0.344	2.45	0.405
3.58	0.360	2.73	0.421
4.07	0.376	3.02	0.439
4.58	0.392	3.30	0.454
5.20	0.408	3.67	0.471
5.70	0.424	4.07	0.488
6.43	0.44	4.38	0.504
7.33	0.456	4.82	0.520
8.13	0.472	5.27	0.537
9.00	0.488	5.80	0.553
9.97	0.504	6.42	0.570
11.08	0.52	7.05	0.581
12.25	0.54	7.72	0.601
15.42	0.57	8.47	0.621
17.15	0.58	9.35	0.642
19.10	0.60	10.38	0.650
21.13	0.610	11.42	0.671
23.75	0.630	12.58	0.681
26.13	0.651	14.13	0.701
29.50	0.660	15.50	0.720
32.62	0.681	17.00	0.732

.....

Appendix-3 contd....

1	2	3	4
37.13	*0.701*	*18.92*	*0.751*
47.78	*0.741*	*24.62*	*0.780*
50.25	*0.740*	*27.12*	*0.801*
57.25	*0.760*	*30.53*	*0.820*
124.50	*0.841*	*34.97*	*0.831*
900.25	*1.0*	*39.87*	*0.8512*
4485.33	*1.0*	*1320.18*	*1.0*
		1401.67	*1.0*
		1718.25	*1.0*
		3030.00	*1.0*

APPENDIX-4

Data on Kinetics of Cumene (Liquid) Sorption in H-ZSM-5 Calcined at 1223K

T = 313 K	
Time, t (min.)	$\frac{h^*}{h^*_{max}}$
0.00	0.00
0.05	0.181
0.10	0.251
0.15	0.280
0.20	0.310
0.25	0.341
0.30	0.370
0.35	0.401
0.40	0.421
0.47	0.430
0.53	0.451
0.60	0.462
0.70	0.481
0.77	0.492
0.87	0.510
0.95	0.521
1.05	0.542
1.20	0.551
1.32	0.570
1.50	0.581
1.67	0.601
1.85	0.612
2.23	0.630
2.68	0.661
3.0	0.670
3.80	0.701
4.30	0.722
5.06	0.730
5.68	0.751
6.65	0.761
7.88	0.780
9.10	0.792
29.17	0.860
30.82	0.871
75.83	0.891
214.30	0.920
241.06	0.931
249.58	0.925
415.50	0.940
4402.33	1.0

APPENDIX-5

Data on Kinetics of Cumene (Liquid) Sorption in H-ZSM-5 Calcined at 1223K and Poisoned with Pyridine

313 K		328 K	
Time, t (min.)	$\frac{h^*}{h^*_{max.}}$	Time, t (min.)	$\frac{h^*}{h^*_{max.}}$
1	2	3	4
0.0	0.0	0.0	0.0
0.23	0.125	0.05	0.191
0.32	0.140	0.17	0.210
0.37	0.151	0.20	0.241
0.48	0.170	0.25	0.272
0.53	0.182	0.32	0.280
0.60	0.201	0.35	0.291
0.82	0.235	0.40	0.301
0.98	0.250	0.47	0.320
1.12	0.261	0.52	0.331
1.25	0.283	0.57	0.340
1.43	0.295	0.63	0.350
1.60	0.310	0.72	0.370
1.83	0.322	0.87	0.381
2.20	0.350	0.93	0.392
2.47	0.375	1.03	0.401
2.75	0.380	1.13	0.420
3.13	0.401	1.25	0.430
3.43	0.410	1.38	0.442
3.90	0.435	1.60	0.451
4.33	0.450	1.73	0.470
4.87	0.468	1.87	0.481
5.45	0.480	2.03	0.492
6.17	0.493	2.20	0.510
6.88	0.510	2.42	0.523
7.58	0.522	2.63	0.531
8.43	0.540	2.92	0.541
9.67	0.550	3.50	0.571
10.97	0.570	3.78	0.582
12.22	0.581	4.17	0.595
13.83	0.601	4.57	0.607
15.83	0.621	5.00	0.620
20.53	0.652	5.52	0.633
23.53	0.663	6.10	0.645
26.97	0.681	6.78	0.658
31.20	0.692	7.45	0.671
37.60	0.711	8.17	0.683
46.50	0.720	9.18	0.697
55.67	0.740	11.27	0.721
66.40	0.751	12.52	0.734

.....

Appendix-5 contd...

1	2	3	4
77.38	0.770	14.15	0.747
95.62	0.782	15.78	0.760
125.83	0.801	17.60	0.772
130.25	0.850	36.66	0.835
4347.0	0.850	41.76	0.848
4506.75	0.912	48.92	0.866
5765.0	1.0	124.82	0.911
		209.88	0.936
		215.75	0.950
		220.25	1.0
		225.33	1.0
		575.00	1.0
		801.25	1.0

APPENDIX-6

Data on Kinetics of Cumene (Liquid) Sorption in Na.H-ZSM-5 at 283 and 298 K

283 K		298 K	
Time, t (min.)	$\frac{h^*}{h^*_{max.}}$	Time, t (min.)	$\frac{h^*}{h^*_{max.}}$
1	2	3	4
0.00	0.00	0.00	0.00
0.05	0.076	0.67	0.130
0.08	0.089	0.82	0.140
1.00	0.096	1.00	0.160
1.44	0.118	1.10	0.170
2.10	0.145	1.32	0.180
3.06	0.187	1.46	0.200
4.00	0.210	1.75	0.210
5.06	0.230	2.13	0.240
6.50	0.250	2.46	0.260
7.56	0.280	2.92	0.270
9.00	0.320	3.72	0.300
12.25	0.340	4.12	0.310
14.56	0.360	5.33	0.340
16.81	0.380	6.40	0.360
18.06	0.390	7.45	0.380
20.25	0.410	9.36	0.410
22.00	0.420	10.37	0.440
27.04	0.430	12.11	0.460
30.24	0.450	14.90	0.480
33.64	0.460	16.46	0.500
42.25	0.490	20.07	0.530
49.70	0.500	22.84	0.540
60.06	0.520	24.60	0.560
68.06	0.530	28.30	0.580
81.90	0.550	30.58	0.600
85.33	0.65	35.52	0.610
92.25	0.78	38.56	0.630
101.33	0.90	48.55	0.750
105.25	0.950	150.25	0.810
112.33	0.960	155.75	0.920
1200.25	0.970	160.33	0.975
1675.33	0.980	225.33	0.982
1579.0	0.992	525.45	0.988
1728.0	1.0	548.5	1.0

APPENDIX-7

Data on Kinetics of Cumene (Liquid) Sorption in Na.H-ZSM-5 at 328 K

Time, t (min.)	$\frac{h^*}{h^*_{max.}}$
1	2
0.0	0.0
0.18	0.161
0.25	0.178
0.28	0.210
0.33	0.226
0.38	0.242
0.43	0.258
0.50	0.274
0.60	0.290
0.78	0.322
1.0	0.355
1.15	0.371
1.25	0.387
1.36	0.403
1.50	0.419
1.67	0.435
1.85	0.451
2.05	0.468
2.25	0.484
2.52	0.500
2.80	0.516
3.07	0.532
3.33	0.549
3.60	0.564
3.90	0.581
4.28	0.596
4.70	0.613
5.17	0.629
5.67	0.645
6.27	0.661
6.78	0.678
7.53	0.693
8.32	0.710
9.40	0.726
10.17	0.742
11.33	0.758
12.67	0.774
14.11	0.790
15.70	0.807
17.58	0.822
20.13	0.839
23.05	0.854
26.92	0.870

.....

Appendix-7 contd...

1	2
41.23	*0.887*
55.45	*0.903*
96.23	*0.920*
145.17	*0.928*
155.25	*0.950*
1450.0	*0.9677*
1462.50	*0.9677*
1504.50	*0.9677*
2807.0	*1.0*
5557.0	*1.0*

APPENDIX-8

Data on Kinetics of Cumene (Liquid) Sorption in NH_4-ZSM-5 at 313 K

Time, t (min.)	$\frac{h^*}{h^*_{max.}}$	Time, t (min.)	$\frac{h^*}{h^*_{max.}}$
0.00	0.00		
0.13	0.140	9.58	0.612
0.18	0.180	10.67	0.633
0.27	0.201	11.92	0.645
0.28	0.210	13.83	0.650
0.32	0.230	14.33	0.671
0.33	0.240	16.0	0.682
0.35	0.250	18.85	0.701
0.40	0.270	19.92	0.713
0.45	0.281	22.83	0.724
0.62	0.300	24.60	0.745
0.77	0.313	27.0	0.756
0.85	0.325	30.75	0.766
1.0	0.345	34.05	0.788
1.11	0.350	38.17	0.790
2.05	0.410	41.33	0.806
2.43	0.436	50.41	0.822
2.50	0.450	59.50	0.834
3.08	0.460	92.50	0.855
3.60	0.483	98.50	0.876
4.50	0.530	143.67	0.898
6.37	0.545	192.75	0.902
7.17	0.576	272.08	0.917
7.75	0.593	1273.75	1.0
8.67	0.601		

APPENDIX-9

Data on Kinetics of Cumene (Liquid) Sorption in H-ZSM-8 at 298 and 313 K

298 K		313 K	
Time, t (min.)	$\frac{h^*}{h^*_{max.}}$	Time, t (min.)	$\frac{h^*}{h^*_{max.}}$
1	2	3	4
0.0	0.0	0.0	0.0
0.20	0.128	0.07	0.286
0.27	0.143	0.17	0.339
0.36	0.158	0.20	0.380
0.40	0.173	0.23	0.415
0.43	0.188	0.28	0.444
0.48	0.203	0.32	0.473
0.53	0.218	0.38	0.497
0.63	0.233	0.42	0.520
0.80	0.248	0.47	0.543
0.92	0.263	0.53	0.555
1.03	0.278	0.58	0.567
1.22	0.293	0.63	0.579
1.72	0.308	0.70	0.590
1.87	0.323	0.77	0.602
2.22	0.353	0.82	0.614
2.48	0.368	0.90	0.625
3.37	0.413	1.02	0.637
3.80	0.428	1.13	0.650
4.23	0.443	1.27	0.660
4.58	0.458	1.40	0.672
5.42	0.473	1.53	0.684
6.08	0.518	1.77	0.696
6.52	0.533	2.00	0.707
7.33	0.564	2.25	0.719
8.57	0.594	2.63	0.736
9.62	0.624	2.97	0.754
11.17	0.639	3.23	0.766
12.28	0.654	3.55	0.778
14.78	0.669	3.92	0.790
17.92	0.692	4.33	0.796
18.75	0.699	4.73	0.813
20.30	0.706	5.13	0.824
21.08	0.714	5.63	0.830
23.50	0.729	6.20	0.848
24.52	0.744	6.87	0.860
26.43	0.759	7.57	0.871
28.63	0.774	8.33	0.877
29.78	0.789	9.30	0.895
32.03	0.804	11.15	0.912

.....

Appendix-9 contd...

1	2	3	4
35.07	0.819	11.83	0.918
38.08	0.834	33.83	0.977
41.75	0.850	38.48	0.988
45.15	0.864	43.03	0.994
49.87	0.880	47.78	1.0
55.20	0.894	60.06	1.0
62.07	0.910	67.16	1.0
70.03	0.925	77.86	1.0
80.97	0.940	82.65	1.0
99.45	0.954	172.25	1.0
116.22	0.970	232.0	1.0
1227.25	1.0		

APPENDIX-10

Data on Kinetics of Cumene (Liquid) Sorption in Na.H-ZSM-8 at 313 K

Time, t (min.)	$\frac{h^*}{h^* max.}$
1	2
0.0	0.0
0.05	0.091
0.58	0.104
0.72	0.117
0.85	0.130
1.15	0.140
1.35	0.156
1.58	0.169
2.05	0.195
2.30	0.208
2.58	0.221
2.90	0.234
3.25	0.247
3.88	0.273
4.25	0.286
4.63	0.299
5.08	0.312
5.47	0.324
5.92	0.337
5.32	0.350
6.90	0.363
7.40	0.376
7.90	0.389
8.40	0.402
8.92	0.415
9.47	0.429
10.12	0.441
10.17	0.454
11.32	0.468
11.92	0.480
12.72	0.493
13.32	0.507
14.12	0.520
14.90	0.532
15.72	0.545
17.53	0.571
18.45	0.584
19.62	0.598
20.57	0.610
21.816	0.623
23.267	0.637
24.750	0.650
26.133	0.662

.....

Appendix-10 contd...

1	2
27.76	*0.675*
29.66	*0.689*
31.77	*0.701*
34.00	*0.714*
36.25	*0.727*
38.50	*0.740*
1162.0	*0.961*
2745.0	*1.0*

APPENDIX-11

Data on Kinetics of Cumene (Liquid) in MgO·H-ZSM-8 at 298 and 313 K

298 K		313 K	
Time, t (min.)	$\frac{h^*}{h^*_{max.}}$	Time, t (min.)	$\frac{h^*}{h^*_{max.}}$
1	2	3	4
0.0	0.0	0.0	0.0
0.03	0.065	0.05	0.169
0.20	0.104	0.15	0.240
0.27	0.117	0.20	0.250
0.33	0.130	0.23	0.278
0.43	0.156	0.28	0.304
0.63	0.182	0.32	0.331
0.78	0.195	0.37	0.358
0.97	0.208	0.43	0.385
1.27	0.220	0.53	0.412
1.53	0.231	0.57	0.426
1.83	0.247	0.67	0.440
2.20	0.260	0.73	0.453
2.83	0.273	0.82	0.460
3.53	0.286	0.92	0.480
4.05	0.299	1.02	0.493
4.67	0.312	1.13	0.507
5.95	0.338	1.33	0.520
6.58	0.350	1.53	0.533
8.25	0.377	1.75	0.547
9.87	0.402	2.10	0.574
10.65	0.415	2.33	0.588
11.50	0.429	2.62	0.601
12.40	0.441	2.90	0.609
13.57	0.454	3.08	0.629
14.80	0.468	3.45	0.642
16.18	0.480	3.92	0.655
17.50	0.493	4.23	0.669
19.48	0.506	4.67	0.682
21.82	0.532	5.08	0.696
30.33	0.584	5.75	0.710
33.03	0.597	6.17	0.723
35.13	0.610	6.80	0.737
38.00	0.623	7.42	0.750
41.23	0.637	8.15	0.763
44.02	0.650	10.87	0.804
47.83	0.662	13.07	0.831
51.05	0.676	14.92	0.844
55.30	0.689	16.20	0.859
60.60	0.701	18.08	0.871

.....

Appendix-11 contd...

1	2	3	4
65.75	0.714	20.12	0.885
72.13	0.728	22.67	0.899
79.4	0.740	25.67	0.912
86.22	0.753	29.70	0.926
93.83	0.767	35.08	0.940
102.62	0.780	78.87	0.987
114.95	0.792	88.62	0.993
129.92	0.805	119.37	1.00
146.43	0.819	128.92	1.00
167.33	0.831	1179.00	1.00
191.10	0.841	1240.00	1.00
225.82	0.858		
1355.0	0.935		
1415.0	0.935		
1447.0	0.935		
10200.0	1.0		

APPENDIX-12

Data on Kinetics of Cumene (Liquid) Sorption in P_2O_5.H-ZSM-8 at 298 and 313 K

298 K		313 K	
Time, t (min.)	$\frac{h^*}{h^* max.}$	Time, t (min.)	$\frac{h^*}{h^* max.}$
1	2	3	4
0.0	0.0	0.0	0.0
0.03	0.0731	0.08	0.232
0.13	0.092	0.15	0.294
0.17	0.102	0.18	0.341
0.20	0.112	0.23	0.372
0.22	0.121	0.27	0.403
0.25	0.131	0.32	0.434
0.28	0.141	0.37	0.465
0.33	0.151	0.42	0.480
0.38	0.160	0.48	0.500
0.43	0.170	0.53	0.511
0.50	0.180	0.65	0.528
0.57	0.190	0.73	0.542
0.63	0.200	0.83	0.559
0.75	0.210	0.95	0.573
0.88	0.219	1.12	0.590
1.02	0.229	1.35	0.604
1.23	0.239	1.67	0.636
1.42	0.249	2.00	0.651
1.63	0.258	2.42	0.682
1.87	0.268	2.67	0.698
2.17	0.278	2.98	0.713
2.45	0.288	3.32	0.729
2.70	0.297	3.68	0.744
3.00	0.307	4.03	0.760
3.60	0.317	4.48	0.775
5.22	0.366	4.92	0.790
5.68	0.376	5.47	0.807
6.13	0.385	6.10	0.821
6.62	0.395	6.67	0.837
7.08	0.405	7.32	0.852
7.73	0.414	8.32	0.868
8.28	0.424	9.30	0.883
8.92	0.434	10.37	0.899
9.68	0.444	11.67	0.915
10.62	0.463	13.32	0.930
12.25	0.483	15.28	0.946
13.00	0.493	17.87	0.961
13.95	0.502	21.38	0.977
14.73	0.512	26.82	0.992

.....

Appendix-12 contd....

1	2	3	4
15.75	0.522	41.73	1.00
16.75	0.532	106.0	1.00
17.92	0.541		
19.20	0.551		
20.32	0.561		
21.50	0.571		
23.08	0.580		
24.73	0.590		
26.07	0.600		
27.78	0.611		
29.23	0.620		
31.08	0.630		
33.20	0.640		
35.22	0.649		
37.50	0.659		
80.25	0.950		
93.25	1.00		

APPENDIX-13

Data on Kinetics of Cumene (Liquid) Sorption in B_2O_3-H-ZSM-8 at 298 and 313 K

298 K		313 K	
Time, t (min.)	$\frac{h^*}{h^*_{max.}}$	Time, t (min.)	$\frac{h^*}{h^*_{max.}}$
1	2	3	4
0.0	0.0	0.0	0.0
0.15	0.061	0.03	0.167
0.37	0.088	0.13	0.218
0.43	0.102	0.18	0.256
0.53	0.116	0.20	0.295
0.72	0.130	0.27	0.320
0.88	0.142	0.30	0.347
1.10	0.157	0.33	0.372
1.37	0.170	0.43	0.423
1.85	0.183	0.50	0.449
2.18	0.198	0.57	0.461
2.47	0.211	0.60	0.474
2.77	0.224	0.65	0.487
3.12	0.238	0.72	0.500
3.50	0.251	0.82	0.512
4.07	0.265	0.88	0.526
4.53	0.279	0.97	0.539
5.08	0.292	1.28	0.564
5.63	0.306	1.38	0.577
6.42	0.320	1.75	0.602
7.08	0.333	2.07	0.628
7.72	0.347	2.13	0.641
8.37	0.360	2.62	0.653
9.25	0.374	2.83	0.667
10.10	0.388	3.12	0.680
11.05	0.401	3.40	0.692
12.02	0.415	3.67	0.705
13.33	0.429	4.08	0.718
14.60	0.442	4.43	0.730
15.75	0.456	4.83	0.743
17.28	0.470	5.30	0.756
18.88	0.488	5.75	0.770
20.42	0.497	6.30	0.782
21.95	0.510	6.80	0.795
23.83	0.524	7.62	0.808
25.83	0.538	8.28	0.820
28.03	0.551	9.02	0.833
30.95	0.564	30.53	0.949

.....

Appendix-13 contd....

1	2	3	4
33.0	0.579	32.0	0.956
35.92	0.591	34.42	0.961
38.73	0.606	42.70	0.968
42.22	0.619	48.10	0.974
45.58	0.647	58.15	0.988
		74.67	0.993
12833	1.0	336.50	1.0
12850	1.0	380.00	1.0